AAiT
ADDIS ABABA INSTITUTE OF TECHNOLOGY
አዲስ አበባ ቴክኖሎጂ ኢንስቲትዩት
ADDIS ABABA UNIVERSITY
አዲስ አበባ ዩኒቨርሲቲ

SCHOOL OF GRADUATE STUDIES

CIVIL AND ENVIRONMENTAL ENGINEERING

MASTER OF SCIENCE IN CIVIL ENGINEERING

(DAM ENGINEERING)

COMPARISON OF MODAL ANALYSIS AND TIME HISTORY FINITE ELEMENT METHOD FOR ANALYSIS OF CONCRETE GRAVITY DAMS: A CASE STUDY OF GILGEL GIBE III DAM.

BY: ESUBALEW MOLLA HUNEGNAW

ADVISOR: DR. ING. ASIE KEMAL JABIR

OCTOBER, 2023 G.C

COMPARISON OF MODAL ANALYSIS AND TIME HISTORY FINITE ELEMENT METHOD FOR ANALYSIS OF CONCRETE GRAVITY DAM: A CASE STUDY OF GILGEL GIBE III DAM.

A Thesis Submitted To The School Of Civil And Environmental Engineering Presented In Partial Fulfillment Of The Requirement For The Degree Of Masters Of Science In Civil Engineering (Dam Engineering)

ESUBALEW MOLLA HUNEGNAW

Addis Ababa University

Addis Ababa Institute of Technology

Addis Ababa

Ethiopia

OCTOBER, 2023

Certification

This is to certify that the thesis prepared by Esubalew Molla, entitled: Comparison of modal analysis and FEM (time history) method for analysis of concrete gravity dam: in the case of Gilgel Gibe III dam, submitted in partial fulfillment of the degree of Masters of Science Civil and Environmental Engineering (Major Dam Engineering) complies with the regulation of the university and meets the accepted standards with respect to originality and quality.

Signed by the examining committee

Dr. Ing. Asie Kemal
Advisor

Signature

Dr. Netsanet Nigatu
Internal Examiner

Signature

Dr. Daneal Fekersillassie
External Examiner

Signature

Abrham Gebre (Dr.)
Dean, School of Civil & Environmental Engineering

Chairperson (Department of Graduate Committee)

Signature

DECLARATION AND COPYRIGHT

I, Esubalew Molla declare that this is my original work and that it has not been presented and will not be presented to any other University for similar or any degree award.

Signature_____

Date_____

Esubalew Molla Hunegnaw

hunegnaw.e@gmail.com

+251912074510

October, 2023 E.C.

ACKNOWLEDGMENT

First I would like to thank my advisor Dr.Ing. Asie Kemal Jabir, who strongly mentored me from the beginning of the course to these days, without his enviable advice no part of this work would be practical. I also acknowledge the Ethiopian Electric Power head office which supplied me with mandatory data. I would also like to thank all Gilgel Gibe III dam EEP staff members for their help and kindness during my visit and for providing supporting staff and information for the study.

I am very grateful to Addis Ababa Institute of Technology, Department of Civil & Environmental Engineering for allowing me to take part in this fascinating work. Finally, my deepest gratitude is reached to my friend Solomon Wondimu Gebre Selasie who supported me while I was struggling to make this work real.

.

Table of Contents

List of Tables

List of Figures

LIST OF ABBREVIATIONS:

FEA Finite Element Analysis

EEPCo - Ethiopian Electric Power Corporation Company

RCC- Roller Compacted Concrete

DBE -Design Basis Earthquake

DOF – degree of freedom

MCE -Maximum Credible Earthquake

SEE – Service Evaluation Earth Quake

GWh- Giga Watt Hour

MW- Mega Watt

DCR - Demand Capacity Ratio

CID - Cumulative Inelastic Duration

ANSYS - Analysis Systems

ABSTRACT

The Gilgel Gibe III Dam is a 243 m-tall roller-compacted concrete dam with a hydroelectric power plant On the Omo-Gibe River in Ethiopia. Concrete gravity dams are stable structures that can withstand external stresses with the help of their weight, shape, and strength. Stresses affect these complex structures, which is developed due to the action of dead loads, reservoir and tail water loads, uplift pressure, earth pressure, and silt pressure. Because it is frequently long and straight, a concrete gravity dam can be conceived of as a plane strain structure. The analysis is carried out using two-dimensional (2D) numerical modeling since the majority of the loads operating on the dam are distributed along the same plane. The design is based on rigid body analysis with "no tensile stress permitted" standards. Nonlinearity in shape, material, and the boundary condition of dams, foundations, reservoirs, and dynamic systems, however, may now be accounted for using finite element analysis methods.

This study examine assessments on a roller compacted concrete dam (RCC) and analyze the effects of seismic loading using 2D numerical modeling in ANSYS software with comparisons between modal analysis and time history finite element analysis are compared in the case of the Gilgel Gibe III RCC dam. The distribution of stress under static and dynamic loading situations is also evaluated. The analysis of the Gigel Gibe III dam is used as a control case, and the number of mode shapes required for each modal approach to produce an accurate analysis is determined.

For the findings, the study provides the time histories of a few significant parameters including directional deformation, the maximum principal stress and minimum principal stress at the dam heel and the horizontal component of displacement at the dam crest. For comparison's sake, the direct method's outcome is also displayed in each graph. The results of each analysis method will also be compared to show how they differ in their correlation concerning the design of gravity dams.

In this work, the researcher visualizes stress distributions and dam displacement patterns using ANSYS software. The study's overall conclusion demonstrates that both analysis methods (time history and modal) have their effective areas like modal in terms of time while the time history method includes non-linearity in the dam structure.

1. INTRODUCTION

1.1. Background

In essence, a gravity dam is a building designed so that external forces are resisted by the weight of the structure itself. Roller compacted concrete dam (RCC) refers to the dam made of dry concrete, with essentially no slump, which is spread in layers and then compacted by rollers(USBR,2017). It is more economical and has shorter construction period, similar to earth and rock-fill dam, and makes full use of the strength and durability of concrete. The primary factor preventing roller compacted gravity dam from collapsing is its weight when faced with the force of accumulated water. Strong and little upkeep is required for this type of construction. The two primary methods for constructing concrete roller-compacted gravity dams are roller-compacted concrete and conventional mass concrete pouring (USBR.2006). Construction of dams can be easily accommodated at any site where the natural foundation is strong enough to support the immense weight of the dam. Under the correct conditions, these dams can be constructed to astounding heights.

Concrete's weight, shape, and strength can endure any external stresses in a stable structure such as a gravity dam. Static stresses affect these complex structures, which include dead loads, reservoir and tail water loads, uplift pressure, earth pressure, and silt pressure. Because it is frequently long and straight, a concrete gravity dam can be conceived of as a plane strain structure. The simulation is carried out using two-dimensional (2-D) numerical modeling since the majority of the loads operating on the dam are distributed along the same plane. There are two forms of earthquake dynamic load analysis: linear and nonlinear. For safety against tilting and sliding, the design is based on rigid body analysis with "no tensile stress permitted" standards. Nonlinearity in shape, material, and the boundary condition of dams, foundations, reservoirs, and dynamic systems, however, may now be accounted for using finite element analysis methods. The three primary operating situations that can occur during the lifetime of a dam usual, unusual, and extreme are taken into consideration when designing and evaluating dams in general(USACE, EM:11110-2-2200). These load combinations have been applied to the dam spillway model in the current investigation, and the structure's related stress and displacement responses have been determined. All applicable static loads that might be present during the structure's regular operation are referred to as the "usual static loading conditions."

Most gravity dam analyses assume that the dam is made up of discrete transverse vertical elements or cantilevers, each of which carries weights to the foundation without any load transfer between adjacent elements. This assumption also applies to the vast majority of RCC dams, including those with transverse joints that divide the dam into many monoliths and those with monolithic construction with no transverse joints. This assumption is usually correct, and stress calculations, including dynamic stress analysis, can be performed using a two-dimensional representation of the dam cross-section The current work presents the findings of a 2-D Finite Element analysis of a reservoir-gravity dam system performed with ANSYS Release 16.0 / 2023R2

According to USACE (1995,2000), Both the movement of tectonic plates apart or together and the rupture of a geologic fault that releases seismic waves are causes of earthquakes. These vibrating waves will spread out in all directions and harm the structure of the earth's surface. The position of the earthquake's epicenter, the size of the tremor, the topography, and the local geology all affect how much damage a structure receives. Seismometers monitor the amplitude, intensity, and frequency of ground acceleration, which is used to express earthquakes. Earthquakes are measured with a seismometer, and their amplitude, intensity, and frequency are used to express them. There is a lot of contact area when large structures, such as concrete dams, come into contact with the foundation.

Time history analysis examines the structure's dynamic response at each time step when its base is exposed to a certain ground motion time history. To find out how structures respond to a given time history, time history analysis is done. It is possible to use the time history analysis for both elastic and inelastic response ranges(Kalyan Kumar et.al (2016). The main purpose of modal analysis is to generate trustworthy models that accurately capture the dynamic behavior of structures. Broadly speaking, modal analysis applications encompass a wide range of goals, including the identification and assessment of vibration phenomena, the development of experimentally based dynamic models, the validation, correction, and updating of analytical dynamic models, the assessment of structural integrity, the detection of damage and modification of existing structures, the integration of models with other dynamics domains like fatigue and acoustics, etc (Zhang Huidong et.al, 2008). It takes a wide grasp of mathematical and physical principles to comprehend modal analysis. linear dynamic methods of analysis such as linear modal response spectrum analysis and linear time history analysis have been applied. Although

time history analysis is widely used in research, structural engineers do not completely accept it as a viable analytical tool.

1.2. A Review of Previous Works on Modal Analysis and Time History Finite Element Analysis on Concrete Gravity Dams

The time history method and modal analysis are two different approaches to study the dynamic response of structures, such as dams buildings, bridges or mechanical systems.

1. The transient(time history) method of dynamic analysis on structural engineering that involves applying a given input force or motion over some time and then using numerical methods to solve for the structure's corresponding output motion, according to USACE: EM-1110-2-6050, 6051, and 6053. When there are no other choices except to rely on past performance measurements, this approach is used. It allows us to measure and simulate the impact of fast changes in load functions, highly detailed seismic events, and other events on the dynamic system. Before making any design commitments, it is also used to assess other design characteristics such as stiffness, damping quality, inertia values, load pathways, and others. Modal Analysis (MA) is an analytical technique usually used to find out how different modes, under different loads or environmental conditions, contribute to overall response characteristics like peak displacement or acceleration at specific locations on the structure. More precision is possible than with conventional single-frequency testing alone because it uses mathematical models known as Eigen solutions to explain each response mode independently, free from interference from other modes.
2. Pavol Lengvarský, Jozef Bocko. (2013). By simulating the actual loads that a structure will experience through time and then solving for the structure's response to those loads, the time history analysis method is a straightforward approach. With time-varying displacements, velocities, and accelerations at every position, this method gives a full picture of the structure's behavior through time. With the help of this technique, you may analyze complex, nonlinear systems and discover how a structure responds to various loading scenarios. Calculating a structure's inherent frequencies, mode shapes, and modal damping ratios is a step in the indirect method known as "modal analysis." The contributions of each of these modes are then added up to estimate the structure's response. To comprehend a structure's underlying behavior and to develop control systems, this method offers a condensed depiction of the behavior of the structure.

3. Niranjan Dilip Patil , 2022, B. Poursartip and V. LotfiModal, 2008), It is challenging to determine which approach is more accurate because it depends on the particular circumstance being studied with the analysis's objectives. Both methods have benefits and drawbacks, and the decision between the two is typically influenced by the particular issue under investigation and the analysis's objectives. In general, the modal analysis provides a simplified representation of the behavior but is less accurate in capturing the response to complex, non-linear loads, whereas the time history method provides a more complete picture of a structure's behavior but is more computationally intensive and time-consuming.
4. Mohammad Ejaz Shahir and Priyanka Dhurvey.(2017). A modal analysis is a technique for determining structure vibration characteristics-a) natural frequencies (What frequencies the structure would naturally vibrate at) b) mode shapes (What shape the structure would naturally vibrate at each frequency) c) mode participation factors (How much mass participates in a particular direction for each mode) The most fundamental type of dynamic analysis.). Time history analysis investigates the dynamic reaction of the structure at each time step when its base is subjected to a specific ground motion. history of time

1.3. Research Motivation

The motivation for comparing modal analysis and time history finite element analysis of concrete gravity dams lies in the need to better understand the dynamic behavior of these structures under different loading conditions. Concrete gravity dams are complex systems that are subjected to various loads such as wind, earthquake, and hydrostatic pressure. The accurate prediction of their dynamic behavior is crucial for ensuring the safety of these structures and preventing potential failure. Modal analysis is a commonly used method for analyzing the natural frequencies and mode shapes of a structure. Time history finite element analysis, on the other hand, involves subjecting the structure to a specific time-dependent load and analyzing its response over time. There has been ongoing debate about the effectiveness of these two methods in predicting the dynamic behavior of concrete gravity dams.

By comparing the results obtained from both modal analysis and time history finite element analysis, we can gain insights into the strengths and limitations of each method. This can help us identify the most appropriate method for predicting the dynamic behavior of concrete gravity

dams under different loading conditions. Ultimately, this research uses a case study on the Gilgel Gibe III dam, as the dam is very huge and used different RCC mix on different zones. So that it can briefly show visible parameters for the comparison and contribute to improving the accuracy of dam safety assessments and maintenance practices.

1.4. Statement of The Problem

The difference between the two analysis methods as stated on the above is found in their respective goals: while time history analysis attempts to model a specific set of inputs over time taken from real-life scenarios, modal analysis seeks out patterns among various frequencies and magnitudes generated through calculations rather than relying on actual observed data measured during physical experiments and tests.

Concrete gravity dams are critical infrastructure that provide water supply , hydropower and flood control. However these dams are also vulnerable to seismic loading, and it is important to accurately assess the seismic performance. Modal analysis and time history finite analysis are the two methods that can be used to analyze seismic response of gravity dams(USBR,2016) (USACE, 1995). And there is luck of comparative studies evaluating the accuracy and efficiency of these two methods for concrete gravity dams, particularly in the context of Gilgel Gibe III dam. This thesis aims to address this gap by comparing the accuracy and efficiency of modal analysis and time history finite analysis for the dynamic analysis of Gilgel Gibe III dam.

1.5. Research questions:

The research was designed to answer the following questions:

- Which analysis (modal or time history) method more accurately predicts the dam's cross-sectional stress versus deflection distribution mechanism on the Gilgel Gibe III existing dam under static and dynamic loading conditions?
- How can the modal analysis and time history finite element analysis methods be used interchangeably to produce similar results in terms of the safe design of Gilgel Gibe III dam?
- Which part of the Gilgel Gibe III dam is most susceptible to deflection under seismic loading and which method (modal or time history finite element) analysis visualizes using contour plots and displacement vectors?

1.6. Objectives

1.6.1.General Objective

The study do analyses, compare the accuracy and efficiency of a roller compacted concrete dam (RCC) and investigate seismic analysis(dynamic) using 2D numerical modeling in ANSYS software with comparisons between modal analysis and time history finite element analysis in concrete gravity dam.

1.6.2. Specific objectives:

The research has been able to:

- Compare the magnitude and behavior of displacement on both analysis methods.
- compare the most un favorable load combinations when calculating compressive and tensile stresses at the heel/toe/any other planes normal to the dam faces.
- Visualize the stress contours and distribution under the given load combinations for the two analysis methods.
- Evaluate the maximum displacement of dam crest along the given load combinations of the two analysis methods.
- Compare the ease of workability and accuracy of the two analysis methods in dynamic loading conditions of RCC dams.

1.7. Scope of the study:

This study compare the accuracy and efficiency of modal analysis and finite element time history analysis for the dynamic analysis of concrete gravity dams using the Gilgel Gibe III dam as a case study the study uses ANSYS software package to perform the analysis applying static and dynamic load cases. Deformation of dam crest, minimum and maximum principal stresses are the main out puts of the study which were used to determine the dam under design basis earth quake(OBE) and service evaluation earth quake (SEE)

1.8. Organization of the study

The research entitled Comparison of modal analysis and time history (FEM) analysis methods in the case of Gilgel Gibe III RCC dam has been organized into five units each of which describes as follows:

Unit 1: introduction : this unit describes the general feature of the problem and the study as a whole.it also includes a brief literature review on RCC dams and the Gilgel Gibe III dam.

Unit2: literature review: this unit tells about the relevant review of literature on RCC dams. It also describes design and loading conditions of Gibe III dam.

Unit 3: materials and methods: this unit describes the materials and methods of this study including the study area, data collection and data analysis methods.

Unit 4: data analysis and discussion: this unit presents the result of the study and discusses findings. the finite element analysis method visualizes the structural analysis of Gibe III dam.

Unit 5: conclusion and recommendation: this unit summarizes the key findings of the study and provides recommendations for the further study.

2. LITERATURE REVIEW

2.1. Roller Compacted Concrete (RCC) Dams Review

Dam construction has a long history that is connected with the Middle Eastern and Far Eastern cultures. In countries such as China, Japan, India, and Sri Lanka, several tiny dams, mainly modest embankment structures, were created for irrigation purposes. Some of these early dams still stand today. The dam in Sadd-el-Kafara, Egypt, erected in 2600 BC, is often considered the oldest known dam of actual significance. Sadd-el-Kafara stands 14 meters tall, with an earth-fill center zone surrounded by rock shoulders and rubble masonry face protection. The dam failed after a relatively short period of service, most likely owing to flood overtopping (P. Novak, A.I.B. Moffat, C. Nalluri, and R. Narayanan, 2007). Several more huge dams were built by early civilizations in the Middle East, most notably in modern Iraq, Iran, and Saudi Arabia. The Marib embankment dam, built in Yemen around 750 BC to serve a vast irrigation operation, was renowned for its final height of 20 meters. Around the same time, Turkey's Kesis Gölü (North) dam, which stands 10 meters tall, was completed.

Later, the Romans made an important contribution to the Middle East and countries surrounding the Mediterranean. Some Roman dams are still in use, and the Romans are likely to be credited with being the first to use the arch principle in dam construction. The beginning of the first Industrial Revolution and the canal age provided significant impetus to embankment dam construction in Britain and Western Europe beginning around 1780. The design was still based on a mix of empirical standards and established expertise. Despite the lack of rational design methodologies, dams grew in size. For example, the Entwistle embankment dam in England was the first of its kind to reach 30 m in height when it was completed in 1838. British engineers progressed and developed embankment design and construction quite successfully in the nineteenth century, with major projects in the UK with its five principal dams, finished between 1854 and 1877.

RCC was originally applied to the construction of pavements in Sweden in the 1930s. Later, with the industry shifting toward environmentally compassionate and economically viable materials to meet the difficulties and goals of the enlarged and various applications in the construction sector, its applications began to be heavily utilized in the early 1960s. RCC has been regarded as a good material for dams since the early 1980s, and by the end of 2012, over 550 RCC dams had been

built globally. Some studies are currently looking into the usage of recycled aggregates in RCC for sustainable concrete. RCC, or roller compacted concrete, is a composite building material that has no slump consistency before it has cured. Its name comes from the construction technique, in which the RCC is laid down using high-density or regular paving machinery and is then compacted or consolidated using rollers (USACE.1995;2005). the most recent method of building concrete dams is the roller compacted concrete (RCC) dam, which has largely replaced the traditional CVC method as the preferred method for building gravity dams. Arch dams are not affected by this condition in the same manner, but it is clear that it has become a handy assumption that RCC is now invariably the least expensive type of concrete dam, even though this is not always the case. Additionally, successes have shown the level of efficiency that may be obtained when building RCC dams, but in practice, this level of efficiency is infrequently attained for a variety of reasons, including poor design and a lack of contractor understanding. According to general guidelines, an RCC structure is considered efficient when the ratio of RCC placement during the peak month to that during the average month is less than two, and when the ratio of placement during the peak month to that during the peak day is greater than twenty. The average monthly placement will equal roughly ten days of placement at full capacity if the peak day of placement represents the RCC manufacturing capacity with roughly 26 to 27 days of construction per month. The height of an RCC dam is realistically limited by an achievable inter-layer tensile strength of approximately 1.5 Mpa (USACE: EM-1110-2- 6051). Depending on the applicable seismic loading, this limitation implies that RCC dams significantly higher than 200 m will require zones of high-tensile strength mass concrete at the upstream face, at least for the lower part of the dam height. On the other hand, very substantially higher tensile strengths can be assured with conventional mass concrete. Concrete dams are critical infrastructure since they are used for energy generation, flood control, and industrial supplies. However, the vast majority of existing concrete dams in wealthy countries were planned using mainly static concepts. Because of the seismic revaluation of some locations and the greater reliability requirements expected by the community many existing concrete dams are now outdated.

2.1.1. Different Types of RCC Dams

roller-compacted concrete (RCC) gravity dams are a specific type of gravity dam constructed using roller-compacted concrete. This construction method involves placing low-slump concrete

in layers and compacting it with vibratory rollers to achieve the desired density. The roller-compacted concrete is typically drier than traditional concrete mixtures(USBR,2017).

The term "roller-compacted gravity dam" itself might be a bit of a misnomer since gravity dams primarily rely on their mass and the force of gravity to resist the horizontal forces from water pressure. However, the use of roller-compacted concrete in dam construction introduces some variations. According to Quentin Shaw. (2017) and EB225.01. (2003) the primary types of RCC gravity dams include:

- **Conventional Roller-Compacted Concrete (CRCC) Dam:** This is the most common type of RCC gravity dam. It follows the general principles of gravity dam design but uses roller-compacted concrete. The concrete is placed and compacted in horizontal layers, with each layer being rolled and compacted before the next one is added. This type is suitable for a variety of dam sizes and applications.
- **Homogeneous Roller-Compacted Concrete (HRCC) Dam:** In a homogeneous roller-compacted concrete dam, the composition and characteristics of the roller-compacted concrete are consistent throughout the dam. This type of dam is designed to have uniform properties, offering simplicity in construction and a relatively homogeneous structure.
- **Zoned Roller-Compacted Concrete (ZRCC) Dam:** Zoned roller-compacted concrete dams have different zones with varying mix designs to optimize the dam's performance. Typically, the mix design may vary in terms of cement content, aggregate size, or other properties to meet specific engineering requirements. Zoning allows for tailoring the dam's properties to different structural and construction needs.

These types of dams offer advantages such as cost-effectiveness, faster construction compared to traditional concrete methods, and suitability for a range of dam sizes and applications. The choice between these types often depends on the project's specific requirements, including the geological conditions, hydraulic considerations, and the desired structural performance.

2.1.2. Design consideration of RCC Dams

Designing roller-compacted concrete (RCC) dams involves careful consideration of various factors to ensure the structural integrity, stability, and long-term performance of the dam. according to USBR,(2017) and USACE (1978)Here are some key design considerations for RCC dams:

1. **Material Properties:**

Concrete Mix Design: The mix design of the roller-compacted concrete is crucial. It involves selecting the right proportions of cement, aggregates, and water to achieve the desired strength, durability, and workability. Most of the gravity-type dams have relatively low stresses in most parts as a result of dead load and water load in the reservoir. The highly stressed areas are restricted to relatively thin strata at the dam's upstream and downstream sides, as well as at its heel and toe, where localized stress concentrations exist. As a result, a leaner RCC mix can be employed inside the internal body of the dams, where a relatively low strength is needed. High tensile stresses are often restricted to the up- and downstream surface layers, and can be brought on by earthquake action, especially in the top part of the dam. For these areas, a richer mix is typically applied to the outside surfaces for increased structural suitability, durability, and abrasion resistance (Wieland, M., and Brenner, R.P., 2004; USBR, 2017).

2. structural design

Gravity Dam Design: While RCC dams are often gravity dams, the design must consider the specific properties of roller-compacted concrete, including its lower slump and higher compressive strength compared to conventional concret(USBR, 2017)..

Stability Analysis: Conduct comprehensive stability analyses, considering factors such as sliding, overturning, and foundation stability. The analysis should also account for seismic forces if applicable.

3.Construction Methods:

Layer Thickness: Determine the optimum thickness of each lift or layer of roller-compacted concrete. The thickness may vary based on the dam's height, the equipment used for placement, and the properties of the roller-compacted concrete. Construction of has resulted in the ability to place larger quantities of RCC faster and at a lower total cost (economic advantage). In addition, for dam rehabilitation projects, the cost of building spillways and embankment overtopping protection with layered, stepped RCC construction techniques.(USBR, 2017).

4.Construction Joints and Lift Lines:

Construction Joints: Plan the location and type of construction joints carefully. Properly designed construction joints are essential for achieving monolithic behavior and preventing the formation of cold joints.

Lift Lines: Establish lift lines to guide the placement of each layer. Lift lines help control the dam's geometry, ensuring it conforms to the design specifications. Often, the design of RCC

structures is dictated by the requirements for bonding lift joints for shear and tension rather than the design compressive strength requirement (USBR, 2017). However, the tensile (bond) strength at the lift joints for well proportioned, well-compacted RCC mix would be very close to the strength attained at the well-prepared lift joints of CMC (USACE 2000, EM 1110-2-2006).

5.Compaction:

Compaction Equipment: Select appropriate compaction equipment, typically vibratory rollers, and establish compaction specifications. Adequate compaction is critical to achieving the required density and strength of the roller-compacted concrete.

6.Seepage Control:

Water stops and Joints: Implement effective water stops and joint detailing to control seepage through the dam. Seepage paths should be carefully considered to prevent any adverse effects on the dam's stability.

7.Temperature Control:

Thermal Considerations: Roller-compacted concrete generates heat during the curing process. Consider the potential for thermal cracking, and implement measures such as cooling pipes or insulation to control temperature differentials.

8. Foundations:

Foundation Preparation: Ensure proper preparation of the foundation, addressing any weak or unstable zones. Foundation conditions significantly impact the dam's stability.

9. Geotechnical Considerations:

Slope Stability: Conduct thorough geotechnical investigations to assess slope stability and potential failure modes. Consider factors such as foundation conditions, seismicity, and reservoir-induced seismicity.

10.Reservoir and Environmental Considerations:

Reservoir Characteristics: Assess the reservoir's characteristics, including water quality, sedimentation, and potential impacts on the dam's performance.

Environmental Impact: Consider environmental aspects and regulatory requirements, including habitat preservation, water quality, and public safety EB225.01. (2003) .

11.Monitoring and Instrumentation:

Instrumentation: Implement a monitoring system to assess dam performance during and after construction. This may include instrumentation for measuring deformation, seepage, and other relevant parameters**.**

It's important to note that these considerations are general guidelines, and the specific design requirements will vary based on the project's unique characteristics and local regulations. Consulting with experienced dam engineers and incorporating the latest industry standards is crucial for successful RCC dam design and construction

2.1.4. Advantages and Disadvantages of RCC Gravity Dams

Advantages of Concrete Gravity Dams:

- **Stability:** The primary advantage of concrete gravity dams is their stability. The weight of the concrete provides resistance against overturning and sliding forces, making them inherently stable.
- **Durability**: Properly designed and constructed concrete gravity dams can have a long service life with minimal maintenance. Concrete is resistant to weathering and deterioration, contributing to the durability of the structure.
- **Hydraulic Efficiency**: Concrete gravity dams are often designed to have smooth surfaces, which can enhance their hydraulic efficiency. The smooth profile minimizes water turbulence, reducing the potential for erosion and improving the flow characteristics.
- **Versatility in Design**: Concrete gravity dams can be designed in various shapes and sizes to suit the specific requirements of a site. This versatility allows engineers to adapt the dam to the topography and geology of the location.
- **Reservoir Support:** Concrete gravity dams can support a reservoir with large storage capacity, providing benefits such as water supply, flood control, and hydropower generation.

Disadvantages of Concrete Gravity Dams:

- **High Initial Cost**: The construction of concrete gravity dams can be expensive, primarily due to the large quantities of concrete required and the complex construction methods involved.
- **Limited Foundation Flexibility**: The design and construction of concrete gravity dams require a solid foundation. Sites with poor foundation conditions may not be suitable for this type of dam.

- **Environmental Impac**t: The construction of concrete gravity dams can have environmental impacts, such as the alteration of river ecosystems and the displacement of communities in the reservoir area.
- **Construction Time**: Building concrete gravity dams can be time-consuming, especially for large structures. The curing time for concrete and the precision required in construction contribute to the extended construction period.
- **Not Suitable for All Locations**: In some cases, the topography or geology of a site may not be suitable for a concrete gravity dam. Alternative dam types, such as arch dams or embankment dams, may be more appropriate.
- **Potential for Cracking**: Concrete gravity dams are susceptible to cracking due to factors like temperature changes, settlement, or differential movements. Proper construction techniques and ongoing monitoring are essential to address this issue.

2.2. Material Property (Theory of Elasticity) of RCC

A body deforms when a load is applied to it. The characteristics of the body, the particular environment, the quantity of the load, how quickly it is applied, and the amount of time that has passed between the application of the load and the observation all affect how much and what kind of deformation occurs (Edward L. Wilson. 2000). The way different materials react when loaded varies substantially.. It is helpful to treat instantaneous and time-dependent responses separately as elastic and plastic deformations, even if they cannot entirely be distinguished from one another.

(i) **Elasticity**: A substance's elastic limit is defined as the highest stress that may be applied to it before it becomes permanently distorted and does not return to its original length. Plasticity: The property of materials that deform under stress but do not return to their former dimensions. Elastic qualities of RCC and traditional concrete include modulus of elasticity and Poisson's ratio, which are affected by parameters such as strength, age, paste volume, and aggregate type.

(ii) **The modulus of elasticity:** is the ratio between the normal stress and the associated strain and is generally a function of strength for a specific aggregate type. It is commonly assumed that the modulus of elasticity in compression and tension is the same. When engineering dams, a low modulus of elasticity is preferred to reduce the probability of

cracking at a given stress level, however this results in increased deformation. It is critical to define an acceptable low modulus of elasticity, which can be accomplished by laboratory measurements on specimens. According to USACE 2000, EM 1110-2-2006 The stresses and strains from the strength tests are shown, and the ratio of stress to strain gives the appropriate modulus of elasticity. $E = \frac{\sigma}{\varepsilon}$, and $\sigma = \varepsilon E$, where E: elastic modules, σ: is the stress and ε: the strain. The Elastic modulus is the ratio of (0,0) and $(\sigma y, \varepsilon y)$.

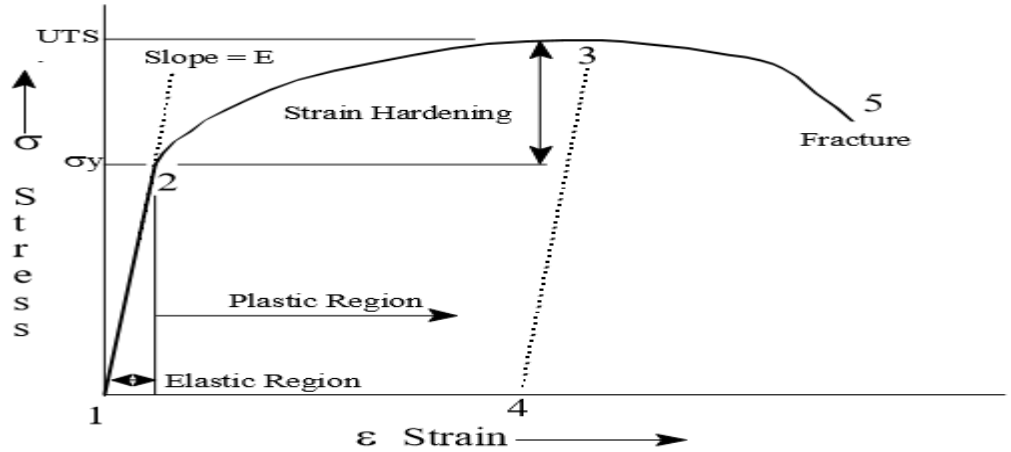

Figure 2. 1. figure showing stress- strain relations of materials

(iii) Poisson's Ratio (ν)

Poisson's ratio is the measure of ratio of the lateral to longitudinal strain resulting from an evenly distributed axial stress applied on the structural component. Poisson's ratio values for RCC are often comparable to those for CMC mixes. For static analysis, values for the majority of RCC dams have ranged from 0.17 to 0.22, with 0.20 being recommended in the absence of testing. When assessing stresses caused by seismic loads, because Poisson's ratio is strain-rate sensitive, the static value may be lowered to 70% of the static value (ACI 207.1R-05; USACE, 2000)The poison's ratio is the ratio between the transverse strain and the axial strain due to a uniformly distributed axial stress. Conventional concrete and RCC has generally similar values of Poisson's ratio and it varies typically between 0.17- 0.22. (ACI, 2011)

(iv) **RCC mixes**: The case studies presented in USACE 2000, EM 1110-2-2006, indicate that RCC mixtures may be designed for a minimum compressive strength of 13.8MPa for durability reasons alone. For seismically active regions, however, higher design

compressive strength is often required in order to achieve the higher tensile and shear strength necessary. Typical compressive strengths of representative 14 RCC dams constructed between the years 1982-2006 in U.S. vary from as low as 8.6 MPa to as high as 48.1 MPa at an age of 1-year, with concrete mixes having nominal maxmum size of aggregates in the order of 37.5, 50 and 75mm (ACI 207.1R-11),

(v) Tensile Strength:

- Numerous techniques, such as the direct tension method, the splitting tensile method, and the flexural test or modulus of rupture method, can be used to gauge the tensile strength of concrete. There are several connections between these tests and compressive strength. The splitting tensile test has been used more frequently to assess the parent tensile strength of concrete (USACE 2007, EM 1110-2-6053; ACI 207.1R-05). ACI 207.1R-05 provides an expression relating tensile strength, f_{dt}', to compressive strength, f'_c, for mass concrete structures as follows:

$$f_{dt}' = 0.6 f_c'^{1/2}$$

- According to the USBR's (2017) study based on collection of a wide range of data set of test results, the following tensile-compressive strength property correlations were determined for RCC lift lines.
  Splitting tensile Strength: $f'_{st} = 0.10 * f_c'$ Direct tensile Strength: $f'_{dt} = 0.05 * f_c'$

USACE (2007) Recommended Static / Dynamic Relationships

As per the guidelines of USACE 2007, EM 1110-2-6053, both strength and elastic properties are strain rate sensitive, and in the absence of test data, the following relationships between static and dynamic properties may be assumed.

Dynamic modulus	= 1.15 x Static Modulus
Dynamic Poisson's Ratio	= 0.70 x Static Poisson's ratio
Dynamic compressive strength	= 1.15 x static compressive strength.
Dynamic tensile strength	= 1.50 x static tensile strength

2.2.1. Review of 2-D Elasticity Theory

In general, stresses and strains at each location in a structure constitute six separate components, which are as follows:

$\sigma_x , \sigma_y , \sigma_z, \tau_{xy}, \tau_{yz} , \tau_{zx},$ for stress and

$\varepsilon_x, \varepsilon_y, \varepsilon_z, \gamma_{xy}, \gamma_{yz}, \gamma_{zx},$ for strain

Isotropic Materials: materials having the same properties in all directions and are used to determine the characteristics of linear elastic materials. The state of stresses and strains can be simplified under specific conditions. In two-dimensional analysis, two types of models are used: plane stress and plane strain. (A. P. Boresi (1985) and Edward L. Wilson (2000)) .

Solid mechanics problems can be expressed as three-dimensional problems and solved using the finite element technique. The geometry and loading in many actual scenarios will be such that the problems can be reduced to two-dimensional or one-dimensional problems with no loss of accuracy.

A. Plane stress problem

The plane stress is defined by using x,y .xy directions and it is a problem visualizing stress variation along the normal direction of the above dimensions. In these cases, it is assumed that no stress component varies over the thickness and that the stress components _z,_yz, and _zx are all zero.

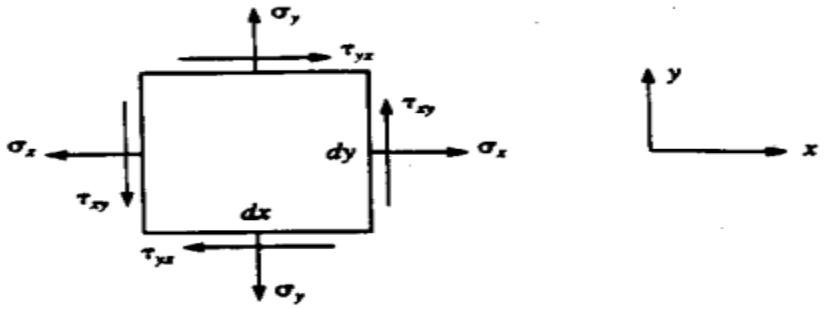

Figure 2. 2. figure showing plane stress problems

The stress is determined to be: $\sigma = \begin{pmatrix} \sigma_x \\ \sigma_y \\ \tau_{xy} \end{pmatrix}$

The maximum and minimum principal and normal stresses are defined by:

$$\sigma_1 = \sigma_{max} = \frac{\sigma_x + \sigma_y}{2} + \sqrt{\left(\frac{\sigma_x - \sigma_y}{2}\right)^2 + \tau_{xy}{}^2}$$

$$\sigma_2 = \sigma_{min} = \frac{\sigma_x + \sigma_y}{2} - \sqrt{\left(\frac{\sigma_x - \sigma_y}{2}\right)^2 + \tau_{xy}{}^2} \quad \ldots\ldots\ldots (2.1)$$

And the principal angle: $\theta_p = \frac{1}{2}(\tan^{-1}(\frac{2\tau_{xy}}{\sigma_x - \sigma_y}))$

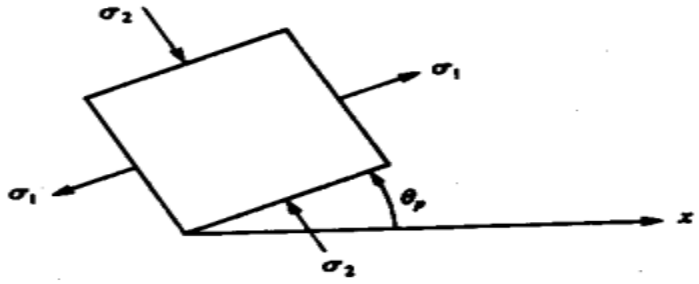

Figure 2. 3 figure showing principal stress and principal angle

Components of stress can be defined using strain in each direction as:

$\varepsilon_x = \frac{\sigma_x}{E} - v\frac{\sigma_y}{E} - v\frac{\sigma_z}{E}$, $\varepsilon_y = -v\frac{\sigma_x}{E} + \frac{\sigma_y}{E} - v\frac{\sigma_z}{E}$, and $\varepsilon_z = -v\frac{\sigma_x}{E} - v\frac{\sigma_y}{E} + \frac{\sigma_z}{E}$,

since σ_z =0, then $\varepsilon_x = \frac{\sigma_x}{E} - v\frac{\sigma_y}{E}$, and $\varepsilon_y = -v\frac{\sigma_x}{E} + \frac{\sigma_y}{E}$, while $\sigma = \varepsilon E$

solving for the two stress components:

$\sigma_x = \frac{E(\varepsilon_x + v\varepsilon_y)}{1-v^2}$, $\sigma_y = \frac{E(v\varepsilon_x + \varepsilon_y)}{1-v^2}$ and $\tau_{xy} = G\gamma_{xy} = \frac{E\gamma_{xy}}{2(1+v)} = \frac{E(1-v)\gamma_{xy}}{2(1-v^2)}$

Finally, we have to write the matrix form of the stress distribution:

$$\begin{pmatrix}\sigma_x\\ \sigma_y\\ \tau_{xy}\end{pmatrix} = \frac{E}{1-v^2}\begin{pmatrix}1 & v & 0\\ v & 1 & 0\\ 0 & 0 & \frac{1-v}{2}\end{pmatrix}\begin{pmatrix}\varepsilon_x\\ \varepsilon_y\\ \gamma_{xy}\end{pmatrix}$$

In general $\sigma = D\varepsilon$ where $D = \frac{E}{1-v^2}\begin{pmatrix}1 & v & 0\\ v & 1 & 0\\ 0 & 0 & \frac{1-v}{2}\end{pmatrix}$

and the strain component can be also written in the form :

$$\begin{pmatrix}\varepsilon_x\\ \varepsilon_y\\ \gamma_{xy}\end{pmatrix} = \frac{E}{1-v^2}\begin{pmatrix}1 & -v & 0\\ -v & 1 & 0\\ 0 & 0 & 2(1+v)\end{pmatrix}\begin{pmatrix}\sigma_x\\ \sigma_y\\ \tau_{xy}\end{pmatrix} \quad \ldots\ldots\ldots\ldots (2.2)$$

All these equations are obtained by assuming the thermal expansion along the plane is neglected. but in reality, if the temperature varies along the plane by a coefficient of β, the above two equations become:

$$\begin{pmatrix}\sigma_x\\ \sigma_y\\ \tau_{xy}\end{pmatrix} = \frac{E}{1-v^2}\begin{pmatrix}1 & v & 0\\ v & 1 & 0\\ 0 & 0 & \frac{1-v}{2}\end{pmatrix}\begin{pmatrix}\varepsilon_x\\ \varepsilon_y\\ \gamma_{xy}\end{pmatrix} - \frac{E\beta T}{1-v}\begin{pmatrix}1\\ 1\\ 0\end{pmatrix}$$

And $\begin{pmatrix}\varepsilon_x\\ \varepsilon_y\\ \gamma_{xy}\end{pmatrix} = \frac{1}{E}\begin{pmatrix}1 & -v & 0\\ -v & 1 & 0\\ 0 & 0 & 2(1+v)\end{pmatrix} + \beta T\begin{pmatrix}1\\1\\0\end{pmatrix}$ ……. (2.3)

Where v = the poison ratio and G = the shear modulus

The loading and boundary conditions of plane stress forces be done according to:

1. the loads must be point or distributed forces applied over the thickness of the body.
2. Supports must be fixed point, fixed edge or roller support.

B. Plane strain problem

Long bodies with little variation in geometry and stress in the longitudinal direction are examples of plane strain problems. In these conditions, a continuous longitudinal displacement corresponding to rigid body translation and linear in z displacements corresponding to stiff body rotation do not result in strain. As a result, the following connections appear (Edward L. Wilson. (2000)).

$$\varepsilon_z = \gamma_{yz} = \gamma_{zx} = 0$$

But here $\sigma_z\ is\ not\ zero.\ 0 = -v\frac{\sigma_x}{E} - v\frac{\sigma_y}{E} + \frac{\sigma_z}{E}$ and $\sigma_z = v(\sigma_x + \sigma_y)$

$\varepsilon_x = \frac{\sigma_x}{E} - v\frac{\sigma_y}{E} - v^2\frac{(\sigma_x+\sigma_y)}{E}$ and $\varepsilon_y = -v\frac{\sigma_x}{E} + \frac{\sigma_y}{E} - v^2\frac{(\sigma_x+\sigma_y)}{E}$

Then the stress and strain components are described:

$$\begin{pmatrix}\sigma_x\\ \sigma_y\\ \tau_{xy}\end{pmatrix} = \frac{E}{(1-2v)(1+v)}\begin{pmatrix}1-v & v & 0\\ v & 1-v & 0\\ 0 & 0 & \frac{1-2v}{2}\end{pmatrix}\begin{pmatrix}\varepsilon_x\\ \varepsilon_y\\ \gamma_{xy}\end{pmatrix} - \frac{E\beta T}{1-2v}\begin{pmatrix}1\\1\\0\end{pmatrix}$$ …….. (2.4)

And $\begin{pmatrix}\varepsilon_x\\ \varepsilon_y\\ \gamma_{xy}\end{pmatrix} = \frac{1+v}{E}\begin{pmatrix}1-v & -v & 0\\ -v & 1-v & 0\\ 0 & 0 & 2\end{pmatrix} + (1+v)\beta T\begin{pmatrix}1\\1\\0\end{pmatrix}$…… (2.5)

Let u and v be displacement vectors along the x and y direction at a given point A shown in the figure below:

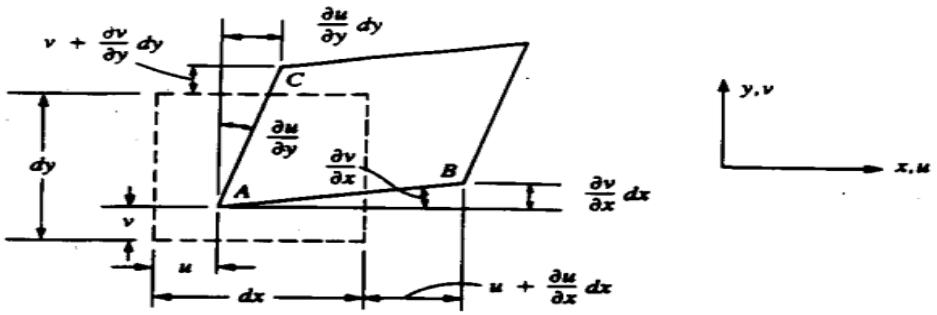

Figure 2. 4 figure showing directional displacement of structure

The relationship between strain and displacement can be simplified and stated as follows.

$$\varepsilon_x = \frac{\partial u}{\partial x}, \quad \varepsilon_y = \frac{\partial v}{\partial y} \text{ and } \gamma_{xy} = \frac{\partial v}{\partial x} + \frac{\partial u}{\partial y}$$

$$\varepsilon = \begin{pmatrix} \varepsilon_x \\ \varepsilon_y \\ \gamma_{xy} \end{pmatrix} = \begin{pmatrix} \frac{\partial u}{\partial x} \\ \frac{\partial v}{\partial y} \\ \frac{\partial v}{\partial x} + \frac{\partial u}{\partial y} \end{pmatrix} \quad \text{..... (2.6).}$$

The loading and boundary conditions of the plane strain problem should satisfy the following:

1. The loads are uniformly distributed over the largest direction (cross-section) and act perpendicular to it. Loading along its thickness is irrelevant.
2. The thickness of the plane is fixed as if the stress is assumed to be generated from this end.
3. Such a method is typically used in the analysis of dam structures, retailing walls, tunnels etc.

2.3. Loading Conditions on analysis of gravity dams

Several loading conditions can be applied to a system. There could be an internal and external load. Load action results in internal stresses/forces and strains/deformations. Since mass is constrained in a volume, "Volume Loads" account for the majority of loads. Wind loads on buildings, reservoir hydrodynamic pressure on dams, waves on offshore structures, pressure distribution on airplanes, and other fluid-structure interaction phenomena can all result in loads. Once more, loads can be quasi-static, dynamic, or static. Line loads, Volume loads Area loads, and Point loads are the major classifications of static loads. The classification is created based on the load's applicability and/or relative relevance.

Primary loads are identified as universally applicable and are always used in design. Secondary loads, such as sediment loads or thermal stresses due to mass concreting, are generally optional and of lesser magnitude. Exceptional loads, such as inertial loads associated with seismic activity, are designed based on limited general applicability or having a low probability of occurrence

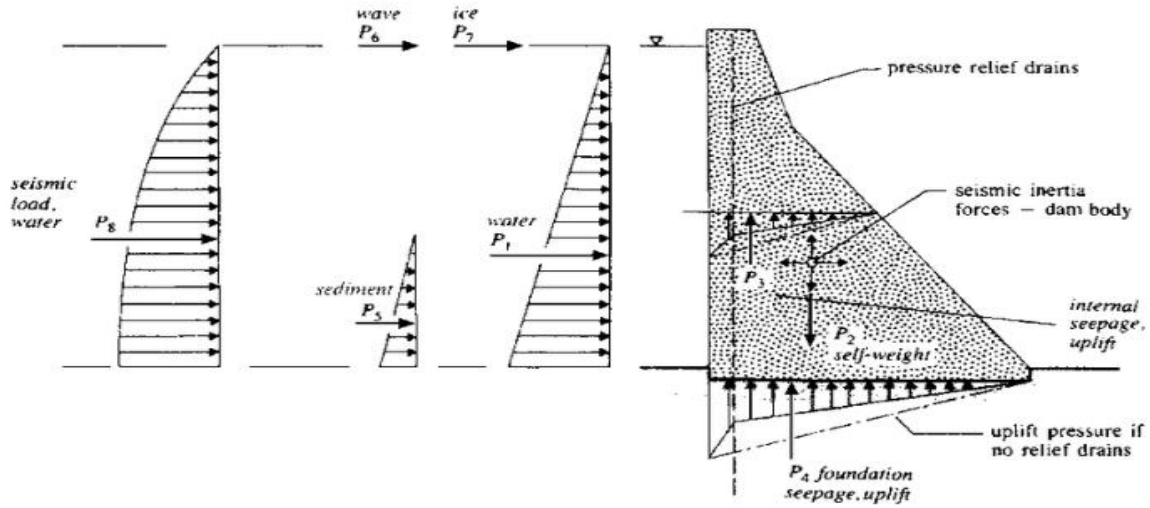

Figure 2. 5 figure showing loading conditions of RCC dam ***(Source: USBR 2016)***

.Technically, the stability of a concrete gravity dam is derived from the gravitational force of the materials in the section. The gravity dam is heavy enough to withstand the stresses and overturning moment created by the water in the reservoir behind it. Because it transfers loads to the foundations via cantilever action, solid foundations are required for the gravity dam.

2.3.1. Seismic Loads

A. Operating basis earthquake (OBE).

The OBE is an earthquake that can reasonably be expected to occur within the service life of the project, that is, with a 50 per cent probability of exceedance during the service life. (This corresponds to a return period of 144 years for a project with a service life of 100 years.) The associated performance requirement is that the projects function with little or no damage, and without interruption of function. The purpose of the OBE is to protect against economic losses from damage or loss of service. (USACE: ER 1110-2-1806).

For the OBE, the linear elastic analysis is adequate for computing the seismic response of the structure and the simple stress checks in which the predicted elastic stresses are compared with

the expected concrete strength should suffice for the performance evaluation. Structures located in regions of high seismicity should essentially respond elastically to the OBE event with no disruption to service, but limited localized damage is permissible and should be repairable.

B. Maximum design earthquake (MDE).

The MDE refers to the maximum ground motion for which a structure is designed or evaluated. While considerable harm or financial loss may be permitted, the project must function without catastrophic failure, such as the uncontrollably releasing of a reservoir, to meet performance requirements. The MDE can be described as a deterministic or probabilistic event (ER 1110-2-1806). When it comes to important structures, MDE and MCE are interchangeable. Critical structures are defined by ER 1110-2-1806 as high downstream hazard buildings whose failure during or immediately following an earthquake could result in fatalities. The maximum potential earthquake (MCE) is the greatest earthquake that might be expected to be produced by a specific source based on seismological and geological data.

C. Safety Evaluation Earth Quake (SEE)

A dam should be planned and analyzed for the most severe seismic event, known as the safety evaluation earthquake (SEE). The stipulation that "there should be no uncontrolled release of water from the reservoir" allows for the acceptance of severe structural damage. It is advised that all components that are essential to safety, like spillway gates and outlets, be made with the SEE in mind. Ensuring public safety, lives, and property is the goal of SEE. The Maximum Credible Earthquake (MCE), which is the largest earthquake that is conceivably possible to occur along a recognized fault or within a geographically defined tectonic province, under the currently known or assumed tectonic framework, can be used to determine the ground motion parameters. The MCE is a deterministic event.

Dynamic analysis is used to assess the overall stability of the dam body, the failure caused by the operating base earthquake and the maximum credible earthquake estimated. The earthquake ground motion parameter typically utilized in the seismic coefficient method of analysis is the peak ground acceleration (typically expressed as a proportion of the peak). At the very least, the earthquake ground motions for dynamic analysis ought to be described in terms of response spectra. If necessary, an earthquake reaction time-history analysis should be carried out utilizing the acceleration time-histories. Whenever possible, the acceleration time-histories should be selected to be similar to the design earthquake in the following aspects:(USACE 1995:2000) the

tectonic environment, the magnitude of the earthquake, fault rupture mechanism (fault type), conditions of the site, design response spectra, and duration of strong shaking. then it is possible to modify the existing data and develop its synthetic record.

a. Peak ground acceleration.

The peak ground acceleration (PGA) is the maximum amplitude of the ground acceleration time history. In terms of structural response, it represents the peak value of the absolute acceleration of a single degree of freedom (SDOF) system with infinite stiffness, that is, with a natural period of vibration equal to zero.

b. Response spectra.

A response spectrum is a plot of the peak values of the response (displacement, velocity, or acceleration) of some SDOF systems with different natural vibration periods subjected to the same seismic input. Therefore, an acceleration response spectrum represents the peak accelerations that a group of SDOF systems with a range of natural periods may exhibit for a given component of ground motion.

c. Site-specific response spectra.

Source-to-site distances, proper attenuation relationships, predicted magnitudes and actual local site characteristics are used to create site-specific response spectra. As a result, it is commonly anticipated that site-specific research will produce more accurate acceleration spectra than normal acceleration spectra. The circumstances necessitating a site-specific ground motion analysis are described in EM 1110-2-6050. A deterministic seismic hazard analysis (DSHA) or a probabilistic seismic hazard analysis (PSHA) can be used to develop site-specific response spectra. The DSHA estimates site ground movements for a specific earthquake, which is defined as a seismic event of a specified magnitude for a specific seismic source happening at a certain distance from the site. The ground motions are represented in terms of the associated site-specific response spectra

2.3.2. Loading Combinations

The dam's self-weight or dead load, reservoir water pressure, and foundation uplift pressure are all significant loadings on a concrete gravity dam. Other loadings occur on an irregular basis, such as seismic forces, or are of a lower magnitude, such as the pressure exerted by waves formed in the reservoir and striking the dam face upstream. The following section explains how

these loadings are integrated to investigate the dam's actual load situations. The following loading combinations are utilized for gravity dam analysis and design (according to USBR2016 and USACE: EM-1110-2-6050).

- **Load Combination A** - unusual loading condition (construction).
    - End of construction, Empty reservoir and tail water
- **Load Combination B** - usual loading condition -normal operating.
    - Normal water level with closed gates, Minimum tail water, Uplift pressure and silt
- **Load Combination C** - unusual loading condition - flood discharge.
    - Maximum Water Level, Gates at appropriate flood-control openings and tail water at flood elevation, Tail water pressure, Uplift, Silt
- **Load Combination D** - **Combination A** + (OBE(Horizontal , upstream)
- **Load Combination E** - **combination B** +OBE(horizontal, downstream)
- **Load Combination F** - **combination B** +SEE (horizontal earthquake, downstream)
- **Load Combination H** - extreme loading condition + PMF

2.4. Finite Element Analysis:

The finite element analysis (FEA), is a computational methodology used in engineering to generate approximate solutions to boundary value problems. Field problems are another name for boundary value problems. The domain of interest is represented by the field, which is most typically a physical structure. The field variables are the variables of interest that are dependent on the differential equation. The boundary conditions are the values of the field variables (or associated variables such as derivatives) that are specified on the field's boundaries.

The finite element method (FEM) is employed in a variety of formulations and is also utilized to analyze nonstructural problems like heat transport, seepage, and general flow issues. Displacement-based FEM is the most popular FEM formulation and is frequently used to solve real-world structural problems. A structure, such as a gravity dam, is idealized as an assemblage of subdivisions (finite elements) coupled at a discrete number of nodal points with a finite number of unknowns using the numerical approach of analysis known as the FEM. The primary unknown variables are represented by the displacements of these nodal points, which are situated at each finite element's boundary.

Finally, the equilibrium equations for the complete system are produced by joining the separate elements in a way that meets the equilibrium and compatibility conditions at their junctions. Numerical methods are used to solve the equilibrium equation, which is effectively a set of alge braic equations.(USACE :EM 1110-2-2200)

2.4.1. General Formulation of FEM

Finite element analysis employs both linear and nonlinear models. The type of analysis is selected based on the structural system and its loadings. The following criteria decide the type of analysis to be performed: Structure type (material and shape), Excitation type (loads), and Response type The following are the State of Equilibrium equations for various cases:

Linear static: $KU = F$

Linear Dynamic: $M\ddot{u}(t) + C\dot{u}(t) + Ku(t) = F(t)$

Non-linear static: $KU + f_{nl} = F$

Non-linear dynamic: $M\ddot{u}(t) + C\dot{u}(t) + Ku(t) + f_{nl}(t) = F(t)$

Here, M, C, K, F and U are mass, damping, stiffness, force and displacement

Displacement Functions: The fundamental concept of displacement-based finite element analysis is that displacements across the system u can be described in terms of element interpolation functions N and nodal displacement vectors U:

$$\{u\} = [N]\{U\} \quad \text{..... (2.7)}$$

the interpolation functions are applied separately to each element m thus:

$$\{u\}^m = [N]^m\{U\}^m = (N_i, N_j, N_k, \ldots\ldots)\begin{pmatrix} U_i \\ U_j \\ U_k \\ \vdots \end{pmatrix} \quad \text{..... (2.8)}$$

Where m indicates that each quantity is referred to as element "m" only The interpolation functions N_i, N_j, N_k satisfy the following relationships:

$$N_i^m\,(x_i, y_i) = I$$

$$N_j^m\,(x_j, y_j) = \quad N_k^m\,(x_k, y_k) = 0 \quad \text{..... (2.9)}$$

- **Strains:** if displacements are known at all points, the strains at any point can be obtained by appropriate differentiation of the assumed displacements. The strains in matrix notation are given by:

  $\{\varepsilon\} = [B]\{U\}$ …….. (2.10)

  For a 2-D problem, the three strain components are defined as follows:

$$\{\varepsilon\} = \begin{Bmatrix} \varepsilon_x \\ \varepsilon_y \\ \varepsilon_{xy} \end{Bmatrix} = \begin{pmatrix} \frac{\partial u}{\partial x} \\ \frac{\partial v}{\partial y} \\ \frac{\partial v}{\partial x} + \frac{\partial u}{\partial y} \end{pmatrix} \text{…….. (2.11)}$$

The strain interpolation matrix [B] is obtained by combining equations 2.8 and 2.11

- **Stresses:** Using the material constitutive law, the stresses in a finite element are connected to the element strains and are given by:

  $\{\sigma\} = [D]\{\varepsilon\} + \{\sigma_0\}$ …….. (2.12)

  Where [D] = the elasticity matrix, $\{\sigma_0\}$= 0 the element's initial stresses. The material law stated in [D] for each element can be arbitrary. However, isotropic material properties are used in most cases and orthotropic material properties are applied to special situations (USACE.1993; 2006).

- **Loads:** the external loads acting on a general 2-D body are surface tractions fs, body forces fb, and concentrated forces Fi. These forces, in general, consist of two components corresponding to the two coordinate axes:

$$\{F^b\} = \begin{bmatrix} f_x{}^b \\ f_y{}^b \end{bmatrix}, \quad , \quad \{F^s\} = \begin{bmatrix} f_x{}^s \\ f_y{}^s \end{bmatrix} \qquad \{F^i\} = \begin{bmatrix} f_x{}^i \\ f_y{}^i \end{bmatrix} \qquad \text{…….. (2.13)}$$

- **Element Stiffness:** Using the virtual displacements principle is the straightforward method for obtaining the stiffness matrix for a finite element (USACE1993: USBR2006). accordingly, the internal and external virtual work done becomes equal for any dynamic compatible minor virtual displacements applied to the body for the body to remain in equilibrium.

$$\int_A \varepsilon^T \sigma \, dA = \int_A U^T f^b dA + \int_S U^S f^s dS + \sum_i U^{i^T} F^i \quad \text{……. (2.14)}$$

The equation's left side is equivalent to internal work. It is equivalent to the real stresses passing through the virtual strains ε that match the virtual displacements that are enforced U. The element nodal degrees of freedom (DOF)-expressed finite element stiffness matrix is obtained.:

$$[k]^m = \int_A \left[[B]^T[D][B]\right]^m dA^m \quad \text{……………………………… (2.15)}$$

The right-hand side of the Equation is equal to the work done by the actual element forces f_b, f_s and F_i going through the virtual displacements {U} and will lead to equivalent nodal forces.

- **Equilibrium Equations**

This is done by taking the displacements within each element and expressing them in terms of the nodal displacements of the overall structure, then rewriting Equation 2.10 as a sum of integrations over the volume and areas of all finite elements., i.e.

$$\ldots\sum_{\mathbf{m}} \int_{\mathbf{A}} [\boldsymbol{\varepsilon}^{\mathbf{T}}\boldsymbol{\sigma}\mathbf{dA}]^{\mathbf{m}} = \sum_{\mathbf{m}} \int_{\mathbf{A}} \left[\mathbf{U}^{\mathbf{T}}\mathbf{f}^{\mathbf{b}}\mathbf{dA}\right]^{\mathbf{m}} + \sum_{\mathbf{m}} \int_{\mathbf{s}} [\mathbf{U}^{\mathbf{T}}\mathbf{f}^{\mathbf{S}}\mathbf{dS}]^{\mathbf{m}} + \sum_{\mathbf{m}} \mathbf{U}^{\mathbf{T}}\mathbf{F}^{\mathbf{i}} \text{………. (2.16)}$$

Where m=1, 2…… N, N = number of finite elements.

the integrations are performed separately for each element, and, thus, local element coordinates may be used for convenience.

$$\mathrm{U^T}[\textstyle\sum_m \int_{A^m}[[B]^T[D][B]dA]^m]U = U^T\,[\sum_m \int_{A^m}\left[[N]^T\left[f^b\right]dA\right]^m] + U^T[\sum_m \int_{s^m}\left[\left[N^S\right]^T\left[f^S\right]ds\right]^m -$$

$$\mathrm{U^T}[\textstyle\sum_m \int_{s^m}\left[[B]^T\sigma^j dA\right]^m + U^T F \quad \text{…………………………………….. (2.17)}$$

where F is now a vector of nodal forces applied at the nodal points of the assembled structure

By imposing unit virtual displacements $U^T = I$ the familiar static equilibrium equations of the element assemblage is obtained:

$$ku = F \text{ Where } F = F_b + F_s - F_i + F_c \quad \text{……………………….. (2.18)}$$

The left side of Equation 2.17 corresponds to the matrix k, which represents the stiffness of the entire structure. The impacts of element body forces, surface forces, beginning stresses, and concentrated loads are all included in the load vector F. To further describe the dynamic behaviour of the system, damping forces and the element of inertia can be added as body forces.

Using the same interpolation functions as in Equation 2.8 to approximate the element velocities and accelerations yields

$$:F_b = \sum_m \int_{Am}[[N]^T[[f^b] - \rho N\ddot{u} - \lambda N u]\dot{d}A]^m \quad \ldots\ldots\ldots\ldots\ldots\ldots\ldots\ldots\ldots\ldots\ldots\ldots (2.19)$$

where $\dot{u}$ and $\ddot{u}$ vectors of nodal velocities and accelerations ρ= mass density λ= damping parameter of the element m.

the entire structure has been analyzed by the dynamic equilibrium equation as:

$$mii + c\dot{u} + ku = F \quad \ldots\ldots\ldots\ldots\ldots\ldots\ldots\ldots\ldots\ldots\ldots\ldots\ldots\ldots\ldots\ldots (2.20)$$

$where\ m$, is the mass matrix, c, is the damping matrix and k is the stiffness matrix

2.4.1. Finite Element Discretization and Approximation Techniques

When solving a mathematical problem numerically, FE reduces the number of degrees of freedom of the system to a finite number. This reduction is, in essence, a discretization. **i. Discretization in time**: The mathematical problems could be subdivided according to whether inertial effects are taken into account or not. these problems are generalized as continuum mechanics. Discretization can take place in both time and space dimensions. In solving dynamic equations to time, two techniques are commonly used: explicit and implicit approximations. In the continuous time domain, discrete time points are identified as $0, \Delta t, 2\Delta t,$ ...t, at which the body's equilibrium is assumed and the equilibrium is hypothesized in the "current" formation $t + \Delta t$. Displacements are expressed as a function of:

$$U(t + \Delta t) = U(t) + \Delta U \ldots\ldots\ldots\ldots\ldots\ldots\ldots\ldots\ldots\ldots\ldots\ldots\ldots\ldots\ldots\ldots (2.21)$$

A..Explicit Approximation

i. Forward Euler method: Given $U(t)$ is a displacement function to a discrete point of time t. The displacement at the time ($t + \Delta t$) in the Forward Euler method is expressed as:

$$u(t + \Delta t) = u(t) + \frac{du(t)}{dt}\Delta t = u(t) + f(u, t) * \Delta t \ldots\ldots\ldots\ldots\ldots\ldots\ldots\ldots\ldots\ldots\ldots\ldots\ldots\ldots\ldots\ldots (2.22)$$

This method uses the slope function (u,) at each point of time, extrapolates and finds the result for the displacement in the next discrete point of time. With a given slope (u,) of the displacement function and the time increment Δt,

ii. Central Difference Method: The other type of explicit method is the central difference method (CDM). A general scheme used in CDM is illustrated in the following figure.

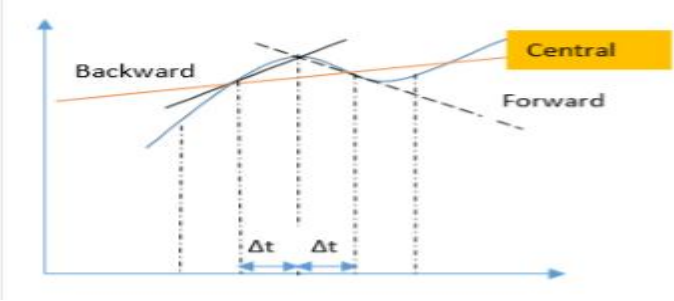

the change in displacement to time can be expressed as:

$$\frac{du}{dt} = \frac{-u^{t-\Delta t} + u^{t+\Delta t}}{2\Delta t} \quad \text{..... (2.23)}$$

B. Implicit Approximation

In the implicit approach, displacements at the current time (t+Δt) are expressed by the displacements at the time t and the displacement increments Δt. . The generic form for the implicit method is as follows:

$$u(t + \Delta t) = u(t) + f(u(t + \Delta t), t + \Delta) * \Delta t \quad \text{..... (2.24)}$$

Two numerical solution schemes using an iterative process are presented in this section, a full Newton Method and a modified Newton Method.

i. Newton–Raphson Method

The Newton-Raphson method is still one of the most powerful numerical methods for determining the roots of algebraic equations. The fundamental notion is detailed further for a function:

$$f(t) = At^3 + Bt^2 + Ct + D \quad \text{..... (2.25)}$$

We begin with a first guess t_0 for a root of the function f given a function defined over the real's t and its derivative'. If the function meets all of the assumptions made in the formula's derivation, a better approximation t_1 is obtained such that $f(t_1) = 0$

It is true that $t = t_0 + h$ for very small number h and $f(t_0 + h) = 0$. Expanding this annotation using Taylor's series

$f(t_0) + hf'(t_0) + \frac{h^2}{2!}f''(t_0) + \frac{h^3}{3!}f(t_0) + \cdots = 0$ truncating the higher terms as 1!, 2!,3!, ... n! are getting larger and larger, then $\frac{h^n}{n!}$ Becomes insignificant. Finally, we can have:

$f(t_0) + hf'(t_0) = 0 \implies h = -\frac{f(t_0)}{f'(t_0)}$ which leads to the expression

$t_1 = t_0 - \frac{f(t_0)}{f'(t_0)}$. In general for N number of discretization like $t_0, t_1, t_3, t_4, \ldots, t_N$

Then any discrete value t_{n+1} is approximated by the prior point t_n using a continues and differentiable function f in the above as:

$t_{n+1} = t_n - \frac{f(t_n)}{f'(t_n)}$, for $n_i = 0, 1, 2, 3, \ldots, N$ ..... (2.26)

2.4.2 . Finite Element Modeling of Gravity Dam:

Modeling complex geometries and range of material properties is possible with the finite element method. A finite element model visualizes the stresses in tension zones, around apertures, and at corners. For calculations that take into consideration the interaction of the dam and foundation as well as linear elastic static and dynamic analyses, finite element models are used. This method has the essential benefit of making complex foundations incorporating diverse materials, weak joints and fractures easily model able. The different modeling approaches are described below:

A. Sub-Structure method.

The foundation is modeled as a viscoelastic half-plane in the substructure technique. An impedance matrix created concerning the nodal points at the dam-foundation rock interface represents the interaction between the dam and the foundation. A separate continuum solution of the foundation region (EM 1110-2-2200) yields the impedance matrix for the viscoelastic half-plane. The frequency-dependent hydrodynamic forces at the dam-water interface are also obtained from a separate continuum solution, assuming that reservoir water may be treated as a fluid domain with constant depth and infinite length in the upstream direction. The seismic input

consists of one vertical and one horizontal component of the free-field acceleration time histories applied at the dam-foundation and water-foundation interface regions.

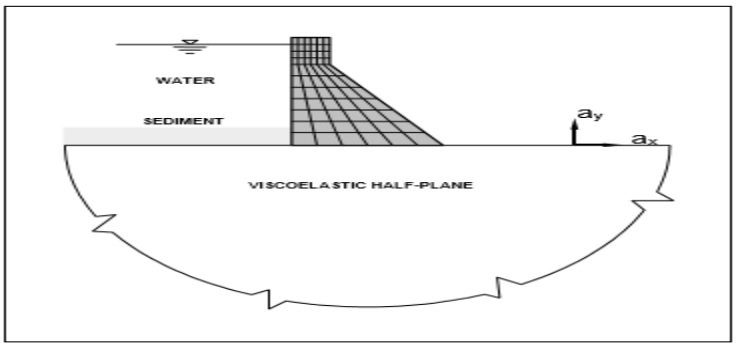

Figure 2. 6 figure showing substructure model

B. Standard method.

The model outlined above applies to a homogeneous foundation in which the same rock qualities are expected to exist throughout the full unbounded foundation region. In general, the characteristics of foundation rock change with depth and along the dam's footprint. The effective modulus of jointed rock at shallow depths may differ dramatically from that at higher depths. In these cases, the viscoelastic half-plane model is inapplicable and should be replaced by a finite element foundation model that can account for variations in rock qualities. The standard method is to create a full finite element model of the dam and an appropriate part of the foundation region. However, to simplify the calculation of the seismic input and minimize the usage of huge foundation models, the foundation model is assumed to be massless. In the upstream, downstream, and downward directions, the foundation mesh must be extended at a distance at least equal to the dam height.

The nodal points at the foundation mesh's base are fixed in both the vertical and horizontal directions. However, the side nodes are connected to horizontal roller supports for horizontal excitation and vertical roller supports for vertical excitation of the dam, as shown in Fig. 2.3 below. The earthquake ground vibrations recorded at the ground surface are used directly as seismic input and are applied at the foundation model's base.

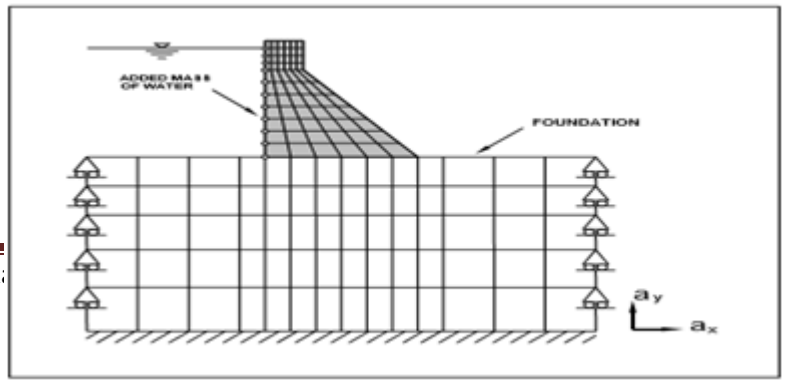

Figure 2. 7 figure showing standard model

C. **Foundation Rock:** A foundation model should ideally encompass key geological elements of the rock and extend to a distance where interaction with the dam is minimal. Because geological data of the fundamental rock are not available or require as much judgment as a measurement to obtain, it is generally impossible to account for all discontinuities in the rock realistically, and the foundation must be analyzed under the assumptions of anisotropy and nonlinear behavior for the rock. Due to the lack of appropriate analytical methods for such models, a foundation model that extends to infinity or a finite distance yet incorporates wave-transmitting barriers is also not practicable. Another major element is the difficulty in identifying free-field motions at dam-foundation contact areas because the foundation model should preferably integrate the main geological features that are neither practical analytical approaches nor sufficient recorded data. For these reasons, an overly simplified idealization of the deformable foundation rock is commonly used in practice (USACE:EM110-2-6053, USBR2006).

A suitable segment of the deformable foundation rock is idealized as part of the gravity dam finite element model, which only includes the flexibility of the foundation rock. As a result, the dynamic analysis ignores the inertial and damping effects of the foundation rock. The material properties are assumed to be linearly elastic, however, the effects of geology are mitigated slightly by using the modulus of deformation rather than the modulus of elasticity of the rock.

D. Impounded Water

A foundation model should preferably integrate the main geological features that are neither practical analytical approaches nor sufficient recorded data. For these reasons, an overly simplified idealization of the deformable foundation rock is commonly used in practice

(USACE: USBR2006). A suitable segment of the deformable foundation rock is idealized as part of the gravity dam finite element model, which only includes the flexibility of the foundation rock. As a result, the dynamic analysis ignores the inertial and damping effects of the foundation rock. In addition, the reservoir water can also be considered in modeling and there are methods used to denote that huge n=mass of water during the analysis stage:

2.4.3. **Generalized Westergaard Model**

The most basic and unrefined reservoir idealization is the Westergaard formulation (Westergaard 1933). The Generalized Westergaard Method (Clough 1977) is another name for this technique, which applies the same added-mass concept that Westergaard created for incompressible reservoirs. The Generalized Westergaard Method, in contrast to the conventional approach, takes into account the curvature and flexibility of the dam by assuming that the hydrodynamic pressure at each position on its upstream face is proportionate to the total acceleration acting normal to the dam at that particular site. Finite element discretization of the fluid domain is not necessary, making this method accessible and computationally efficient. Nevertheless, the method only provides a crude approximation of the hydrodynamic forces operating.

i).Incompressible Reservoir Model

The iterative impacts of the impounded water can be represented by a similar added-mass matrix if the compressibility of the water is omitted. A finite element method is used to idealize reservoir water as a collection of incompressible liquid elements and calculate the added-mass matrix. Although complex reservoir geometry can be described in general by finite element discretization, practical applications only require a prismatic model that extends to a finite distance upstream. Pressures at the free surface are therefore assumed to be zero since surface wave effects are usually disregarded. At other reservoir boundaries, the normal component of acceleration and the pressure gradient must be proportionately established to satisfy the acceleration boundary criterion.

ii). Compressible Reservoir Model

According to field measurements and analytical methods, recent studies on the Morrow Point Dam indicate that water compressibility can be important for dam-reservoir interactions (Ankle. A. Chopra, 1995, cited by USACE manual). A frequency domain solution is required for the

interaction between the dam and the imprisoned water when water compressibility is considered. To properly transmit pressure waves upstream, it can be helpful to conceptualize the fluid domain as a limited zone close to the dam that is connected to a prismatic body of water that extends infinity. In the infinite region, an assemblage of infinite elements is considered, whereas the finite region is represented as an assemblage of liquid finite elements (much like in the incompressible case). Additionally, by assuming absorptive bounds, this analytical process permits the energy loss into the reservoir floor.

2.5. Structural Analysis:

The analysis is either linear or non-linear. Linear model analysis assumes that the material does not plastically deform (permanent deformation). There are two general types of finite element analysis in solid mechanics. Static and dynamic analysis:

2.5.1 . Static Analysis

To identify the amount and distribution of stresses within the structure under static and dynamic load conditions, as well as to assess the substructure and foundation structural adequacy, a stress analysis of gravity dams is conducted.

For Static Problems, the finite element method solves the equilibrium equations $\sum F = 0$ (external and internal forces act on the solid sum to zero). In this case, it may not be necessary to calculate the time variation of motion. However, some materials are history-dependent (e.g. metals deformed in the plastic regime). In addition, a static equilibrium problem may have more than one solution, depending on the load history In some cases, we may be interested in the dynamic behavior of a solid body. Examples include modeling vibrations in structures, problems involving wave propagation, explosive loading and crash analysis. Depending on the level of refinement needed for the specific level of design as well as the type and configuration of the dam, gravity dam stresses are either analyzed using approximate simplified methods or the finite element method. As stated in the US Bureau of Reclamation (USBR), "Design of Gravity Dams" simplified methods using cantilever beam models for two-dimensional analysis or the trial load twist method for three-dimensional analysis are suitable for preliminary designs. If a more precise stress study is necessary, the finite element technique is typically used for the feature and final design stages.

2. 5.2. Dynamic Analysis (seismic)

Currently, hydraulic structural safety evaluation and earthquake-resistant design are done using linear dynamic analysis methodologies. Either the response spectrum or the time-history modal superposition approach is used to carry out the linear dynamic analysis. The main characteristic of a modal analysis is that the overall response of a structure is determined by adding the individually estimated responses of each of its different modes of vibration. For structures whose responses to earthquakes fall within the linear elastic range, the response spectrum analysis is suitable. However, in structures where a large earthquake might exceed the concrete's cracking strength and the reinforcing steel's yield strength, a linear time-history analysis offers extra information crucial for estimating damage or the anticipated degree of inelastic response behavior.

2.5.3. System Equations of Motion

The system's equation of motion on a finite element analysis is described as:

$$M\ddot{U} + C\dot{U} + KU = F(t) \quad \text{..... (2.27)}$$

where M, C, and K are the system's mass, damping, and stiffness matrices U = vector of finite element node displacements F(t) = time-varying external force vector or effective load resulting from earthquake ground motion. In the event of earthquake ground motion, no dynamic external forces are immediately applied to the structure. Rather, the base of the structure is susceptible to ground accelerations. Inertia forces are produced by the base excitation in proportion to the overall accelerations of the DOFs brought on by relative motion inside the structure as well as the influence of support motions. Thus: $\ddot{u}^{\iota} = \ddot{u} + d\ddot{u}_g$

where $\ddot{u_g}$= the vector of three components of the free-field ground accelerations at all support points d = influence coefficient matrix which represents structural displacements resulting from a unit displacement in each component of the support motions and then the equations of motion for a dam-foundation-reservoir system subjected to earthquake ground motion can be written as:

$$m\ddot{u} + c\dot{u} + ku = -md\ddot{u} + f_h \quad \text{..... (2.28)}$$

where m and c =mass and damping matrices of the dam k stiffness matrix of the dam and foundation rock-margin effective earthquake loads f_h = vector of hydrodynamic forces acting on the dam-water interface only

Note that the foundation rock contributes only to the stiffness matrix because its inertia and damping effects are ignored. Procedures for calculating hydrodynamic forces f_h for the incompressible reservoir water are presented in the following section.

A. Westergaard Analysis of Added-mass

The first person to examine how reservoir water affected concrete dam seismic response was Westergaard (1933). He created the concept of added mass for an incompressible reservoir, which is now widely used to determine how most gravity dams will react. His analysis ignored surface wave effects and envisioned the dam as a 2-D rigid monolith with a vertical upstream face. It also assumed that reservoir water was endlessly long and incompressible. The hydrodynamic pressures imposed on the dam face as a result of earthquake ground motion are equivalent to the inertia forces of a prismatic body of water attached firmly to the face of the dam and moving back and forth with the water, according to Westergaard's conclusion, based on these oversimplified assumptions.

The pressures normal to the dam face, however, differ at different locations. When making this adjustment, it is also useful to consider dam flexibility by keeping in mind that the hydrodynamic pressure applied to the dam at any given place is directly proportional to the total normal acceleration at that location. The added mass determined by this method is called the generalized added mass since it pertains to the whole shape of the upstream face of flexible gravity dams. The pressure at each given point I on the dam face is expressed by the Westergaard parabolic form, as seen in the image below, which is the basis for the analysis of the Generalized Westergaard Method (Clough 1977).

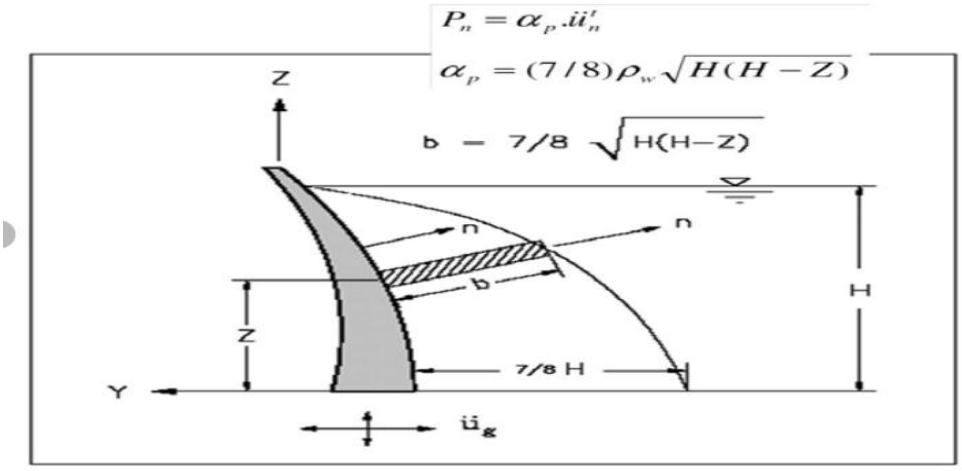

[source: USACE,1993 manual]

Figure 2. 8 figure showing generalized Westergaard's added mass model

There is a principle which is applied to determine the hydrodynamic force of the dam presented as the normal pressure p_i is now converted to an equivalent normal hydrodynamic force at node i by multiplying by the surface area A, tributary to point i:

$F_{ni} = -\rho_i A_i$ …… (2.29)

The normal force Fn, can also be described using Cartesian coordinates:

$F_i = F_m \emptyset_i^T$ …… ….. (2..30)

Finally, we have a general equation combining all the above forms as

$F_i = -m_{oi}(\ddot{u} + d\ddot{u_g})$ …… (2.31)

Where,$m_{oi} = \alpha_{ni} A_i \emptyset^T{}_i \emptyset_i$, m_{ni} is a full added-mass matrix associated with node I on the upstream face of the dam? Following the direct stiffness assembly procedure, the vector of hydrodynamic forces acting on the upstream nodes of the dam is given by:

$f_h = \sum F_i = m_{oi}(\ddot{u} + d\ddot{u_g})$ …….. (2.32)

where $m_{oi}$is the added-mass matrix resulting from the hydrodynamic pressures acting on the upstream face of the dam. The added-mass terms associated with each node form a full sub-matrix along the diagonal of m_{oi} but the sub-matrices are not coupled.

Coupled Dam-Water Equations of Motion and hydrodynamic load can be expressed as:

$\boldsymbol{(m + m_{oi})\ddot{u} + c\dot{u} + ku = (m + m_{oi})d\ddot{u_g}}$ …… (2.33)

B. Analysis of Incompressible Water

The Westergaard added mass discussed previously is computationally efficient, however, it does not accurately depict the hydrodynamic forces occurring on gravity dams. A more realistic simulation of the complex geometry of an arch dam reservoir can be achieved by idealizing the impounded water using the finite element approach. An equivalent added-mass matrix represents the finite element solution of the dam-water interaction, assuming that the water is incompressible. Kuo (1982) and Zienkiewicz (1971), as noted by USACE (1995), summarize the

finite element formulation of an incompressible reservoir model with nodal pressures as unknowns. The equation of motion for hydrodynamic pressures of an incompressible and viscid fluid is given by the wave equation:

$\nabla^2 P = 0,$ …….. (2.34)

where ∇^2 = Laplacian operator in two dimensions p = $p(x, y, t)$ = hydrodynamic pressure over the static pressure in the fluid domain Ω. The hydrodynamic pressures operating on the face of a dam are obtained by solving this equation with appropriate boundary conditions. The boundary condition at the free surfaceΓ_F is zero in the absence of surface waves.

i.e p=0

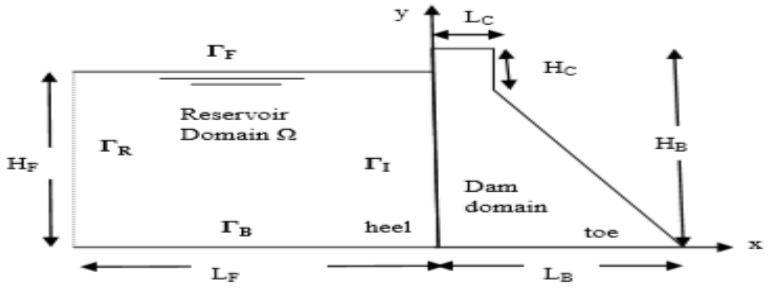

Figure 2. 9 figure showing reservoir-dam boundary

On the upstream face of the dam where the pressure is normally applied the boundary condition is given by: $\frac{\partial p}{\partial n} = -\rho \ddot{u}_n$ on Γ_1. By assuming the horizontal movement of the earth and the rigidity of the reservoir bottom, the pressure gradient and reservoir bottom absorption effects are ignored.

It should be noted that in numerical modeling, the reservoir length is considered to be finite, LF. As a result, an artificial boundary is used to replicate the effect of an infinite reservoir. Based on the Sommerfeld boundary, this boundary is modeled as: $\frac{\partial p}{\partial n} = \frac{1}{c}\frac{\partial p}{\partial t}$ on Γ_R where $c = \sqrt{\frac{k}{p}}$,

c = aquatic fluid wave speed, k = bulk modulus of water and p = pressure.

2.6. Modal Analysis A Review

One method for determining how the structure will vibrate is modal analysis. Certain frequencies can cause the structure to vibrate in the absence of any weight. These are natural frequencies, with unrestrained vibrations. The structure's distortion at each frequency is referred

to as the mode shape. If a structure is designed to vibrate at a particular frequency, it may do so at frequencies other than its inherent frequency.

This frequency of vibration is an excitation frequency; it is a forced vibration. If the natural frequency is close to the stimulation frequency, resonance phenomena may occur. In other words, if the structure is made to vibrate at its inherent frequency, resonance will occur and large amplitude vibrations will be observed.

2.6.1. The Un-damped/Conservative System

In this paper, we do not discuss dynamic-degree-of-freedom (DOF) selection for no-homonymic systems, which is converting continuous systems to discrete models At this point, think of a discrete, un-damped, simplified n-degree-of-freedom structural model that is devoid of any gyroscopic effects. These consist of the sway multistory shear frameworks and the translational toy mechanical system. Every scenario has the required number of imagined finite degrees of freedom (DOFs)

$$M\ddot{u}(t) + K\,u(t) = F(t) \quad \ldots\ldots\ldots\ldots\ldots\ldots\ldots\ldots \text{(2.35.)}$$

where M and K are the constant symmetric mass and stiffness matrices (n x n) $\ddot{u}$(t) and u(t) are the column matrices or vectors (nx1) of accelerations and displacements expressed in physical coordinates varying with time t and F(t) the vector (n x1) of the externally applied (not motion dependent) dynamic loads.

This coupling is a coordinate coupling that perplexes the solution of Eq. 2.35. Especially in the common case of large alternatively, a different formulation practised in finite element (FE) derivations for either M or K, entitled consistent form, leads in general to non-diagonal forms for both these matrices each one of these equations includes components of the vectors u(t) and $\ddot{u}$(t) corresponding to various DOFs and not only to one DOF. And exactly, the modal analysis aims at decoupling these equations. If Eq.2.35. gets uncoupled, this will yield n-independent equations of motion, i.e., each one of which refers to only one DOF, with the result that the MDOF system described by Eq. 2.35 can be treated as n-equivalent uncoupled SDOF systems. Each of them corresponds to a so-called natural mode of vibration, which is characterized by a particular frequency and shape (modal/Eigen frequency ω_i) and modal/eigenvector $\varphi_i(n \times 1$).

Such an advantageous simplification can be established by transforming the vector u(t) into a new vector q(t), (n x 1), whose components are called normal or principal coordinates, as well as generalized displacements. This transformation is equivalent to the separation of variable technique, exercised in partial differential equations and described as:

$$u(t) = \Phi q(t) = \sum_{i=1}^{n} \varphi_i q_i(t) \quad \text{..... (2.36)}$$

alternatively for the displacement vector $u_i(t)$corresponding to each mode i

$$u_i(t) = \varphi_i q_i(t) \quad \text{..... (2.37)}$$

Where Φ is the modal matrix$(n \times n)$ consisting of all n-mode shapes φ_i arranged as its columns, which includes the entire modal shape information. And q(t) is a vector (i.e., column matrix) of n components, with the arbitrarily chosen ith component $q_i(t\ )$ representing the unknown time-functioning generalized displacement for the ith mode. after setting $F(t) = 0$ and recognizing the pure harmonic nature of the associated q(t). Specifically speaking, considering the free/unforced counterpart of Eq. 2.35, i.e., the free-vibration equations

$$M\ddot{u}(t) + K\,u(t) = 0 \text{..... (2.38.)}$$

And considering each modal response $u_i(t) = \varphi_i q_i(t)$ is the solution for equation 2.8. implies that

$$M\varphi_i \ddot{q}_\iota(t) + K\,\varphi_i q_i(t) = 0 \text{..... (2.39)}$$

Multiplying by ${\varphi_i}^T$(transposed mode shape)

$${\varphi_i}^T M\varphi_i \ddot{q}_\iota(t) + {\varphi_i}^T K\,\varphi_i q_i(t) = 0 \text{..... (2.40)}$$

and defining the frequency ω_i as:

$$\omega_i{}^2 = \frac{{\varphi_i}^T K\,\varphi_i}{{\varphi_i}^T M\varphi_i} \text{..... (2.41)}$$

Equation 2.8 becomes

$$\ddot{q}_\iota(t) + \omega_i{}^2 q_i(t) = 0 \text{..... (2.42)}$$

and substituting it into eq. 2.28.

$$(M - \omega_i{}^2 K)\,\varphi_i = 0 \text{..... (2.43)}$$

which have a non-zero solution φ_i then the zero determinant

$|M - \omega_i{}^2 K| = 0$ is the characteristic equation of the system. Because of the indeterminacy of the problem the resultant vectors φ_i are not unique solutions, but rather represent families of solutions of the type $\alpha\varphi_i$, where α is an arbitrary scalar constant. A solution's computing effort/time is proportional to n^3. It has been observed that finding such sets of ω_i, φ_i, solutions

for complex structural systems have opened up a whole new idea for devising efficient solvers. Referring to orthogonal concepts:

$\varphi_i{}^T M\varphi_i = \varphi_i{}^T K\,\varphi_i = 0$, for all $i \neq j$ ……. (2.44)

Using the symmetrical form of the mass and stiffness matrices M and K, respectively, and allow Eq. 2.35 to be uncoupled into n SDOF equations. Indeed, pre-multiplying Eq. 2.35 with $\varphi_i{}^T$ and replacing $u(t)$ with $\Phi q(t)$ according to Eq. 2.36, one gets

$\varphi_i{}^T M\Phi\ddot{q}(t) + \varphi_i{}^T K\,\Phi q(t) = \varphi_i{}^T F(t)$ …… (2.45)

With the help of the orthogonality concept eq.2.35 is equal to:

$\varphi_i{}^T M\varphi_i\ddot{q}_\iota(t) + \varphi_i{}^T K\,\varphi_i q_i(t) = \varphi_i{}^T F(t)$ …… (2.46) or is equal to

$M_i\ddot{q}_\iota(t) + K_i\, q_i(t) = f_i(t)$ …….. (2.47)

The division makes eq.2.37 to:

$\ddot{q}_\iota(t) + \omega\, q_i(t) = \frac{f_i(t)}{M_I}$ ……. (2.48)

Where $K_i = \varphi_i{}^T K\,\varphi_i$, $M_i = \varphi_i{}^T M\,\varphi_i$ and $\omega_i = K_i/\,M_i$ and $f_i(t) = \varphi_i{}^T F(t)$…….. (2.49)

with Ki, Mi, oi and Pi(t) being the so-called scalar modal stiffness, mass, frequency, and force, respectively. A common scaling, or else referred to as normalization, used for φ_i is the one that results in unit modal masses. Namely, if each φ_i is divided by $\frac{1}{\sqrt{M_i}}$ then eq.2.49 becomes:

$\frac{\varphi_i{}^T}{\sqrt{M_i}} M \frac{\varphi_i}{\sqrt{M_i}} = I$ …… (2.50)

With all of the above information in hand, one can now move on to the initial challenge of calculating the response of the un-damped system to some generic forcing F(t). The modal solution$q_i(t)$ of Eq.2.39 consists of a free-vibration solution$q_i{}^c(t)$) due to only the initial conditions $q_i(0)$and $\dot{q}_i(0)$and a special forced-vibration solution $q_i{}^p(t)$due to exclusively the imposed modal force $P_i(t)$in particular, the time domain solution$q_i(t)$) equals

$q_i(t) = q^c{}_i(t) + q^p{}_i(t)$ ……. …….. (2.51)

$q^c{}_i(t) = q_i(0)cos\omega_i t + \frac{\dot{q}_i(0)}{\omega_i}\sin\omega_i t$ …….. …… (2.52)

And $q^p{}_i(t) = \frac{1}{\omega_i}\int_0^\tau \frac{P(\tau)}{M_i} sin\omega_i(t-\tau)d\tau$…… (2.53)

The forced-vibration solution $q^p{}_i(t)$ defined in the time domain by Eq. 2.53 is the Duhamel integral expression, which can be calculated using a variety of numerical approaches It should be noted that retrieving the modal beginning conditions $q_i(0)$ and $\dot{q}_i(0)$ from the initial conditions $u(0)$ and $\dot{u}(0)$ is a simple result of Eq. 2.36 and the orthogonality criteria (2.49). Specifically, by multiplying Eq. 2.36 by $\varphi_i{}^T\ M$ and accounting for the orthogonality properties (2.49), it follows that:

$\varphi_i{}^T MU(0) = \varphi_i{}^T M\Phi q(0) = \varphi^T{}_i M\varphi_i q_i(0) = M_i q_i(0)$ …… (2.54)

$\varphi_i{}^T M\dot{U}(0) = \varphi_i{}^T M\Phi \dot{q}(0) = \varphi^T{}_i M\varphi_i \dot{q}_\iota(0) = M_i \dot{q}_\iota(0)$ …… (2.54)

From which the magnitudes $\frac{\varphi_i{}^T MU(0)}{M_i} = q_i(0)$ and $\frac{\varphi_i{}^T M\dot{U}(0)}{M_i} = \dot{q}_\iota(0)$ are derived.

Finally solving Eqs. 41 and 42 for the unknowns $q^c{}_i(t)\ and\ q^p{}_i(t)$ and then Eq. 2.41 for the unknown$q_i(t)$), Equation.2.26 will be used for synthesizing the total response time histories u(t) from the individual synchronous modal contributions $q_i(t)$ which have been determined as the products $\varphi_i q_i(t)$ of the evaluated modal shapes φ_i and generalized displacements $q_i(t)$

Then $u(t) = \sum_{i=1}^n u_i(t) = \sum_{i=1}^n \varphi_i q_i(t)$ …… (2.55)

2.6.2. The damped System

The earlier discussed conservative (un-damped, i.e., no energy losses) system must be the starting point for any dynamic inquiry. But it's not a true reflection of reality. All structures are intrinsically able to disperse and reduce energy inputs. In addition to being a structural feature, effective damping can also result from the way the structure interacts with other kinds of loads or external loads. An initial modeling of the damping property is nearly impossible. This is due to many factors. There are numerous mechanisms to dissipate excess energy, and intrinsic material damping is not well understood. It highlights the challenge of accurately representing links, fracture holes, and inter-element friction. It is reasonable to consider damping in terms of a linear viscous component.

$M\ddot{U}(t) + C\ddot{U}9t) + KU(t) = F(t)$ …… (2.56)

where C denotes the damping matrix (n x n).

In general, this is non-diagonal. Connecting C to the easily derived structural matrices K and M provides a workaround for estimating its many unknown constituents. The approach of stiffness-proportional damping, which is intuitive, may readily be proven to result in damping increasing with frequency combining the two proportionality approaches provides Rayleigh damping, which appears to be a good and widely used idealization for the energy dissipation mechanism of evenly distributed structures. And rewriting equations 2.36, 2.37 and 2.39 leads to an equation of the form:

$m_i\ddot{q}_i(t) + C_i\dot{q}(t) + k_i\, q_i(t) = f_i(t)$ …… (2.57)

Which leads to:

$\ddot{q}_i(t) + 2\xi\omega\, \dot{q}(t) + \omega\, q_i(t) = \frac{f_I(t)}{m_I}$ …….. (2.58)

Where $\xi = \frac{c_i}{2\omega_i m_i}$ called the global damping rato. Any such damping model greatly reduces the complexity of any further dynamic calculations and is categorized as classical damping. It is also necessary to categorize the previously discussed mass-proportional and stiffness-proportional damping subcases as classical damping. After that, the process of calculating modal replies is the same as it was in the earlier explanation: each modal equation is solved separately, and the few lower modal contributions are added to the total answer in a specific order.

$$q_i(t) = q^c{}_i(t) + q^p{}_i(t)$$

$$= e^{-\xi_i\breve{\omega}_i t}(q_i(0)cos\breve{\omega}_i(t) + \frac{\dot{q}_i(0)+\xi_i\breve{\omega}_i\, q_i\,(0)}{\breve{\omega}_i}\, sin\breve{\omega}_i t) + \int_0^t \frac{p_i(\tau)}{m_i} h_i\,(t-\tau)d\tau \ldots\ldots\ldots \text{(2.59)}$$

2.7. Time History Analysis (FEM)

Time history analysis is a dynamic analysis method that solves the dynamic differential equations of structures iteratively. It is sometimes referred to as the elastic-plastic dynamic analysis approach. Initially, the displacement, acceleration, and velocity dynamic reactions of each mass point with time may be obtained by applying the time history analysis method to compute the time history of the internal force and component deformation. The detailed application and computing process of the time history analysis approach is demonstrated in the following. The ground motion time t is first divided into a sequence of time intervals Δt depending on a predetermined amount and time interval. Subsequently, the overall structural system is estimated as a linear system for every time Δt. the equation of motion can be written as

$$m\ddot{u}(t) + C\dot{u}(t) + ku(t) = -m\ddot{u}_g(t), \text{ ……..(2.60)}$$

The mass matrix m in a standard finite-element formulation with a massless foundation and incompressible water contains both the structure mass and the extra mass of water. The combined stiffness of the structure and the foundation is represented by the matrix k. The effective load vector $m\ddot{u}_g(t)$ resulting from the earthquake ground shaking comprises inertia loads caused by the structure's and water's massIn sub-structuring finite-element formulation, the interaction with water is frequently represented by hydrodynamic forces that are incorporated into the effective load vector. Dynamic stiffness or impedance matrices, which also include interaction forces with the foundation, are used to express the damping and stiffness. The substructure needs to be constructed with the frequency-dependent hydrodynamic forces and foundation impedance in mind.

2.7.1. . Direct Integration

Direct integration is integrating the equations of motion in (2.52) step-by-step through a numerical procedure without first converting the equations into a new form. Through the use of step-by-step integration procedures, the approximate solution is produced at discrete intervals of n time. The following is an expression for the equation of motion: 0, Δt, 2Δt, 3Δt, …, t, t+Δt, …T, where T is the duration of the input motion or loading and Δt =T/n.

Many techniques have been developed for numerical integration. However, only a very brief synopsis of the most often used methods is given to show how they are applied in seismic analysis of hydraulic structures. Generally speaking, implicit and explicit direct integration techniques come in two varieties. Implicit techniques are typically applied in linear time-history evaluations of hydraulic infrastructure. Nevertheless, explicit methods are briefly discussed here because many commercial computer programs include them and the reader may find them helpful in tackling specific problems.

a. **Explicit Methods**. Creating the equations of motion for the first time step, approximating the starting velocity and acceleration terms with finite difference expressions, and then solving for the response at the end of the time step constitute the general notion underpinning the majority of explicit approaches. Because of this, the response values that are produced in each phase are exclusively reliant on the amounts that were gathered in the stage prior. The numerical

procedure thus proceeds step by step without interruption. Explicit techniques are extremely helpful, but they will "blow up" if the time step is too tiny and are only conditionally stable.

The central Difference Method: The central difference method is a very simple explicit method that uses the following finite-difference expressions for approximation of the initial velocity and acceleration terms (Clough and Penzien 1993, Bathe and Wilson 1976).

$$\ddot{u}_t = \frac{1}{\Delta t^2}(u_{t-\Delta t} - 2u_t + u_{1+\Delta t}),\ \dot{u} = \frac{1}{2\Delta t}(-u_{t-\Delta t} + u_{t+\Delta t})$$

The displacement solution from the time step is given by assuming the general motion equation

$m\ddot{u}(t) + C\dot{u}(t) + ku(t) = F_t$Substitution leads to :

$$\left(\frac{1}{\Delta t^2}m + \frac{1}{\Delta t}C\right)u_{t+\Delta t} = F - \left(k - \frac{2}{\Delta t^2}m\right)u_t - (\frac{1}{\Delta t^2}m - \frac{1}{2\Delta t^2}c)u_{t-\Delta t} \quad \text{..... (2.61)}$$

b. **Implicit Methods**. The formulations for new values at $t + \Delta t$ in an implicit approach employ equilibrium equations at t+Δt and hence incorporate one or more values from the same step. The following are some examples of implicit integration methods.

(1) Newmark-β Method. The Newmark method is a general step-by-step process with the integration equations for displacement and velocity at time step t+Δt as shown below (Clough and Penzien 1993, Bathe and Wilson 1976).

$$u_{t+\Delta t} = u_t + \Delta t\dot{u}_t + \Delta t^2(\left(\frac{1}{2} - \beta\right)\ddot{u}_t + \beta\ddot{u}_{t+\Delta t}$$

$$\dot{u}_{t+\Delta t} = \dot{u}_t + \Delta t((1-\gamma)\ddot{u}_t + \gamma\ddot{u}_{t+\Delta t} \quad \text{..... (2.62)}$$

where β and γ are weighting factors and can be chosen to obtain optimum stability and accuracy

(2) Wilson θ Method. The duration of the highest mode is connected to the qualities of the individual elements for a general type of structure. A relatively small mass element results in a very short period of vibration, requiring an incredibly short time step of integration, as stated above. Although the unconditionally stable constant acceleration approach can be employed in this case, an unconditionally stable linear acceleration method, such as the Wilson -method (Clough and Penzien 1993, Bathe and Wilson 1976), is preferable for accuracy reasons. The Wilson $\boldsymbol{\theta}$-method is predicated on the premise that acceleration varies linearly over a long computational interval $\boldsymbol{\tau = \theta\Delta t,}$ **where** $\boldsymbol{\theta > 1.}$ The method reverts to the normal linear

acceleration method for $\boldsymbol{\theta = 1}$, but it becomes unconditionally stable for $\boldsymbol{\theta > 1.37}$. However, the Wilson approach dampens out higher modes and can result in huge inaccuracies when higher modes contribute significantly. As a result, using this method is no longer recommended.

2.7.2. **Mode Superposition**

The number of operations and the number of time steps have an inverse relationship in the direct integration approach. Direct integration can generally be performed successfully when the reaction is required for a short time. Nevertheless, it might be more effective to convert the motion equations into a style that makes step-by-step integration less costly if the integration is to be carried out over a large number of time steps. For this reason, the equations of motion for linear analysis are usually transformed to produce the eigenvectors or normal-coordinate systems. The decoupled equation of motion for each mode is presented below, which can be obtained by applying the normal-coordinate approach of Clough and Penzien (1993) to equation $m_n\ddot{u}_n(t) + C_n\dot{u}_n(t) + k_n u_n(t) = F_n(t)$, where the modal coordinates mass, damping, stiffness and load are defined as:

$$M_n = \emptyset^T{}_n m\, \emptyset_n \quad ,$$

$$C_n = \emptyset^T{}_n c\, \emptyset_n$$

$$K_n = \emptyset^T{}_n k\, \emptyset_n$$

$F_n = \emptyset^T{}_n f\, \emptyset_n$ where the modal equation can be defined in the form:

$$\ddot{u}_n(t) + 2\xi_n\omega_n\, \dot{u}_n(t) + \omega^2{}_n\, u_n(t) = \frac{F_n(t)}{M_n} \quad \text{..... (2.63)}$$

where n = ξ is the modal damping ratio, and n = ω is the un damped natural frequency. Now the time integration can be carried out individually for each decoupled modal equation. This can be accomplished using any of the above integration schemes or by numerical evaluation of the Duhamel integral (Clough and Penzien, 1993) cited on USACE. (2007).

$$U_n(t) = \frac{1}{M_n\omega_n}\int_0^t F_n(\tau)e^{(-\xi_n\breve{\omega}_n(t-\tau)}sin\omega_n(t-\tau)d\tau \quad \text{..... (2.64)}$$

Where $\omega_{dn} = \omega_n\sqrt{1-\xi_n{}^2}$ is the damped natural frequency then the displacement of the structure in the geometric coordination can be computed as:

$u(t) = \phi_1 u_1(t) + \phi_2 u_2(t) + \cdots . + \phi_n u_n(t)$..... .....(2.65)

2.7.3. Stability and Accuracy Considerations

As a dependable method of examining the behaviour of dams during seismic events, linear time-history studies can be seen as an essential stage in the study process. Compared to the simplistic pseudo-static methods of analysis that are typically used in the initial stages of a gravity dam's design, they constitute a major upgrade. The output of linear time-history analyses is typically displayed as maximum stress envelope maps. Nevertheless, this type of result displays peak values that are frequently not simultaneous and provides no information regarding the length of the overstress cycles. An approach was proposed by Eugenia Correa et.al., (2020) to evaluate the seismic performance of a structure by integrating the positive values of the maximum primary stress time history. Several other performance indicators have been proposed in the literature as substitute analysis techniques that allow for a methodical assessment of the impacts of different ground motions, according to (USACE, EM110-2-6050). Currently, the most reliable and widely used method of assessing a dam's stability under seismic events is the DCR (Demand Capacity Ratio) - CID (Cumulative Inelastic Duration) method, as described in USACE "Time-History Dynamic Analysis of Concrete Hydraulic Structures" (USACE, EM110-2-6051) and (USACE: EM110-2-6053).

With this approach, it is possible to evaluate a dam's seismic performance using straightforward stress assessments from a linear elastic analysis along with engineering expertise. For dynamic loadings, a specific number of stress excursions above the tensile strength is permitted. The magnitudes of the Demand Capacity Ratios (DCR), cumulative duration, and damage level are used to establish the performance evaluation and damage level assessment, based on the magnitudes of Demand Capacity Ratios (DCR), the cumulative duration of stress excursions over the tensile strength of the RCC, and the spatial area of overstressed locations, performance evaluation and damage level assessment are developed. The tensile strength or capacity of the plain concrete used in the computation of DCR is obtained from the uni-axial splitting tension tests or the static tensile strength $f_t = 1.7\, f'^{\frac{2}{3}}_c = \frac{2P}{\pi LD}$, Raphael's suggestion as cited by USBR,2006 and USACE,EM:1110-2-6053, where L and D are the length and diameter of specimen, p stands for the applied load and fc' is the compressive strength of the concrete. A performance curve displays the permissible level of damage based on the linear-elastic analysis, as shown in figure below

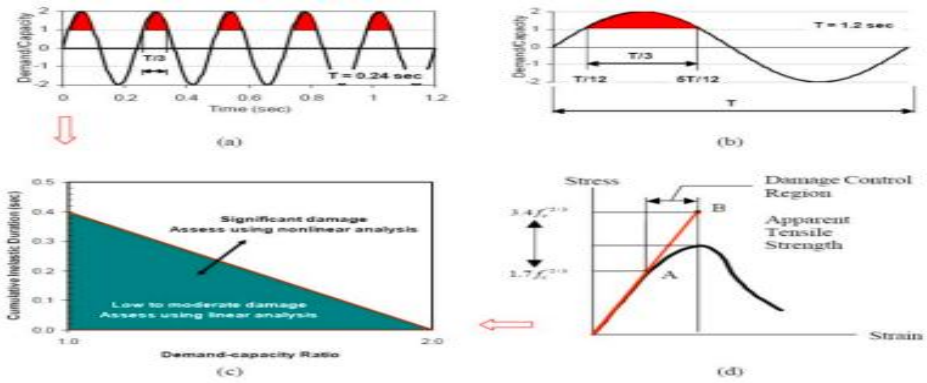

(Source USACE time history dynamic analysis of concrete dams)

Figure 2. 10 figure showing basis for upper limit demand capacity and cumulative inelastic duration

For a dam's linear transient dynamic analysis, a DCR of two is the maximum allowed. This translates to a stress demand twice the concrete's static tensile strength. The stress demand associated with a DCR of 2 corresponds to the concrete's so-called "apparent" dynamic tensile strength, which is utilized to assess the outcomes of linear dynamic analysis, as shown by the stress-strain curve in the previous image. If the calculated stress demand-capacity ratios are less than or equal to 1.0, the dam response to an earthquake is regarded as being within the linear-elastic range of behavior with no likelihood of damage. If the predicted stress demand-capacity was exceeded, the dam would respond nonlinearly by cracking its concrete and/or opening its construction joints.

3. MATERIALS AND METHODS

3.1. Study Area and overview of the dam

3.1.1. Location

Water resource in Ethiopia is properly used since they can be the eminent cause for the reduction of poverty but Ethiopia is known for building hydroelectric plants, reservoirs, irrigation and diversion canals, and dams. Dams have benefits beyond just producing power. Numerous dams are multifunctional buildings that supply water for drinking, irrigation, and flood control. The Gibe III project region is roughly 400 kilometers southwest of Addis Ababa and 50 kilometer's east-southeast of Awasa, as seen in the map below Mareka Gana Wereda of the Dawro Zone and Kindo Koyisha Wereda of the Sodo Zone of the Southern region of Ethiopia(EEP report, 2007).

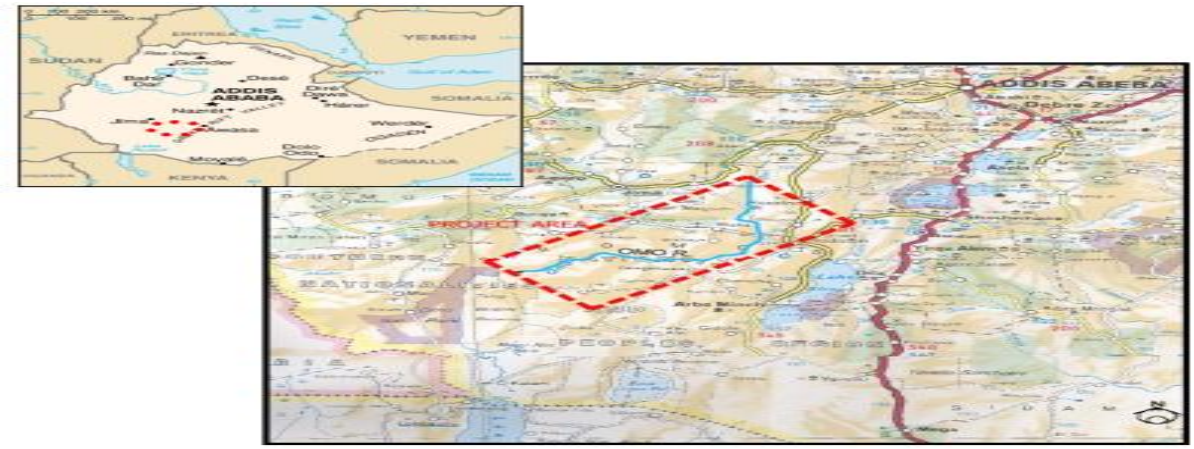

Source: EEPCO GIBE III environmental and social impact assessment report 2009

Figure 3. 1 figure showing site location of Gilgel Gibe III dam

3.1.2. Climate

Tropical humid climates characterize the highlands of the research region, which include places around Jimma and the Gojeb River's sources. The remainder of the watershed is characterized by a tropical sub-humid climate, which lies between the hot, arid environment found in the floodplain's southern portion and the tropical, humid climate. The extreme southern plain receives 400 mm of the country's total annual precipitation of 1140 mm, whereas the highland receives 1900 mm. The average yearly temperature in the basin ranges from roughly 29°C in the south lowlands to around 17°C in the west highlands (Awulachew, S. et. al (2007) The headwaters of the Gojeb River and the areas surrounding Jima are part of the tropical highlands.

The northwest of Jima, beyond the Gibe Basin, experiences the greatest rainfall. The lower-lying southern regions of the basin receive a significant amount of rainfall. The basin receives roughly 1900 mm of rain annually in the western and northern portions and 1200 mm in the lower portion of the project area. South of Lake Turkana, annual rainfall rates drop sharply to less than 300 mm. The yearly average air temperature in the project region is 20.4^{o}C (Pages 81–100, EEP report 2009)

3.13. Geology

The dam location is located on the Jima volcanic rock, which dominates the South-Western Ethiopian highlands. The tertiary volcanic sedimentary strata formation is mostly made of trachyte, basalts, pyroclastics, and rhyolite (Shayma Al Baghdady and Linnea Khan, 2018; EEPCO,2009) The RCC barrier is supported by the central trachytic body. The blocky structure of the massif is defined by sub-vertical joints that are typically filled with calcite and have a moderate to significant separation from one another. These joints are nearly parallel and perpendicular to the river's alignment. The granite rock shallow part shows sub-horizontal and low persistent joints. Except for the 5-10 m region, except for the region, 5-10 m below the RCC-rock contact, where the permeability is often greater than 1 UL, the upper zone of the trachytic body has a relatively low permeability. The dam's foundations are defined by the presence of a sequence of volcanic and volcano-sedimentary rocks. Despite differences in thickness and placement of some units, the ecology on both sides of the Omo valley is comparable (EEPCO,2009). SW-T outcrops, reaching a maximum height of approximately 150 meters at the right abutment. It is substantially thinner on the left abutment (10-40m). These rocks are porphyric, fine-grained, slightly carious locally, frequently blocky or very blocky, and slightly weathered. They are grey to yellow in variety. The Un-weathered Trachyte (U-T) unit outcrops in the valley's bottom. According to petrographic analysis, it is a volcanic rock (trachyte flows) with a sufficiently high evolutionary degree.

3.1.4. Structural Description of Gibe III Dam

According to the EEPCO report geometric design was done by studio Pietrangeli a sister company of Salini contractor who passionately took the overall project contact. The upstream face slopes 0.25:1 (H: V) below elevation 770 m above sea level and 0.2:1 (H: V) above elevation 770 m. The average slope of the stepped downstream face is 0.65:1 (H: V), with a local slope reduction near the toe below 700 m asl. 35 monolithic blocks that make up the dam

are divided by cutting joints into the newly compacted RCC. For this study, the non-overflow geometry was used in different loading conditions.(EEPCo, 2009)

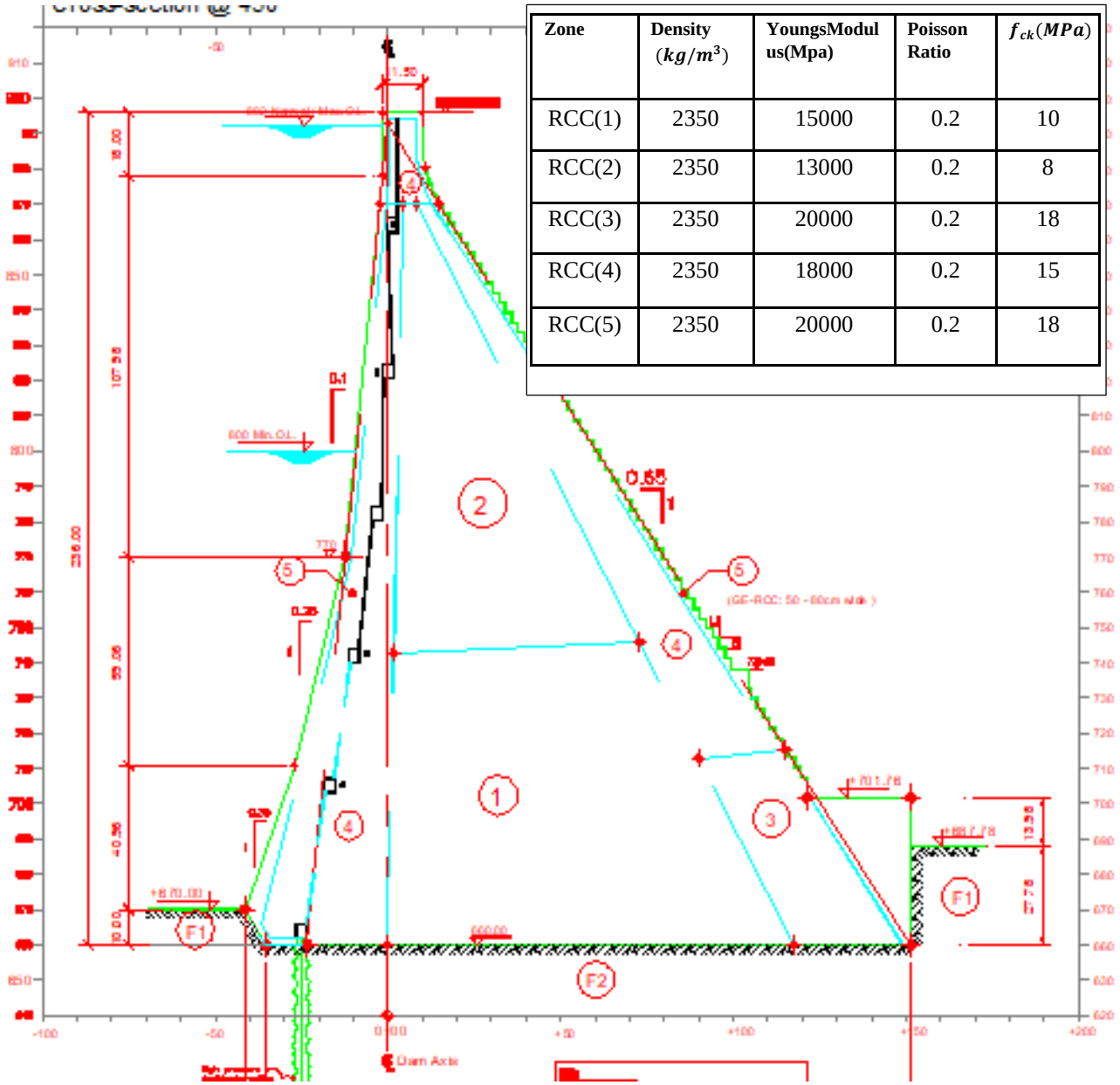

Zone	Density (kg/m^3)	YoungsModulus(Mpa)	Poisson Ratio	$f_{ck}(MPa)$
RCC(1)	2350	15000	0.2	10
RCC(2)	2350	13000	0.2	8
RCC(3)	2350	20000	0.2	18
RCC(4)	2350	18000	0.2	15
RCC(5)	2350	20000	0.2	18

Figure 3. 2 figure showing geometry of Gilgel Gibe III dam non- over flow section

According to the EEP study from 2009, Gilgel Gibe III is a roller compacted concrete (RCC) dam the biggest and tallest Roller Compacted Concrete (RCC) dams in the world. Ethiopian Electric Power Company (EEP) is the owner, while Salini-Impregilo SpA is the main contractor. While the project began in 2006, impounding did not begin until 2015. Now that the dam's construction is finished, the facility is running at maximum capacity.

Table 3. 1 . Table showing physical background of Gilgel Gibe III dam (EEP,2006)

1. Main dam body and accessories	
Name of dam	Gibe III
Location	Southern regional state, Ethiopia
Name of river	Omo
Type of structure	RCC
Foundation level (lowest)	650 m a.s.l (maximum overflow section)
Maximum height	243m (maximum overflow section) 236m (maximum non-overflow section)
Length of dam	610m
Spillways	7 in number, each with discharge capacity of 10600 m^3/s
2. Reservoir	
Normal (maximum) operating water level	892 m a.s.l
Reservoir storage capacity (active)	11.75 x 10^9 m^3.
Standard Project Flood (SPF) level - 10600 m3/s	887.5 m asl
Probable Maximum Flood (PMF) level-18600m3/s	893 masl
Minimum operating level	800 masl
Full reservoir level (sill)	875 masl (top of spillway)
Dam crest (non-overflow section)	896 masl
Maximum (flood) tail water	695 masl
Silt elevation after 50 years	689masl
Normal operating level	681 masl
Minimum tail water level	677 masl
Standard Project Flood (SPF) level - 10600 m3/s	695 masl
Probable Maximum Flood (PMF) level-18600m3/s	701 masl
3.capacity	
Headrace tunnel	2 in number, length 1.0 km, diameter 11m
Power house	Outdoor; 10 Francis turbines, installed power 1870 MW.
Transmission lines	Length 3km, 400 kV

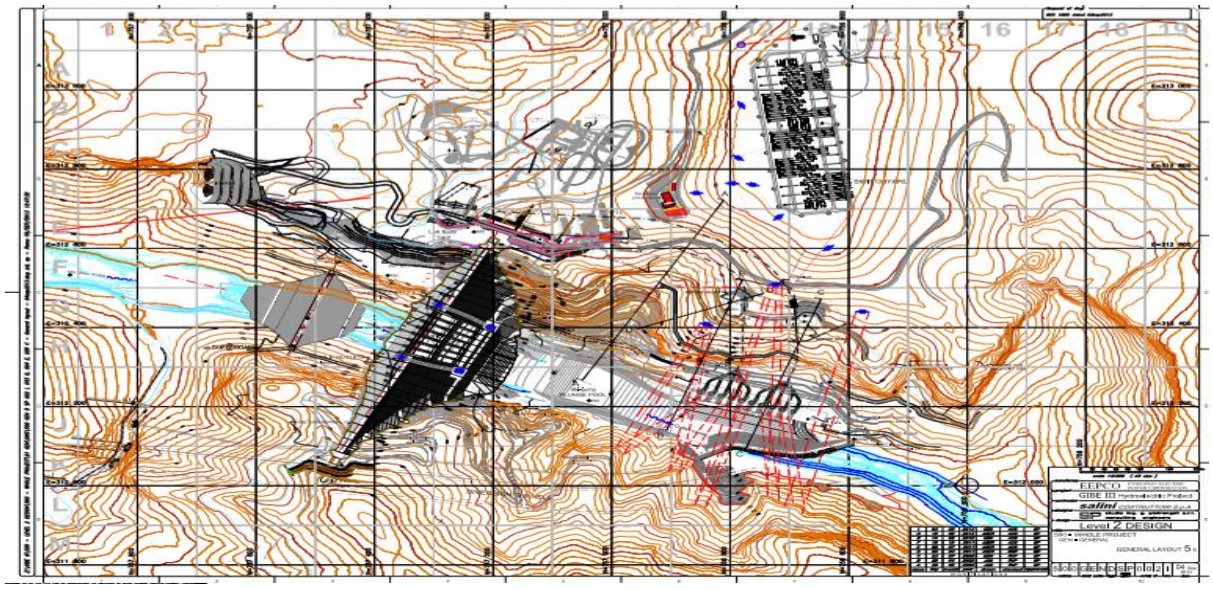

Source EEP level I design report

Figure 3. 3 figure showing general layout of Gigel Gibe III dam

upstream view of the dam

View of the dam from downstream

Figure 3. 4 figure showing upstream and downstream view of Gilgel Gibe III dam

3.2. Research Type

This study was a quantitative type comparative study of modal analysis and time history finite element analysis which was done based on a case selected in a particular project for the seismic analysis of RCC dams. Modal analysis and time history finite element analysis (FEA) are two different approaches used in structural analysis to understand the dynamic behavior of structures under various loading conditions. Let's explore each method, along with their definitions, advantages, and disadvantages

(i). Modal Analysis: Modal analysis is a technique used to study the dynamic characteristics of a structure by determining its natural frequencies, mode shapes, and damping ratios. It is based on

the assumption that the structure can be represented as a set of discrete mass, stiffness, and damping elements.

Advantages:

Modal analysis provides the eigenvalues (natural frequencies) and eigenvectors (mode shapes) of the structure, which give insights into how the structure responds to different modes of vibration.

Modal analysis simplifies the complex structural system into a series of modes, making it easier to understand and analyze the dynamic behavior.

Disadvantages:

Modal analysis assumes linear behavior, which may not accurately represent the response of structures under large deformations or nonlinear conditions. Accurately modeling and extracting damping ratios can be challenging, and the assumption of proportional damping may not always hold true.

(ii). Time History Finite Element Analysis (FEA):

Time history analysis in finite element analysis involves solving the equations of motion for a structure subjected to dynamic loading over a specified period. Unlike modal analysis, it considers the time-varying nature of the applied forces or displacements.

Advantages:

Time history analysis allows for the consideration of realistic time-varying loading conditions, making it suitable for studying dynamic events such as earthquakes, impacts, or blasts. It can handle nonlinear material behavior and large deformations, providing a more accurate representation of the structural response under extreme conditions.

Disadvantages:

Time history analysis can be computationally intensive, especially for large and complex structures, requiring significant computational resources and time. Modeling the time-dependent behavior of materials, nonlinearities, and accurately representing the loading history can introduce complexity and uncertainty into the analysis.

3.2.1.Comparative overview of the two methods

Applicability: Modal analysis is often used for linear systems with simple loading conditions, while time history analysis is more suitable for structures subjected to dynamic and time-varying loads.

Accuracy: Time history analysis is generally more accurate for nonlinear and dynamic scenarios, but modal analysis provides a quick overview of the structure's natural frequencies and mode shapes.

Computational Efficiency: Modal analysis is computationally more efficient compared to time history analysis, which can be computationally expensive.

In summary, the choice between modal analysis and time history FEA depends on the specific characteristics of the structural system and the loading conditions under consideration. Both methods have their strengths and weaknesses, and they are often used complementarily in structural engineering analyses.

3.3. Data collection

the study uses the following data sources to collect secondary data and validation of data was done as it is stated in each data collection.

1. Ethiopian electric power main office and project office
   - Geometry of the dam
   - Stability analysis report publicized in 2007E.C.
   - Seismic analysis report publicized in 2007 E.C.
   - Geotechnical report publicized in 2008 E.C.
2. Previous works on the dam site (seismic data)
   - Amn Ali. (2020) . Seismic Vulnerability Analysis of Major Ethiopian dams. PHD dissertation.
   - Ayele. Atalay, (2016), Probabilistic seismic hazard analysis (PSHA) for Ethiopia and the neighboring regions.

3. Standards (design and analysis codes), publications.

   - USACE(Us Army Of Corps Of Engineers) publications and manuals
   - USBR(United States Berau Of Reclamations) manuals
   - ACI (American concrete institute) standards
   - ICOLD Publications
   - ES (Ethiopian standard for seismicity)manual (ES-8)

3.3.1 Earthquake Acceleration Data

The two key issues for a project are the effects of soil strata and topographic circumstances (basin effects, or ray path focus), and the consequences of ground motion on the site (such as weakening of foundation materials and instability of natural slopes). These could affect how ground motion from a rock outcrop spreads to a particular project feature. The study's objective is to gather all the data on on-site conditions required for a project's safe design or operation. The study collected earthquake time history data using the EEPCO seismic report document analysis and reviewing the different studies on the seismicity of the area, observing the historic earthquake events around GILGEL GIBE III.. The historic earthquakes formed around the site were tried to be collected and were used as support for the use of other studies and own decisions the study tried to see some historic earthquakes which occurred around the dam site up to 150km distances and the result was given with the following table.

Table 3. 2 table showing historic earthquake around Gibe III dam

Date	Magnitude(NEJC)	Magnitude(Gouin)	distance from GIBE III (km)
23, August 1906		6.6	35
28, Octo. 1906		6.7	-----
14, July, 1960		6.3	23
27,jan, 1968	5.1		152
2, Dec. 1983	5.1		40
20, Aug,1985	5.4		42
10, July,1987	5.3		11
25, Oct, 1987	5.6		19
28,oct1987	5.4		3
8, June 1989	5		15
13, feb1993	5		11
20, Jan,1995	5		17
19, dec,2011	5.1		59

Source :Gouin (1979) advanced national science system(ANSS)database, walter in (Carr,2012)

The first task here was determining site-specific peak ground acceleration PGA for this work three documents that were studied on seismic behavior of the region and specifically done on Gilgel Gibe III dam were used.

i. The EEPCO (2007) “seismic hazard assessment report on Gibe III dam project”

ii. The research studied by, Aman Ali,(2020), “Seismic Vulnerability Analysis of Major Ethiopian Dams with Emphasis on Dam Safety Evaluation”

iii. The research was done by Ayele. Atalay, (2016), " Probabilistic seismic hazard analysis (PSHA) for Ethiopia and the neighboring regions"

iv. The Ethiopian Building Standards (ES) (2013), the Ethiopian building code for seismic regions

1.(EEPCO, 2007) design report:- According to the report, the distribution of the current tectonic movements across time and space can be seen in the seismicity analysis that was done within a 100 to 150 km radius area centered on the study location with rock shear velocity $V_s = 700m/s$. The report was summarized as follows:

Table 3. 3 table showing PGA developed by EEP report

Design Earthquake	Average Return Period (T_R)	Probability of Exceedance (P_E)	Service life (T_L)	Damping	Method of estimation	Estimated magnitude of PGA
MCE	N/A	N/A	N/A	5%	DSHA	0.15g
MDE	950yrs	10%	100yrs	5%	DSHA	0.11g
OBE	145yrs	50%	100yrs	5%	DSHA	0.06g

2.Aman A. (2020) - PhD dissertation (AAU) assumption for the development of site-specific peak ground acceleration:- According to the research, data was collected from instrumentally measured six historical earthquakes magnitude above 6 Ms with a distance of 150 km around the dam, Vs = 760 m/s based on USACE manual and ICOLD recommendations. It was summarized as seen below:

Table 3. 4 table showing PGA developed by Aman A.(2020)

Design Earthquake	Return Period (T_R)	Probability of Exceedance (P_E)	Service life (T_L)	Damping	Method of estimation	PGA
SEE	10000yrs	1%		5%	PSHA	0.34g
	4975	1%	50	5%	PSHA	0.26g
	4950	2%	100	5%	PSHA	0.26g
	2475	2%	50	5%	PSHA	0.18g
DBE	475	10%	50	5%	PSHA	0.12g

The study developed uniform hazard spectra for different return periods

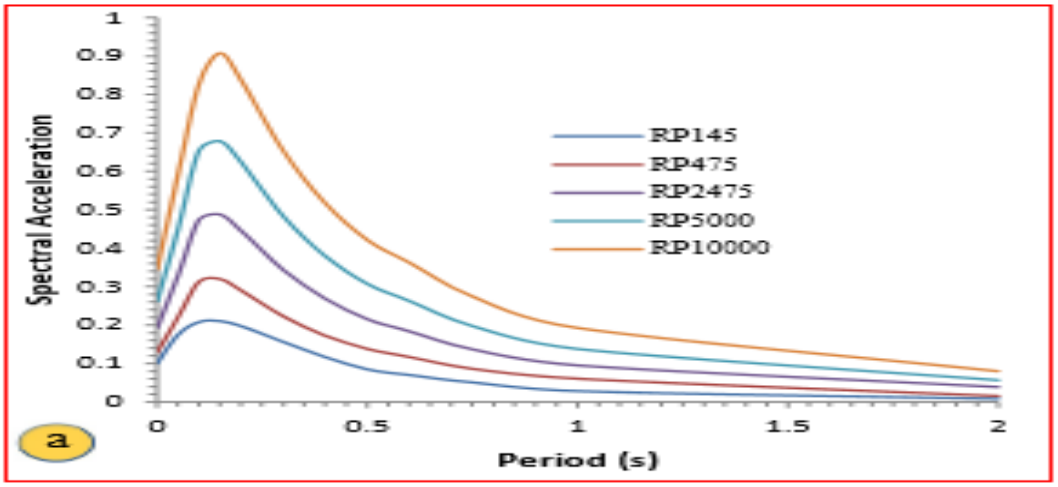

Adapted from Aman Ali's (2020) PhD dissertation

Figure 3. 5 figure showing uniform spectra for Gibe III dam area

1. **Ayele A. (2016):-** In his research region sources were zoned using the seism tectonic map of the study region that was available from recent studies. The study region was divided into small grids of 0.5°X 0.5° to calculate the seismic hazard parameters, which were then calculated at the Centre of each grid cell by taking contributions from all seismic sources. Using a generic rock site with Vs = 760 m/s, the peak ground acceleration (PGA) corresponding to 10% and 2% likelihood of exceeding 50 years was estimated for each grid point.

Table 3. 5 table showing PGA developed by Ayele a.(2016)

Design Earthquake	**Average Return Period (T_R)**	**Probability of Exceedance (P_E)**	**Service life (T_L)**	**Damping**	**Method of estimation**	**Estimated magnitude of Horiz.PGA**
OBE	475	10%	50	5%	PSHA	0.10g
MDE	2475	2%	50	5%	PSHA	0.18g

Finally, the researcher developed a seismic hazard map for the above two exposure times and the contour shown below shows the different levels of PGA which enables any user to identify the seismic exposure of a specific site throughout Ethiopia and the Horn of Africa.

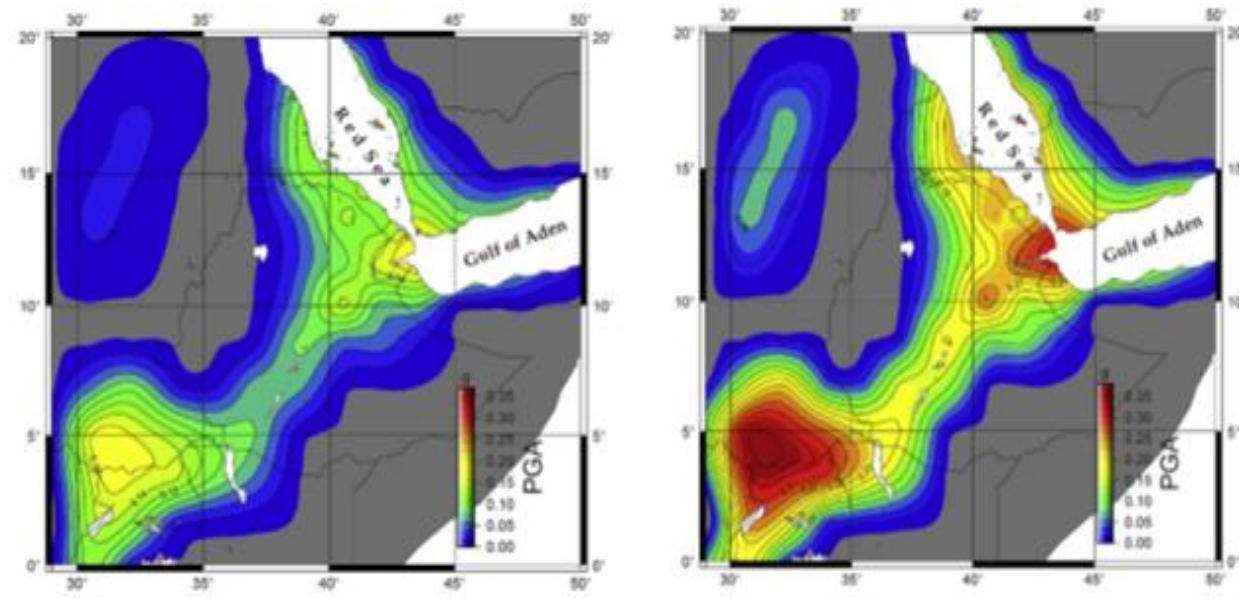

seismic hazard map for 10% probability of exceedance seismic hazard map for 2% probability of exceedance

Figure 3. 6 figure showing seismic hazard map of Gibe III water shade

4. **The Ethiopian building standards (ES)**

Accordingly, the standard describes seismic zones of the country, depending on the local hazard analysis manual (ES 8). The hazard is described in terms of a single parameter, the effective peak ground acceleration, a_g, in the rock of firm soil, called "design ground acceleration". But data recommended for the study was summarized below.

Table 3. 6 table showing PGA developed as per ES-8

Fundamental requirements	**Average Return Period**	**Probability of Exceedance**	**Exposure Period**	**Damping**	**Method of estimation**	**Estimated Magnitude of PGA**	**Remark**
Non-collapse requirements	T_{NCR}= 475yrs	P_{NCR}= 10%	T_L= 50yrs	5%	PSHA	0.10g	Ground type: A (rock) Seismic zone: 3

Finally, the peak ground acceleration for the Gibe III dam site area was determined based on the method of data used by each report to satisfy the seismicity of the area and its relations with the historic earthquake records in the region. Accordingly: The site-specific peak ground acceleration (PGA) for operation basis earthquake (OBE) was determined to be 0.10g which was

recommended by all three studies except study recommended by EEP. But in the case of safety evaluation earthquake (SEE), the study done by **Aman A. (2020)** was used due to the criteria set at the beginning of this paragraph and was determined to be 0.34g. He had also developed uniform site-specific spectra and that was completely adopted as a base for the development of site-specific hazard spectra.

Table 3. 7 table showing PGA developed for the analysis of this study

Design Earthquake	Average Return Period (T_R)	Probability of Exceedance (P_E)	Service life (T_L)	Damping ratio	Method of analysis	Estimated magnitude of PGA	Ground condition
SEE	10000yrs	-	-	5%	PSHA	0.34g	Average rock site Vs30 = 760 m/s
OBE	145yrs	50%	100	5%	PSHA	0.10g	

i). Development of site-specific hazard spectra

At the beginning of this sub-topic PGA was developed by Aman Ali. (2020) was adopted. As a result, The site-specific spectra (target spectra) for the dam site were determined as given below which were used for the generation of ground motion time history data from the Pacific Earthquake Engineering Research Centre (PEER). Here are the steps to perform site-specific spectra in ES -8 for a damping ratio of 5%

1. Determine the damping correction factor $\eta = \sqrt{\frac{10}{\xi+5}} = 1$

2. Get the basic natural periods of vibration of the dam

   Empty case $T = 0.7\ sec$

   Full reservoir case $T = 1.1\ sec$

4. Determine $s, T_b, T_c, and\ T_0$ using ground-type description

Parameters to describe the horizontal elastic response spectrum

Ground Type	S	T_B	T_C	T_D
A	1	0.05	0.25	1.2

4. After this determination set your time interval and use the formula

$$0 \le T \le T_B:\ S_e(T) = a_g \cdot S \cdot \left[1 + \frac{T}{T_B} \cdot (\eta \cdot 2.5 - 1)\right]$$

$$T_B \le T \le T_C:\ S_e(T) = a_g \cdot S \cdot \eta \cdot 2.5$$

$$T_C \le T \le T_D:\ S_e(T) = a_g \cdot S \cdot \eta \cdot 2.5 \left[\frac{T_C}{T}\right]$$

$$T_D \le T \le 4s:\ S_e(T) = a_g \cdot S \cdot \eta \cdot 2.5 \left[\frac{T_C T_D}{T^2}\right]$$

Then you should have a jagged shape picture after you are drawing it as given below.

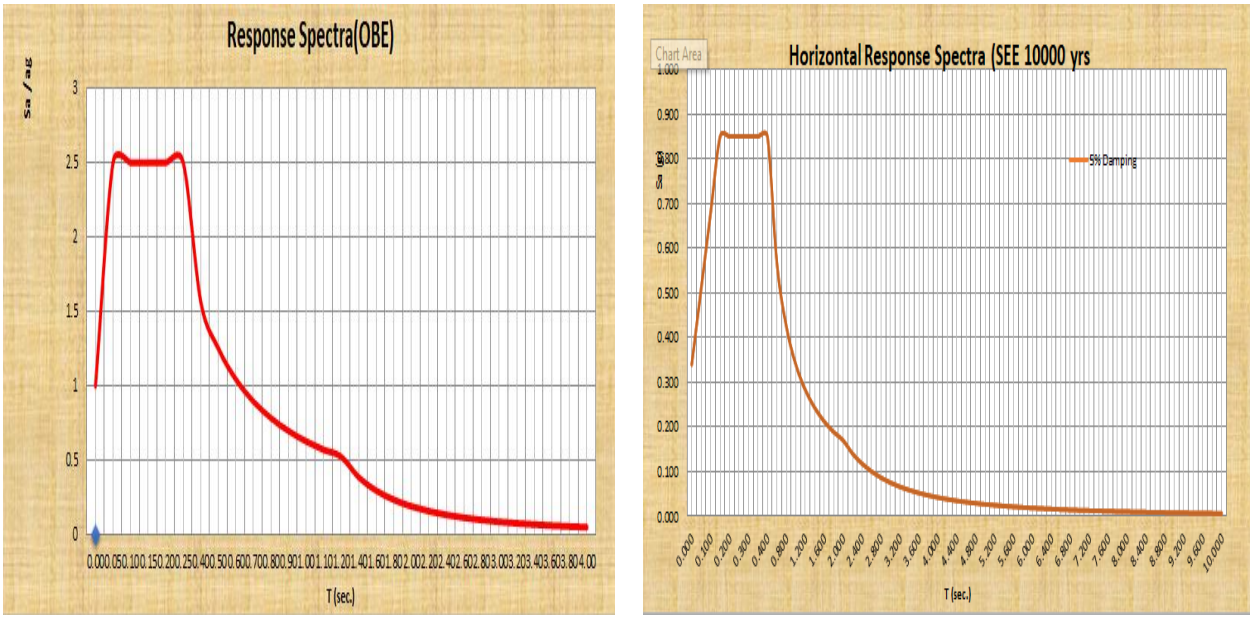

Figure 3. 7 figure showing site specific spectra of Gilgel Gibe III dam

ii). Generating representative ground acceleration time histories

The following broad assumptions, per the USACE (1995) guideline and the ES-8-based criteria covered below, served as the basis for the selection of acceleration time histories in the current study. the resemblance between geology and tectonic environments; resemblance in the subsurface circumstances or local locale; compatibility with the design response spectrum or UHS, especially in the fundamental period range of interest; matching the magnitude and epicenter distance of the design earthquake; and Similar length of time for intense shaking Based on these site-specific hazard spectra on the site the acceleration time history data was generated from PEER (Pacific Earth Quake Engineering Research Center). As per the specific criteria set for the PEER data generation requirement below it was decided to generate scaled acceleration time histories for 20 destinations while the matched three earthquake destinations were selected for this study purpose which is listed in table 3.9 and table 3.10. Below.

Table 3. 8 table showing PEER ground motion database search criteria

PEER Ground Motion Database West2 -- 2023-04-27 Summary of PEER Ground Motion Database Search Criteria					
Magnitude Min:	4.5				
Magnitude Max:	8				
Rrup Min (km):	10				
Rrup Max (km):	200				
Rjb Min (km):	10				
Rjb Max (km):	200				
Vs30 Min (m/sec):	700				
Vs30 Max (m/sec):	1000				
D9-95 Min (sec):	-0.000001				
D9-95 Max (sec):	99999				
Scale Factor Min:	0.25				
Scale Factor Max:	4				
Period Array:	0.05	0.15	0.4	4	10
Weight Array:	1	1	1	1	1
Record Sequence Number:					
Earthquake Name:					
Station Name:					
User-Defined Maximum Number of Records:	20				
Pulse:	3				
Damping Ratio:	0.05				
Scaling Method:	Minimize MSE				
Suite Average:	Arithmetic				
Single-Period-Scaling Period (sec):					
Component:	SRSS				
Fault Type:	SS+Normal				

Table 3. 9 table showing selected earth quake destinations for OBE case

Quake name	**Record serial number**	**station**	**Year**	**magnitude**	**Epic. Distance(km)**	**Fault type**
Morgan Hill	RSN-476	UCSC	1984	6.19	45.2	strike-slip
Chichi Taiwan	RSN-2753	CHY102	1999	6.2	90	strike-slip
Totori Japan	RSN-3925	OKYH07	2000	6.61	15	Strike slip

Table 3. 10 table showing selected earth quake destinations for SEE case

Quake name	Record serial number	station	Year	magnitude	Epic. Distance(km)	Fault type
Hector mine	RSN-1787	Hector mine	1999	7.13	10.3	Strike-slip
Totori Japan	RSN-3932	OKYH14	2000	6.61	21	Strike slip
14151344	RSN-9071	Pinon flats	2005	5.12	13	Strike-slip

All these six time history data were un-scaled and we should have to match each data with the site-specific response hazard spectral acceleration. When acceleration time histories are required for the structure dynamic analysis, they should be developed to be consistent with the design site-specific response spectrum (USACE, EM:110-2-6050; Em-1110-2- 6053). The general approach used to develop acceleration time histories was selecting a suite of recorded motions that, best fits the design spectrum; or synthetically modifying one or more recorded motions to produce motions having spectra that are a close match to the design spectrum ("spectrum matching" approach). For this step data must be scaled and matched with respect to the site response spectral PGA using the Software" SeismoMatch2022".

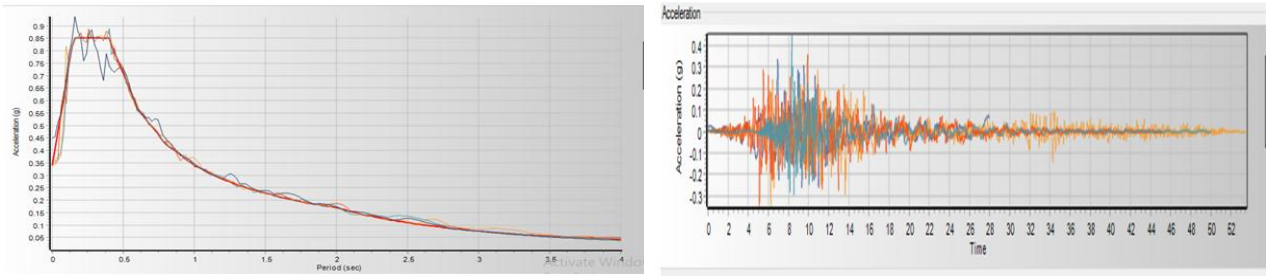

Figure 3. 8 figure showing spectral matching

finally, the scaled-matched time history data was set to use for the analysis.

Table 3. 11 table showing acceleration time history used in seismic loading on Gilgel Gibe III dam

	Quake name	R.serial Number	station	Year	magnitude	Epic.Distance (km)	Fault type
OBE	Morgan Hill	RSN-476	UCSC	1984	6.19	45.2	strike-slip

SEE	Hector mine	RSN-1787	Hector mine	1999	7.13	10.3	Strike-slip

3.3.2. RCC Data and Dam Zoning

The RCC data was collected based on the properties of the selected materials which were prepared on each zone of the dam. 5 types of concrete mix design were briefly described in the corresponding sections (EEP, 2009). The different mixes have been identified according to their strength (f'c), as shown in the table below.

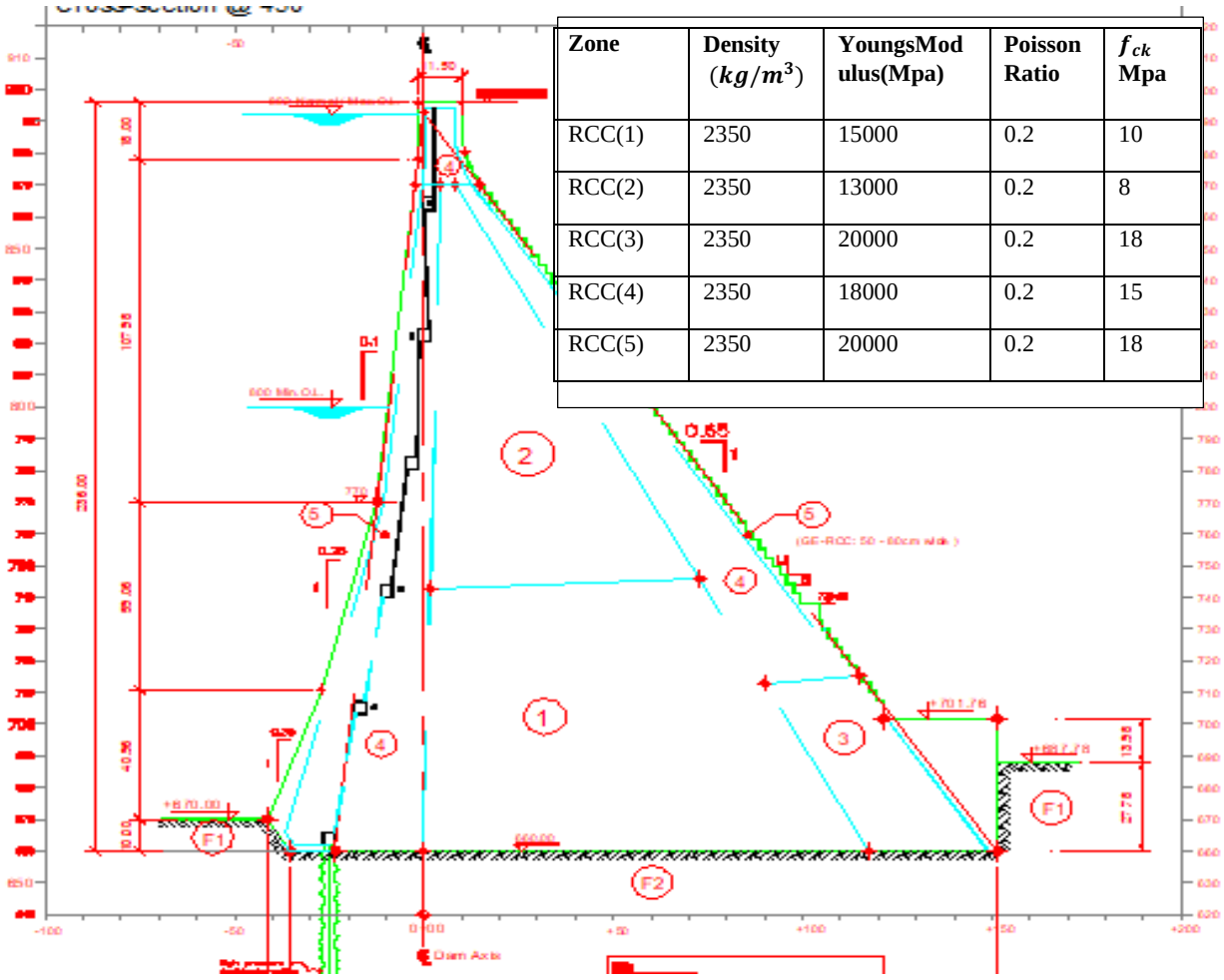

Zone	Density (kg/m^3)	YoungsModulus(Mpa)	Poisson Ratio	f_{ck} Mpa
RCC(1)	2350	15000	0.2	10
RCC(2)	2350	13000	0.2	8
RCC(3)	2350	20000	0.2	18
RCC(4)	2350	18000	0.2	15
RCC(5)	2350	20000	0.2	18

Figure 3. 9 figure showing dam zones with the corresponding mix design of RCC on Gilgel Gibe III dam

(i). Dynamic isotropic Properties:- according to Bruhwiler, 1990; quoted by USACE: EM 110-2-6050,51, the dynamic properties of concrete material are determined.

Table 3. 12 table showing dynamic material property of RCC mix

Zone	Density(kg/m^3)	Youngs Modulus(Mpa)	Poisson Ratio	$f_{ck}(MPa)$
RCC(1)	2350	17250	0.14	11.5
RCC(2)	2350	14950	0.14	9.25
RCC(3)	2350	23000	0.14	20.7
RCC(4)	2350	20700	0.14	17.25
RCC(5)	2350	23000	0.14	20.7

(ii). Strength of RCC(joint) materials:

The strength and elastic characteristics of RCC depend on the mix's constituents and amounts. The primary determinants of strength and elastic qualities are aggregate quality and cementation content, but these attributes may be as dependent on field management of mixing and putting processes as on mixture ingredients or mixture proportions. Compressive strength, tensile strength, shear strength, elastic modulus, Poisson's ratio, and density are characteristics that are significant to the seismic study of RCC dams. The strain rates that occur during significant earthquakes are on the order of 1,000 times greater than those utilized in routine laboratory testing, and all of these properties aside from density are strain-rate sensitive. (EM 1110-2-2006) The estimate of flexural tensile strength the modulus of rupture or the cracking strength of concrete from cube compressive strength is obtained by the relations fcr = 0.7 fck N/mm^2. The tensile strength of concrete in direct tension is obtained experimentally by split cylinder test. It varies from 1/8 to 1/12 of cube compressive strength.

Table 3. 13 table showing strength of joint materials

Static properties			Shear parameters		Dynamic Properties	
Zone	Compressive Strength(Mpa)	Tensile Strength static, Mpa	Cohesion (c')(Mpa)	∅ in degree	Compressive Strength(Mpa)	Tensile Strength (Mpa)
RCC(1)	10	0.6	0.6	45	11.5	0.9
RCC(2)	8	0.48	0.4	45	9.25	0.72
RCC(3)	18	1.2	1	45	20.7	1.8
RCC(4)	15	1	0.8	45	17.25	1.5
RCC(5)	18	1.2	1	45	20.7	1.8

(iii). Rock Mass Strength

The RCC gravity dam had the foundations mainly in trachytic rocks un-weathered or slightly weathered. The structure of the rock mass is generally favorable for the foundations since no weak planes sub-horizontal, or sub-parallel to the dam excavations, were found. The most relevant lithological types found along the dam foundations were classified by the following rock mass units:

U-T –Un-weathered trachyte, SW-T -Slightly Weathered Trachyte

The following typical zones can be considered for the general stability analysis along the dam foundations

Table 3. 14 table showing foundation rock mass isotropy property

Zone	Density(kg/m^3)	Deformation Modulus(Mpa)	Poisson Ratio
F(1)-SW-T	2400	25000	0.15
F(2) U-T	2400	30000	0.15

According to USACE (2003) – EM-1110-2-6051, the static and dynamic properties of rock mass are used the same. And for the Silt soil:-Saturated unit weight = 17 KN/m^3, $\emptyset = 25^0$ was taken.

3.3.3. Loads

The effects on the dam structure due to loads, as discussed below, are determined by conventional static and dynamic analysis methods. The results of the dynamic and static analyses are combined by superposition to determine the total stresses for the earthquake load case. According to the USBR (2006), the following are typical recommendations for incompressible water: Modulus of elasticity(E) = 1.31MPa**,** Density (ρ) = 981 Kg/m3**,** Poisson's ratio(ν) = 0.4999**,** Bulk modulus: K=Ew / [3 (1 – 2 n)] = 21,800 MPa**,** Speed of sound in water =1438m/s.

A. Static Loads:

Hydrostatic loads. Load cases were included to cover reservoir pool elevations to have a reasonable chance of occurrence at the time of the design earthquake. The Normal Operating Condition level for the reservoir is at 892 m a.s.l while the base of the dam is at 670 m a.s.l where measurements during loading is taken and Tail water pressures on the downstream face of the non-overflow (gravity) section have been determined considering the minimum tail water depth. The minimum level for tail water is at 677 m a.s.l

- **Horizontal loads:**

$P_R = \frac{1}{2} * \gamma_w * H^2$ at $z = \frac{H}{3}$ and $P_t = \frac{1}{2} * \gamma_w * h^2$ at $z = \frac{h}{3}$..... (3.2)

Table 3. 15 table showing horizontal hydrostatic loading

	Loading Description	Loading reference
1.	Original ground level (OGL)	670 m a.s.l
2.	Maximum water level	892 m a.s.l
3.	Minimum tail water level	677 m a.s.l
4.	Unit weight of reservoir water	10 KN/M

- distributed load $(p) = \gamma_w H$

- **Vertical loads**: this is happened at the reservoir (up-stream) side only

This load is determined based on the elevations where dam geometry is changing slope and the first slope change is at 710 m a.s.l, second at 770m a. s. l and the third one is at 870 m a.s.l.

$$p_{rv1} = \gamma_w * area\ of\ rectangle$$
$$p_{v2} = \gamma_w * area\ of\ trapezium$$
$$P_{v3} = \gamma_w * area\ of\ trapezium$$
$$P_{v4} = \gamma_w * area\ of\ triangl$$

Table 3. 16 table showing vertical hydrostatic loading

	Loading Description	Loading reference
1.	Original ground level (OGL)	670 m a.s.l
2.	Maximum water level	892 m a.s.l
3.	Minimum tail water level	677 m a.s.l
4.	First slope change from OGL	710 m a.s.l
5.	Second slope change from OGL	770 m a.s.l
6.	Third slope change from OGL	870 m a.s.l
7.	Unit weight of reservoir water	10 KN/M

- **Siltation load.** During the life of the dam, silt may build up against the upstream face to a depth of 689 m a.s.l which may cause a moderate increase in the tensile stresses in load cases where tension in the upstream face is critical. The silting loads have been considered assuming Mohr Coulomb's behavior.

$$P_{Silt} = \frac{1}{2} * K_a * \gamma_{sub} * h^2 \quad \text{where, } k_a = 1 - sin\emptyset, \emptyset = 25^0 \ldots\ldots\ldots\ldots (3.3)$$

- **Gravity loads**. Gravity loads shall include the weight of the RCC, the weight of backfill or silt on faces of the dam, and the weight of equipment if significant.
- **The uplift pressure**: The uplift pressure trend adopted should be considered a reasonable conservative assumption since the downstream drainage curtain and grouting screen allow foreseeing a generally lower uplift pressure at the dam-rock contact and within the foundations. Uplift pressures have been considered to vary from the hydrostatic pressure relative to :

  a. at u/s toe H_1 =the reservoir water level at 892 m a.s.l
  b. at d/s toe H_2 = full tail water level at 677 m a.s.l
  c. at drainages $H_3 = K\,(H_1 - H_2) * \frac{L-X}{L} + H_2$

  Where $k = 0.25 - 0.5$ (USACE) and gallery height is less than tail water height.

Then $P_U = \frac{1}{2}\gamma_w[H_1(LK + X) + H_2(L(2 - K) - X]$..... (3.4)

Uplift pressure distribution

H3 = K (H1-H2)*(L-X)/L +

H2= 84m

H1= 222m

H2= 7m

L= 193m

X= 20m

K= 0.25 - 0.50 ---= 0.4

Xi (m)	Formula	p_x (KN/m2)
0	$\gamma w * H_1$	2177.82
10		1501.36
20	$\gamma w * H_3$	824.90

B. **Dynamic loads:**

Both the dam structure and the water contained in the reservoir vibrate as a result of the earthquake forces. The force generated by the dam is known as the Inertia Force, and the force generated by the water body is known as the Hydrodynamic Force. Because earthquake forces are generated by the vibration of the ground itself, which can shake horizontally in both directions as well as vertically. For design purposes, one must examine the worst-case scenario, and hence the combination that appears to be the least advantageous to the dam's stability must be evaluated.

(i). Hydrodynamic loads: Hydrodynamic forces are imposed on the dam due to the motions of the dam reacting with the surrounding water, and motions of the reservoir bottom. Horizontal acceleration acting towards the reservoir causes a momentary increase in the water pressure, as the foundation and dam accelerate towards the reservoir and the water resists the movement owing to its inertia. The extra pressure exerted by this process is known as hydrodynamic pressure this load was determined according to Westergaard's generalized added mass approach.

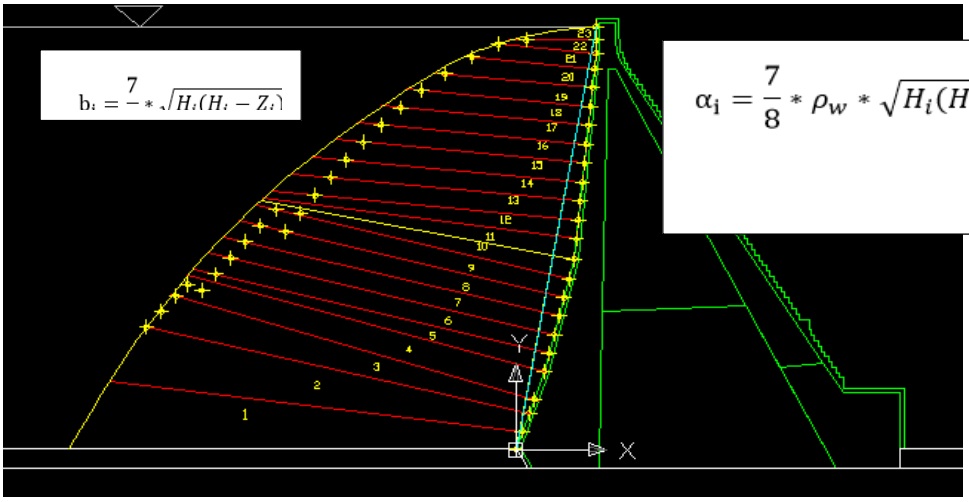

Table 3. 17 showing westergaard's added mass calculation

Node, ni	Point masses		Zi	H_i=H-Zi	bi	αi	Node	Ai	mi = Ai*ρw (kg)
	X-Coordinate	Y-Coordinate							
1	0.0000	0.0000	0.0000	222.0000	194.2500	194250.000	1	6098.931	6098931.40
2	6.6500	19.0000	19.0000	203.0000	185.7516	185751.598	2	4811.132	4811132.10
3	14.3201	40.9146	40.9146	181.0854	175.4390	175439.047	3	3984.034	3984034.00
4	18.1716	56.3206	56.3206	165.6794	167.8104	167810.371	4	3160.325	3160325.10
5	21.8096	70.8727	70.8727	151.1273	160.2714	160271.389	5	2655.154	2655154.30
6	25.4477	85.4249	85.4249	136.5751	152.3598	152359.768	6	2467.153	2467152.70
7	29.0857	99.9770	99.9770	122.0230	144.0142	144014.224	7	2427.501	2427500.60
8	30.9284	118.4037	118.4037	103.5963	132.6956	132695.643	8	2118.732	2118732.10
9	32.4209	133.3292	133.3292	88.6708	122.7651	122765.081	9	1746.507	1746507.10
10	33.9135	148.2548	148.2548	73.7452	111.9570	111957.043	10	1525.485	1525484.90
11	35.4060	163.1803	163.1803	58.8197	99.9876	99987.554	11	1473.601	1473600.70
12	36.8986	178.1059	178.1059	43.8941	86.3749	86374.911	12	1252.982	1252981.50
13	38.3911	193.0314	193.0314	28.9686	70.1695	70169.486	13	1113.447	1113447.20
14	39.8837	207.9570	207.9570	14.0430	48.8556	48855.615	14	598.643	598642.70
15	39.8837	222.0000	222.0000	0.0000	0.0000	0.000	15	100.000	100000.00

(ii). Inertia due to ground motion:

The inertia forces acting on the structure's various levels are proportional to the masses and overall accelerations of the sub-structures and are calculated using Newton's Laws. These accelerations are the second derivatives of the displacements to time, and they vary far more to time than the structure's displacements.

(Iii). Wind Load: as per USBR, (1981)the wind load's impact is actually seen in two different forms. It can be applied as a direct load exerted on the exposed surface of the dam but it is not that much usable in this dam since the face of dam is covered with water so that there isn't a significant height of dam exposed on this direct wind load or it can also be applied according to the wave developed through the reservoir which is determined based on wind speed, height of the wave and straight fetch length of the reservoir. This is highly recommended for the design of free board specially in embankment dams and it is also applied in concrete gravity dams The simpler method is prescribed as that given by the Stevenson formula.

$h_w = 0.032\sqrt{VF} + 0.763 + 0.271(F)3/4$ for $F < 20$ km ……..(3.5)

$h_w = 0.032\sqrt{VF}$ for $F > 20$ km ……(3.6)

where; h_w – height of the wave in meters, V – wind velocity in km/h, F – straight length wave expands in km. The maximum pressure Pw can be calculated as follows

$Pw = 2.4\gamma_w h_w$ acts above $h_w/2$ above the maximum water level.Further, the pressure distribution is considered as triangular and having the height $5h_w/3$. Hence, total force(F_w) due to wave action can be calculated as:

$F_w = 0.5\ (2.4\gamma_w h_w).5h_w/3 = 20h_w^{2}$.Force will be acting $\frac{3hw}{8}$ above the reservoir water level according to EEPCO,2009 impact assessment report the straight fetch length of reservoir is about 12km. The average wind speed of the site is 35m/s according to GetinetM.et.al. 2021, in Ethiopia. Hw= 3.15m and and pressure (p)= 2.4*1000*3.15 =7560 pa= 0.00756 Mpa is very low as compared to other loads. Therefore it is impact is insignificant and it is not taken as part of decisive loads.

3.3.4.Load Combination:

Among the seven load combinations stated by USACE (2007): EM 1110-2-6053; USBR(2016), on unit two of this study the load combination forms were used for this study purpose and loads were organized based on the above loading conditions, input methods were also applied

according to the requirement of modeling the dam. The extreme type of loads are used for the study since , it was decided to visualize the dynamic loading conditions.

Table 3. 18 table showing load combination used for this study

	Static		Dynamic		
load	Combination 1 (empty reserve.)	Combination 2 (MWL)	Combination 1 (Empty+ OBE)	Combination 2 (MWL+OBE)	Combination 3 (MWL+SEE)
Dam weight	√	√	√	√	√
Horizontal hydrostatic		√		√	√
Vertical hydrostatic		√		√	√
Tail water hydrostatic		√		√	√
Silt horizontal		√		√	√
Silt vertical		√		√	√
Uplift		√		√	√
Hydrodynamic load				√	√

3.4. Data Analysis Methods

With a defined methodology, finite elements have been frequently used in the analysis of concrete gravity dams. The dynamic time history analysis and modal analysis of a concrete gravity dam using ANSYS Workbench version 2016 and 2023/R2 student version software are the main topics of this study. Gilgel Gibe III is a 243-meterhigh concrete gravity dam. An ANSYS model of the dam was created to conduct modal and time history analyses. During the modeling and analysis, the dam was considered in 2 different cases:

1) Dam with empty reservoir and flexible foundation.
2) Dam with full reservoir and flexible foundation.

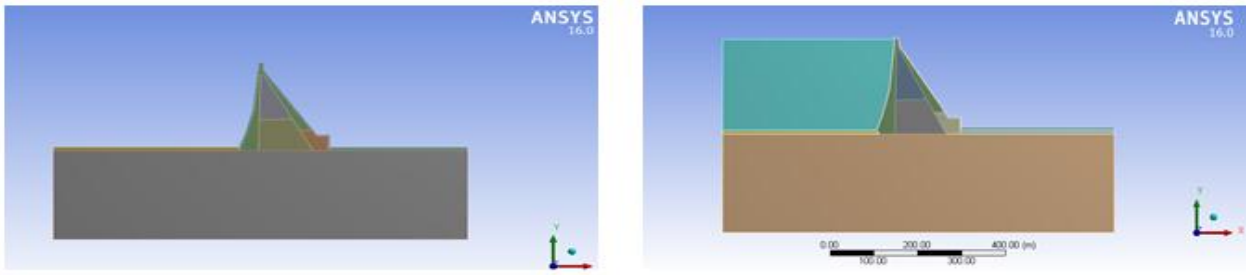

a. Empty reservoir model b. Full reservoir model

Figure 3. 10 figure showing dam models used to the study

3.4.1. Capabilities of ANSYS for Dynamic Analysis

The finite element approach is currently applicable to a wide range of engineering disciplines where the physical description leads to a mathematical formulation with some characteristic differential equations that can be solved numerically. Originally, the method was created to handle problems in structural mechanics. Over the years, there have been several advancements in numerical modeling that have allowed engineers to run simulations that are today fairly accurate. Large deformations, problems, and nonlinear material behavior are examples of nonlinear phenomena that are increasingly included in structural mechanics modeling projects. (ANSYS INC. 2016). It is not unexpected that the FEM's popularity has spurred the creation of various finite element programs, both research- and commercial-focused, given that it is a numerical/computational analytical tool. Commercial software that is backed by appropriate graphical user interfaces (GUI) to facilitate use is frequently advertised by private companies. NASA's effort to create a computer code for assessing aeronautical structures led to NASTRAN, the first commercial program. The initial effort was led by the MacNeal - Schwendler Corporation (MSC) in the late 1960s. Another well-known program that included nonlinear analysis early on was ANSYS. E. Wilson's endeavors at UC Berkeley significantly accelerated the development of software and gave rise to two different types of programs.

The first type was created using SAP code and ultimately led to certain software solutions that Berkeley, California-based Computers and Structures, Inc. sold. SAP 2000, ETABS, and Perform3D are the primary applications in this family that are utilized by the civil structural engineering sector and place a strong emphasis on seismic design. Subsequently, two well-known industrial commercial applications are LS-DYNA (originally developed by John Hallquist at Livermore National Laboratories and currently distributed by Livermore Software

and Technology Corporation (LSTC)) and ABAQUS (originally invented by David Hibbitt and currently marketed by Simulia). These two applications are quite flexible and can do structural and nonlinear solid analysis. Academics find them particularly interesting since they allow the introduction of user-defined code simultaneously. (Ioannis Koutromanos, et.al, 2018)

Table 3. 19 table showing software package and their difference

Software package	Methods used	Application problem
ABAQUS	FEM(implicit, explicit)	Structural analysis, acoustics, thermal analysis etc
LS-DYNA	FEM(explicit)	Structural dynamics, computational fluid dynamics, fluid-structure interaction
NASTRAN	FEM(implicit)	Structural analysis, acoustics, thermal analysis
MARC	FEM(implicit)	Structural analysis, acoustics, thermal analysis
MSC-DYTRAN	FEM+VM	Structural dynamics, computational fluid dynamics, fluid structural interaction
ANSYS	FEM(implicit, explicit)	Structural analysis, acoustics, thermal analysis, multi-physics
ADINA DIANA	FEM(implicit)	Structural dynamics computational fluid dynamics fluid-structure interaction

Problems of Structural Dynamics:-

Numerical Methods in ANSYS Here we give a general overview of typical problems in structural dynamics. Based on D'Alemberts principle and due to the discretization process of a continuous structure with finite elements the following equation of motion can be derived:

$$M\ddot{U} + C\dot{U} + KU = F(t) \quad \text{.....(3.7)}$$

M, C, K: System mass, damping and stiffness matrix respectively. The vectors of nodal accelerations, velocities and displacements are U and $\ddot{U}$ $\dot{U}$ & f(t)is the vector of applied forces. Dynamical equilibrium is obtained if the equation holds for all times « t ». All problems in structural dynamics can be formulated based on the above equation of motion. A coarse classification is obtained by taking different representations for the time-varying applied forces. This classification presents a diagram where several analysis types of structural dynamics are listed according to the representation of the applied load. Furthermore, a structural analysis that accounts for damping has to be distinguished from an analysis where damping is neglected. Finally, since not every engineering application results in the formulation of symmetric system

matrices, we should further distinguish between analyses with symmetric and un-symmetric matrices. In the following sections, we briefly describe the different analysis types.

3.4.2. Modal Analysis

When designing a structure, the vibration characteristics are ascertained by the use of a modal analysis. Identification of the natural frequencies and mode shapes is therefore the aim of a modal study. f(t) = 0, or the right-hand side of the equation of motion, is regarded as zero. Another more in-depth dynamic study that can be started with a modal analysis is a transient dynamic analysis, harmonic analysis, or even a spectrum analysis based on the modal superposition technique. A linear modal analysis is performed. Any nonlinearity the user may have provided is not taken into account. However, one could take into account pre-stress effects.

(i). Solution Algorithms for a Modal Analysis

Calculating natural frequencies and mode shapes is mathematically analogous to solving an eigenvalue issue. The amount of numerical work required to solve the eigenvalue problem will vary depending on whether the damping is present and the shape of the system matrices that are produced. But ANSYS offers a wide variety of eigenvalue solvers. Numerous of them are made for specific application goals, thus it's critical to understand which eigenvalue solver best matches the problem's specific physics.

Damping effects are frequently disregarded and symmetric system matrices are used in engineering applications. ANSYS offers the following Eigen solvers for those problems:

- Block Lanczos Method,
- Subspace Method,
- Reduced Method,
- Power dynamics Method

The Block Lanczos: In this study the Block Lanczos method is applied since it is the default algorithm and the structure (Gilgel Gibe III dam is very big) with some program controlled adjustments due the lumped mass added on the nodes of the structure. For big models, the Method is a very effective modal analysis algorithm. It is a quick and reliable method that serves as the default solver in the majority of applications. The Lanczos algorithm block version is designed to reduce I/O effort. Spectral transformations are used to divide the lengthy Lanczos

procedure into several shorter ones. It significantly reduces computation time when a big number of eigen pairs (100 - 1000 or more) are required. The following is the original natural vibration problem:

$K\phi - \lambda M\phi = 0$ …… (3.8)

where K is a positive definite symmetrical stiffness matrix and M is a positive definite or semi-definite lumped or consistent mass matrix.

The physical product of the modal damping coefficient and the un-damped natural frequency is represented by the real component. Those kinds of applications The Damped Method Eigen solver is offered by ANSYS. This approach takes into account the damping matrix when formulating the eigenvalue problem under consideration. For determining an appropriate number of modes to extract, the mode participation factor and effective mass are essential. The mass travelling in a certain direction for each mode is indicated by the mode participation factor. A higher value means that, given the force or excitation delivered in that direction, the mode may be excited. The following equation is used to compute the participation factor:

$\gamma_i = (\emptyset)_i^T [M][D]$, …….. (3.9)

And Effective mass is calculated by the following equation: $M_{effi} = \gamma_i^2$

Where, $\{\varphi\}_i^T$ is the transpose of mode shape or eigenvalue matrix, [M] is the mass matrix, and {D} is the excitation direction matrix which represents the direction, the participation factor is calculated The effective mass and participation factors both suggest the significance of a particular mode..

3.4.3. Transient (time history)Dynamic Analysis

A transient dynamic analysis is a method for figuring out how quickly a structure reacts to arbitrary pressures that change over time. Any load vector function may be supplied on the right side of equation 3.7 With this kind of study, you may find out how a structure responds to various combinations of transient or harmonic loads in terms of displacement, strain, stress, and force over time. A temporal integration must be done to solve the motion equation 3.7. Broadly speaking, they can be divided into implicit and explicit ways. When comparing the stability of these two different integration techniques, implicit techniques are typically unconditionally

stable. Conversely, explicit approaches are only stable if the time step size is less than a crucial one, which often relies on the structure's maximum natural frequency. For short-duration transient problems in structural dynamics, explicit methods are frequently utilized due to the tiny time step required for stability considerations.

a. Implicit Time Integration: The Newmark method is the implicit time integration algorithm used by ANSYS. Two default settings for the method's stability parameters ensure that the scheme is unconditionally stable and that the impact of numerical damping is kept to a minimum. A linear system of equations is produced for each time step when the Newmark method is applied to the equation of motion 3.7. Since the stiffness matrix is on the left, each time step in the incremental solution method requires that it be inverted.

Newmark-β Method. The Newmark method is a general step-by-step process with the integration equations for displacement and velocity at time step t+Δt

$$u_{t+\Delta t} = u_t + \Delta t \dot{u}_t + \Delta t^2 (\left(\frac{1}{2} - \beta\right) \ddot{u}_t + \beta \ddot{u}_{t+\Delta t} \quad \ldots\ldots\ldots\ldots\ldots\ldots (3.10)$$

$$\dot{u}_{t+\Delta t} = \dot{u}_t + \Delta t((1-\gamma)\ddot{u}_t + \gamma \ddot{u}_{t+\Delta t} \quad \ldots\ldots\ldots\ldots\ldots\ldots\ldots\ldots (3.11)$$

where β and γ are weighting factors and can be chosen to obtain optimum stability and accuracy

The implicit solution technique in ANSYS is always a good choice to perform a transient analysis if the problem is not crucially dominated by nonlinearities because its inversion is computationally expensive, especially for highly nonlinear problems.

- Full Method
- Modal Superposition Method

In this particular study , Direct integration method in ANSYS is applied in steps through the approximate solution produced at discrete intervals of n time.(0, Δt, 2Δt, 3Δt, …, t, t+Δt, …T, where T is the duration of the input motion or loading and Δt =T/n.). Since original matrices are employed to compute the answer, the Full Method does not diminish the dimension of the problem under consideration. As a result, it is easy to use, allows for the specification of all types of nonlinearities, provides automated time stepping, allows the specification of all types of loads, does not assume that masses are concentrated at the nodes, and compute all results in a single computation. The fundamental drawback of the Full Method is that as the size of the model

under consideration increases, more time must be spent solving the problem. The global damping ratio $\xi = 0.05$ was applied with the following procedures:

3.5. Finite Element (FEM) Modeling

The numerical computations and analysis for this work were done using the ANSYS Mechanical workbench version 2016 and 2023 student version. Finite Element Analysis (FEA) Software for Structural Engineering. One of the most popular simulation programs for engineering simulations is this one. In this work, the stress and deformations in the Gibe III dam with the freshly built wall were precisely analyzed, simulated, and modeled using this program. The PLANE182 element type from the ANSYS element library is used to mesh the finite element models. four nodes with two degrees of freedom each make up the element. Two-dimensional planar strain models were used to simulate the dam. In other words, the condition where the strains perpendicular to the analysis plane are maintained at zero. In this study, the foundation is uniform and homogenous, and all materials are assumed to have linear elastic behavior. Using 2-D plain strain isotropic elements.

3.5.1. 2D Finite Element Geometry: Two models were employed for the 2D finite element representation based on the modeling criteria set in different manuals as stated in unit two of this study which was determined to be the standard modeling method one represents the dam with empty reservoir and foundation while the other represents the dam with full reservoir and foundation. This geometry was modeled by using ANSYS 2016 and ANSYS 2023design modelers, and isotropic material characteristics were involved in the element input data.

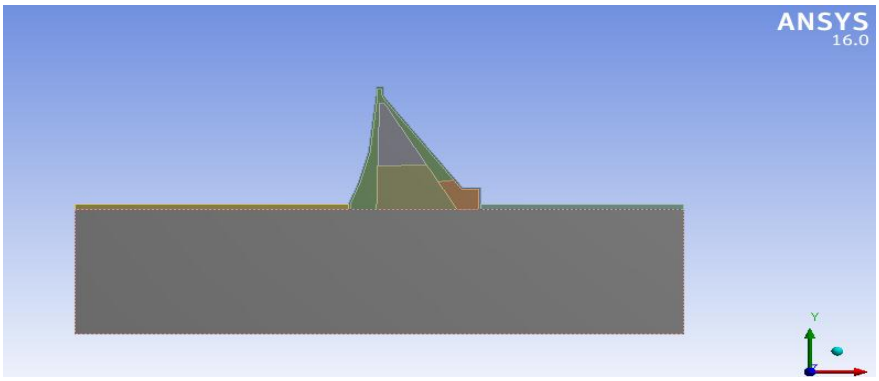

Figure 3. 11 figure showing general 2-D assembly of Gilgel Gibe III dam (non-overflow section)

3.5.2. Finite Element Equivalent Mass System(dam-foundation) Model.

This method models both the dam and the foundation as an assembly of discrete finite elements. Either solid quadrilateral plane stress or plane strain elements are used for 2-D models. The foundation consists of a rectangular block with a width in the upstream-downstream direction (horizontal length) about three times the dam height and depth equal to the dam's height in the vertical direction.(USACE(1995),USBR(2006;2018)).

(i). Reservoir effects.

The reservoir effects are modeled by developing an equivalent mass system which consists of adding mass to the finite element model to correctly alter the dynamic properties. The added mass is active in the direction normal to the vertical upstream face of the dam. This method also allows the reservoir bottom absorption characteristics to be incorporated into the analysis by using Chopra's standard hydrodynamic pressure function curves to determine the added mass. Although the use of these curves in developing the equivalent mass system is only approximate, it is reasonably accurate.

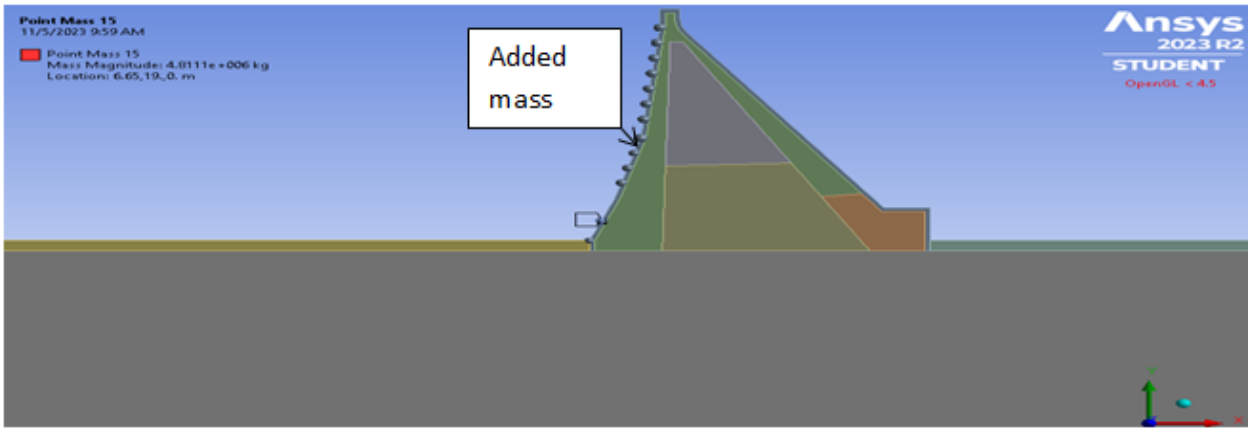

Figure 3. 12 figure showing Westergaard's added mass model

(ii). Boundary conditions.

The stiff boundary is where the earthquake ground motion is introduced in this kind of model. Instead of being stated at the ground surface (dam-foundation interface), where the design earthquake ground motion is given, this boundary runs along the sides and bottom of the rectangular foundation block. The foundation is taken to be massless to account for this. Since there is no wave propagation in the massless foundation, the ground motion is transferred unchanged to the contact between the dam and the foundation. Both rock and concrete were assumed to be elastic and isotropic;

- The boundaries of the rock mesh were specified at a horizontal length of three times the dam height from the upstream and downstream toe and the same depth as the dam height in the vertical direction.
- The restraints imposed on the nodes at the limiting surfaces of the overall FEM model are the following:
  - Nodes at the base of the dam - fixed in all directions;
  - Nodes at the left and right edges of rock - fixed in horizontal (u/s to d/s) direction;
  - All the other nodes – free.

(iii). Flexibility in Modeling.

The composite finite element model may be formulated to represent a variety of design conditions for both 2-D models. For example, almost any geometric shape was accommodated, various zones of superior RCC mix were incorporated in the dam model, and changes in deformation modulus in the foundation were also included.

(iv). Assembly Contacts:

The dam was divided into different RCC zones so that there were contacts between these zones and it was modeled by considering contact conditions needed to describe how different contacting bodies can move relative to one another. Bonded, no-separation, friction, rough and frictionless contact types are available for assembly analysis, as listed along the model extended In most cases, contact regions can be automatically detected and generated in the FEA program. They can also be manually modified if needed. but in this study bonded type of contact was applied in most cases.

(v). Mesh and loading

Mesh:- Meshing is an essential component of the simulation process. In ANSYS, meshing structural models is all about finding a compromise between computational cost and correctness. But eventually, the mesh becomes sufficiently fine-tuned to represent the outcomes accurately. It is necessary to select an appropriate size for each component based on mesh convergence to have accurate results. PLANE182 element type from the ANSYS element library is used to mesh the finite element models. four nodes with two degrees of freedom each make up the element. In this work, mesh convergence was employed to give a precise estimation of the outcomes. By reducing the mesh size until a convergent deformation and primary stress value are obtained, the model has been solved.in this study quadrilateral and triangular mesh elements with different mesh size, finer 5m mesh size to coarser 12m mesh size were applied.

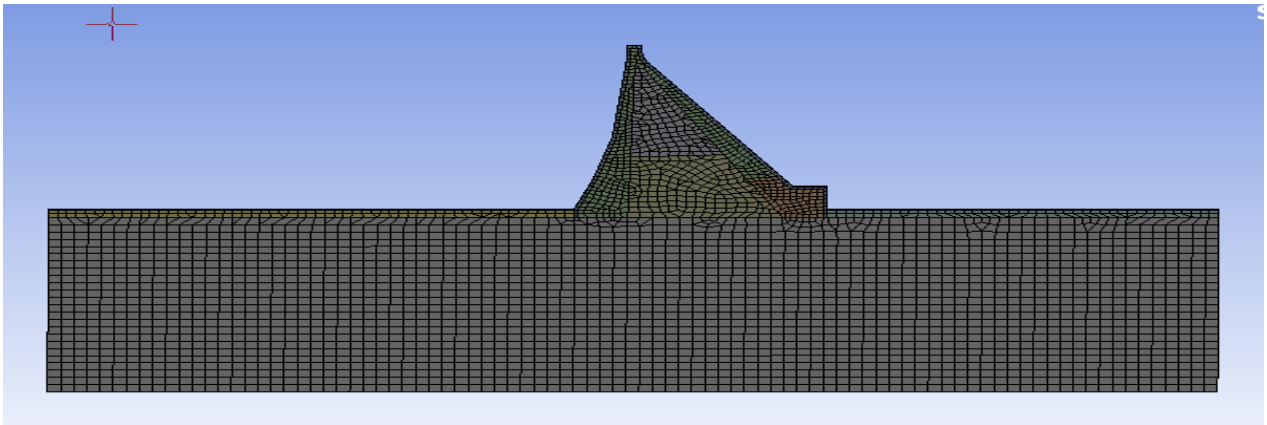

Figure 3. 13 figure showing quadrilateral meshing of Gilgel Gibe III dam model

Loading:- loads applied in this study were organized as distributed loads some were surface loads, body loads and others were edge loads. But almost all the loads were loaded on the structure using the load tabulation method which was expressed in terms of either time or x and y variables where the software program seeks an implicit type of programming.

3.6. Presentation and comparison criteria

The presentation and evaluation-specific parameters of the Gilgel Gibe III dam were described with the following results

1. **Dam Crest Acceleration (optional):**. To accurately describe the impacts of the dam-water interaction, more realistic simulations of the imprisoned water's dynamics are needed. The seismic demand would either rise or decrease depending on whether the lower modes of the dam lie on the ascending or descending part of the earthquake response spectrum. The resistance of such a shake is incredibly shown on the dam's crest and here this movement is directly related to displacement and stress developed at the dam's body
2. **Diformation histories.** It is important to display and assess the sizes and time histories of nodal displacements at important sites like the crest. The results are visually validated by displacement patterns, but the magnitudes of the displacements are also checked to make sure they are minor and don't compromise the dam's overall stability.
3. **Maximum and minimum principal stresses.** Determine the maximum and minimum principal stresses resulting from static and seismic loads, and display them as contours or vector graphs. Stress vectors show both the amount and direction of the primary stresses, making them more informative than contour plots in terms of predicting the likely direction of tensile

cracking. The biggest tensile (positive) and largest compressive (negative) stresses, which typically occur in the dam at different moments during the earthquake excitation, are represented by the maximum and minimum stress (USACE: EM 110-2-6051)

4. ANALYSIS AND DISCUSSION

4.1. General

Most gravity dam analyses assume that the dam is made up of discrete transverse vertical elements or cantilevers, each of which carries weights to the foundation without any load transfer between adjacent elements. This assumption also applies to the vast majority of RCC dams, including those with transverse joints that divide the dam into many monoliths and those with monolithic construction with no transverse joints. This assumption is usually correct, and stress calculations, including dynamic stress analysis, can be performed using a two-dimensional representation of the dam cross-section The current work presents the findings of a 2-D Finite Element analysis of a reservoir-gravity dam system performed with ANSYS Release 16.0 / 2023R2(ANSYS users guide theory and reference). Dynamic analysis of a dam with hydrodynamic pressure on the upstream face assumed as virtual mass moving in phase with the dam (Westargaard 1933) is commonly referred to as coupled analysis when incompressible fluid is used to perform a numerical simulation of the influence of ground movement on a concrete gravity dam. The structure (gravity dam) was considered to be linearly elastic, and plane strain formulation was used to analyze it. The water in the reservoir was classified as an incompressible fluid.(USACE: EP 1110-2-12 30 ,1995).

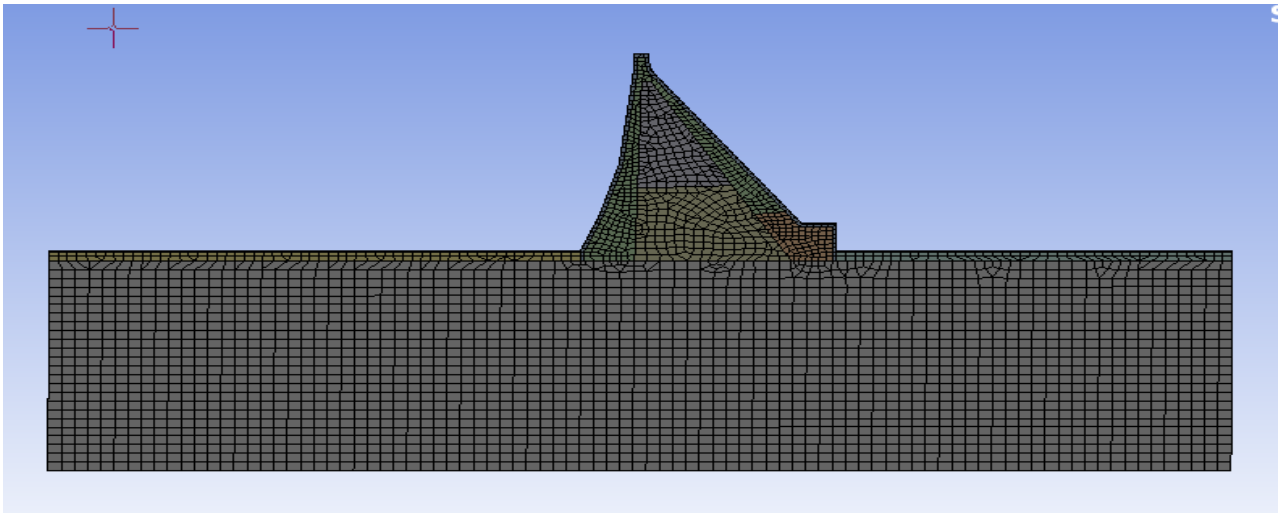

Figure 4. 1 figure showing finite element 2D model of Gibe III dam

4.2. Linear Static Analysis Over Gibe III Dam

The hydrostatic level and temperature, in addition to the gravity load, are used to perform a linear elastic static analysis of the structure to assess the static behavior of the FEM model. The direct plumb line measures the effect quantity, which is the displacement of the dam's crest at its center portion. It measures the displacement of the dam body to the dam foundation's two plan metric components (upstream, downstream, and left-right). A dam regime in the Apennines typically exhibits an increase in hydrostatic level during the winter/spring and a decrease during the summer due to seasonal water requirements. Such displacement is related to seasonal changes in the hydrostatic level and the air/concrete temperature. The static analysis for all model cases, as shown in Fig. 4.2 below was used and the hydrostatic force at the dam's u/s and d/s faces with the constant tail water level at 7 m height, as well as its self-weight, to determine the critical locations of stress, deformation, and their distribution over the dam's body. Here the static analysis was intended to be used as firsthand information in which part of the dam body and what amount versus the intensity of stress is being distributed. This kind of analysis gave some kind of inception about the stress-p susceptible parts of the dam. This is done with static loads imposed on empty reservoirs and reservoir conditions

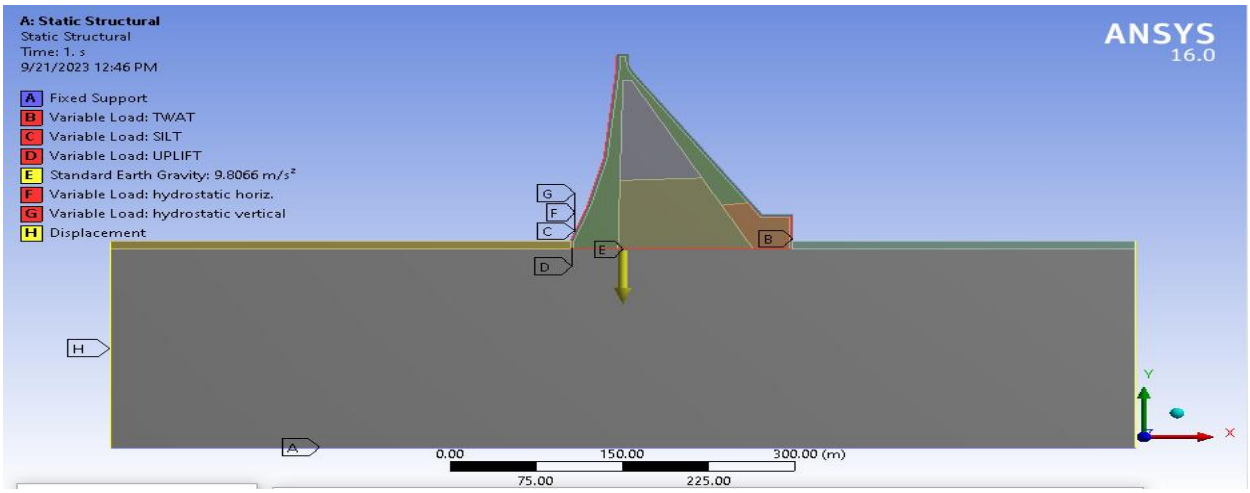

Figure 4. 2 showing static loading of GibeIII dam (full reservoir)

4.2.1.Deformation Dam Crest under static Analysis

In this analysis type dam with full reservoir and dam under the final stage of construction were used for the observation and the required parameters are taken from the overall time step of loading effects.

Table 4. 1 table showing maximum deformation under static analysis of dam crest

Loading condition	Reservoir condition	Maximum displacement (cm)		Reference
		Total	Directional	
Load comb.1	Empty	4.95	-2.98	Figure 4. 3
Load comb.2	Full(NWL)	5.11	-2.96	Figure 4. 3

1.

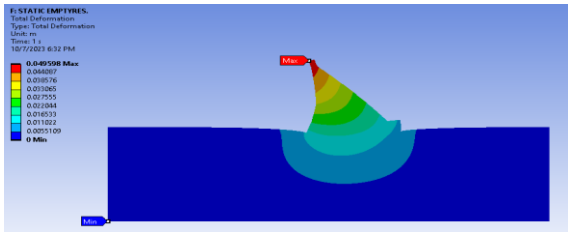

a. Total deformation (empty reserve.)

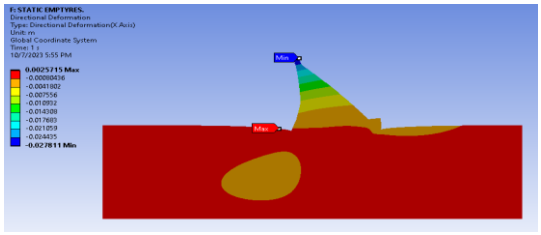

b.Directional deformation (empty reserve.)

2.

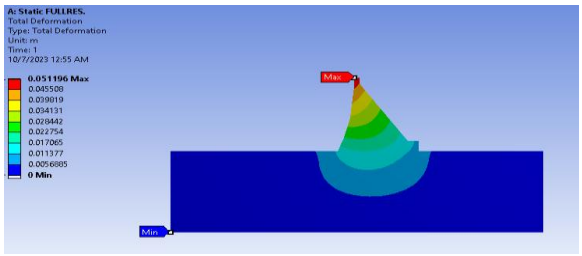

a. Total deformation (full reserve.)

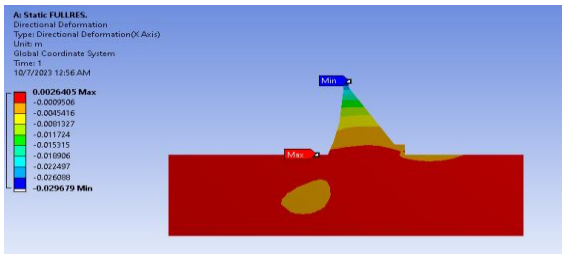

b.Directional deformation (full reserve.)

Figure 4. 3 figure showing deformation envelope on static analysis

Observation: Observing from the above table and pictures under static loading the dam crest is deflecting 2.98 cm towards the downstream direction in the empty reservoir case which is the governing directional deformation while the total structure is deflected at a distance of 5.11 cm which is observed in the full reservoir case. Here we can observe that total deformation of the dam is maximum when the dam is exposed under full reservoir case, which gives an emphasis that the overall deformation of the dam is occurred due to water pressure that punches the dam continuously along the upstream direction. But the maximum directional deformation is occurred when the dam is in its final stage of the construction, which in turn shows the dam's body composition with various

mixes rearrangement causes this deformation and it also shows that pressure in some part is also used for stability of the dam.

4.2.2.Stress Envelope In Static Loading

Table 4. 2 table showing the maximum and minimum stress along the dam body

Loading condition	Reservoir condition	Orientation	Stress (Mpa)	
			Maximum principal (tension)	Minimum principal(compression)
Load comb.1	Empty	Maximum	1.08	0.0011
		Minimum	1.07	-9.8
Load comb.2	Full(NWL)	Maximum	0.825	0
		Minimum	0	-10

1

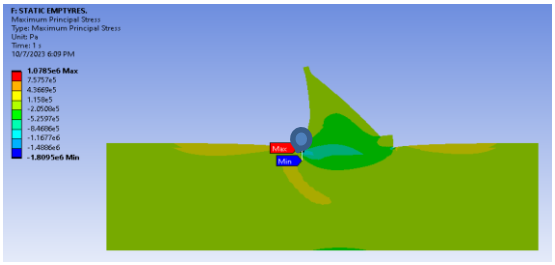

a.Maximum principal stress(Empty Resrv.)

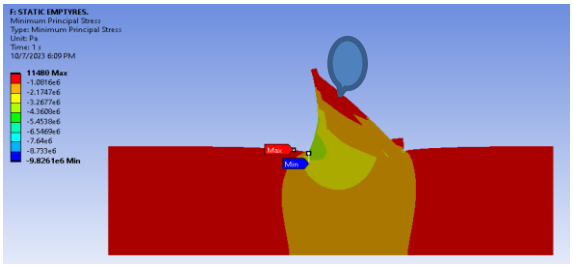

b.Minimum principal stress(Empty Resrv.)

2

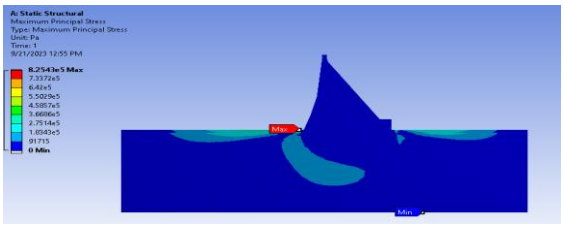

a.maximum principal stress (full Reserve.)

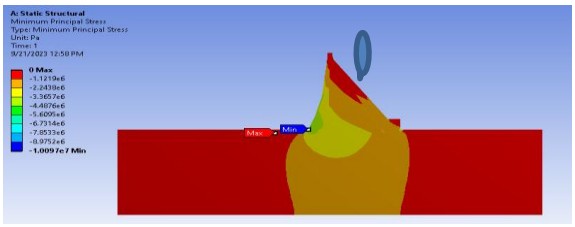

b.minimum principal stress(full Reserve.)

Figure 4. 4 Figure showing stress envelope along static analysis

Observation

Stress in static loading may cause development of crack at some selected points where the dam became stressed i.e. the places where slope change will occur, the dam crest and toe and at heel side the compressive and tensile stress are characterized based on their action on dam body. the table shows the amount of stress developed in the dam structure and each picture visualizes the maximum principal stress(tensile stress) and the minimum principal stress (compressive stress) distribution along the dam body. The maximum principal stress is a little bit high when the dam is empty which is 1.08 Mpa but in the full reservoir system, it is 0.825 Mpa. Whereas the compressive stress(minimum principal stress) is high at the full reservoir 10 Mpa at the up-stream side near the dam heel in which most studies assumed as the region where stress contours at that area show relatively large value. The maximum and minimum stresses are developed under RCC5 dam section whose tensile and compressive strength are 1.2 Mpa and 18 Mpa respectively so the developed stresses in both load combinations are on the allowable region and the dam is safe along this loading conditions.

4.3. Modal Analysis of Gibe III Dam Profile

The inherent frequencies and mode shapes of the structural system were determined using modal analysis. During the analysis, the contact parts behaved as linear springs. The natural frequencies of the bonded foundation model for the two-dimensional dam monolith with a full reservoir system were reported. The deflection forms of the first six modes were shown to visualize the character of each mode form and deflection along each shape plot.

Loading: It should be noted that static loads, such as weight and hydrostatic pressures, are represented as imposed in discrete time increments. As a result, the same 0.005 second for OBE and 0.01 second for SEE case time step that is used for dynamic analysis is also taken into account for the application of time increments for static loading. It is observed that time for static analysis is only a useful instrument for applying the load one after the other, but that in the process, inertia and damping effects are ignored. In this regard, a single increment of the dead load and a subsequent increment of hydrostatic pressures are delivered within a negative time range. The real dynamic analysis starts at time zero, applying the static displacements and stresses as initial conditions.

4.3.1. Damping

The Rayleigh damping parameters, which could explain a significant amount of the discrepancies in participant results. shows that for damping in the range of 3–7%, the difference in loads and displacements for the gravity dam is not substantial. Consequently, a critical damping of 5% is used in all analyses; however, the key issue is how the damping is applied to the model. And in this analysis method the setting for damping was used to match the Rayleigh damping at 1 Hz and 10 Hz.

4.3.2. Representative Mode Shapes Of The Dam

The dam structure has oscillated with different vibration patterns with infinite in number but the first three to four mode shapes usually represent the overall structural sway. When a structure vibrates at its inherent frequency, it takes on its mode shape. Undoubtedly, the study investigates how a structure behaves dynamically in response to different loadings. It suggests the natural vibratory frequency of the structure, the shape in which it vibrates at various frequencies, as well as the mass involvement for each mode in a given direction. In general, it is wise to perform a modal analysis before carrying out any more dynamic assessments. due to the importance of vibrational features in predicting how a structure will react to various excitations.(USACE:EM110-2-6051)

For determining an appropriate number of modes to extract, the mode participation factor and effective mass are essential. The mass travelling in a certain direction for each mode is indicated by the mode participation factor. A higher value means that, given the force or excitation delivered in that direction, the mode may be excited. The following equation is used to compute the participation factor:$\gamma_i = (\emptyset)_i^T [M][D]$, Where, $\{\varphi\}_i$ ^{T}is the transpose of mode shape or eigenvalue matrix, [M] is the mass matrix, and {D} is the excitation direction matrix which represents the direction, the participation factor is calculated The effective mass and participation factors both suggest the significance of a particular mode. Effective mass is calculated by the following equation: $M_{effi} = \gamma_i^2$. If the ratio of effective mass to total mass is close to '1′, suggests that the significant modes have been extracted. The dam was subjected to the Morganhill (1984) earthquake on the OBE case and the Hectrmine (1999) earthquake on the SEE case in the upstream-downstream direction The study developed 25 mode shapes for the effectiveness of representing results but six of these mode shapes are determined to represent the whole structure which were identified by observing the

participation factor of each mode to the total. From the chart below the participation factor for the first six modes are determined to be :

Table 4. 3 table showing selected modes and frequency of mode shapes

Mode	frequency	Participation factor	Effective mass to total mass (ratio)
1	1.54337	667.76 – y-direction	0.0085
2	3.07988	33220.4- y- direction	0.21
3	3.28257	5993 – y direction	0.686
4	5.102326	525.8- y-direction	0.00528
5	7.387645	1865 – y direction	0.06646
6	7.46487	300.34- y- direction	0.00172

Participation factor and effective mass of each mode (y- direction)

***** PARTICIPATION FACTOR CALCULATION ***** Y DIRECTION

MODE	FREQUENCY	PERIOD	PARTIC.FACTOR	RATIO	EFFECTIVE MASS	CUMULATIVE MASS FRACTION	RATIO EFF.MASS TO TOTAL MASS
1	1.54338	0.64793	667.76	0.111422	445899.	0.853455E-02	0.852076E-02
2	3.07988	0.32469	3320.4	0.554034	0.110247E+08	0.219549	0.210674
3	3.28258	0.30464	-5993.0	1.000000	0.359166E+08	0.906996	0.686336
4	5.10233	0.19599	525.88	0.087748	276550.	0.912289	0.528464E-02
5	7.38765	0.13536	-1865.0	0.311196	0.347828E+07	0.978864	0.664670E-01
6	7.46488	0.13396	300.34	0.050114	90201.1	0.980590	0.172367E-02
7	9.62766	0.10387	126.94	0.021181	16112.8	0.980898	0.307902E-03
8	10.0300	0.99701E-01	-26.222	0.004375	687.577	0.980912	0.131390E-04
9	11.0227	0.90722E-01	54.385	0.009075	2957.77	0.980968	0.565204E-04
10	11.6808	0.85611E-01	821.10	0.137008	674200.	0.993873	0.128834E-01
11	13.1131	0.76260E-01	342.01	0.057068	116970.	0.996111	0.223520E-02
12	13.4829	0.74168E-01	193.56	0.032298	37466.1	0.996828	0.715945E-03
13	14.7609	0.67747E-01	20.138	0.003360	405.534	0.996836	0.774942E-05
14	15.8526	0.63081E-01	135.30	0.022576	18305.8	0.997187	0.349809E-03
15	16.1614	0.61876E-01	-50.087	0.008358	2508.75	0.997235	0.479400E-04
16	17.2425	0.57996E-01	-149.12	0.024883	22237.5	0.997660	0.424940E-03
17	17.4840	0.57195E-01	-179.18	0.029898	32105.8	0.998275	0.613515E-03
18	18.4933	0.54074E-01	35.856	0.005983	1285.68	0.998299	0.245682E-04
19	18.7737	0.53266E-01	-219.53	0.036631	48193.3	0.999222	0.920934E-03
20	19.7112	0.50732E-01	-123.85	0.020665	15337.9	0.999515	0.293095E-03
21	20.6177	0.48502E-01	49.946	0.008334	2494.64	0.999563	0.476705E-04
22	21.0254	0.47561E-01	4.2991	0.000717	18.4819	0.999563	0.353173E-06
23	21.9873	0.45481E-01	-15.665	0.002614	245.382	0.999568	0.468904E-05
24	22.6403	0.44169E-01	31.632	0.005278	1000.60	0.999587	0.191206E-04
25	23.1882	0.43125E-01	146.84	0.024502	21563.3	1.00000	0.412056E-03
sum					0.522464E+08		0.998384

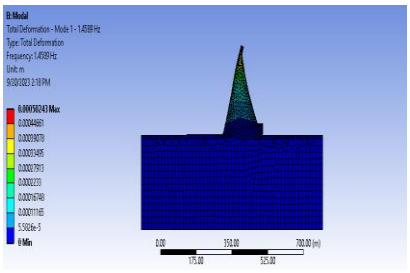

Mode 1

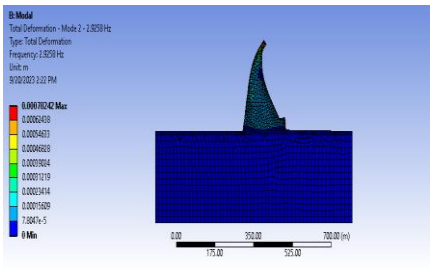

Mode 2

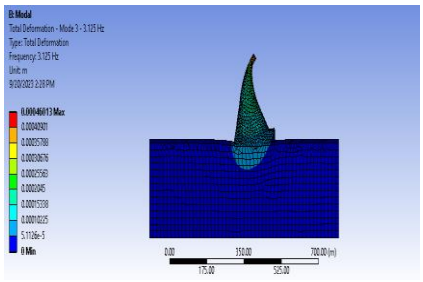

Mode 3

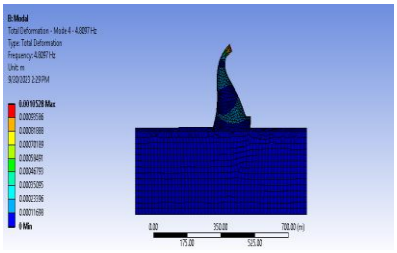

Mode 4

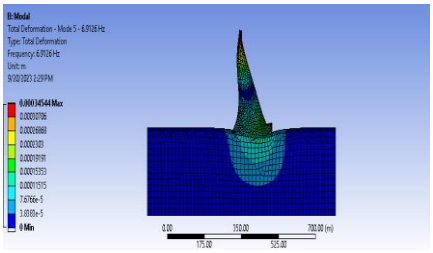

Mode 5

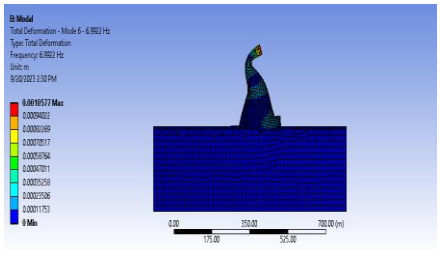

Mode6

Figure 4. 5 figure showing the first six natural mode shape of the dam

4.3.3. Deformation Along the Dam Body

The deformation along the dam crest can visualize how much the dam body is displacing while it has interacted with different scenarios**.** Within this analysis method, the three cases are selected as it is believed to be good to show the movement of the dam crest plus the whole dam body in the worst-case earthquakes. Here the following table tries to show the deformation profile of the Gilgel Gibe III dam under dynamic loading cases in modal analysis.

Table 4. 4 table showing deformation along the dam crest

Loading condition	Earthquake ground motion	Reservoir condition	Deformation cm)	
			total	directional
Load comb.1	OBE in upstream direction	Empty	10.71 at t=0.33sec	-10.71 At t=0.33sec
Load comb.2	OBE in downstream direction	Full (normal pool)	40.95 At t=0.5sec	40.59 At t=0.5sec
Load comb.3	SEE in downstream direction	Full (normal pool)	40.96 At t=0.49sec	40.69 At t= 0.49sec

.

1.

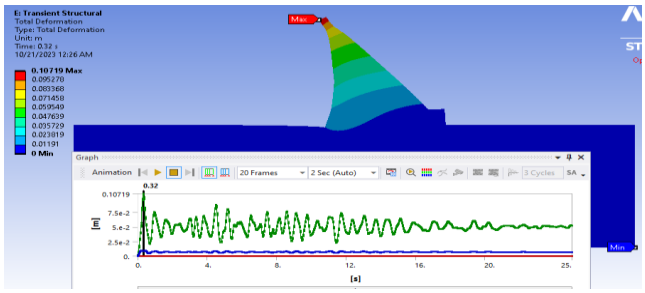

a.total deformation (Empty +OBE.)

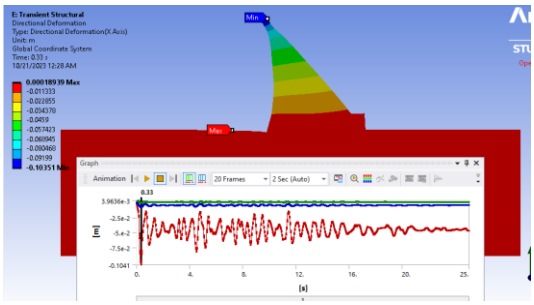

b.directional deformation(empty+OBE)

2.

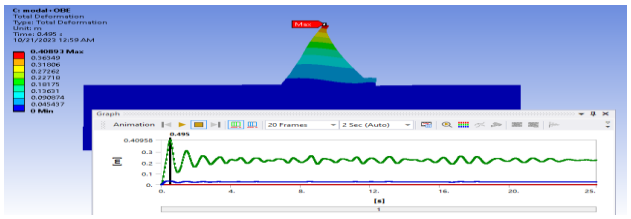

a.total deformation(MWL+OBE)

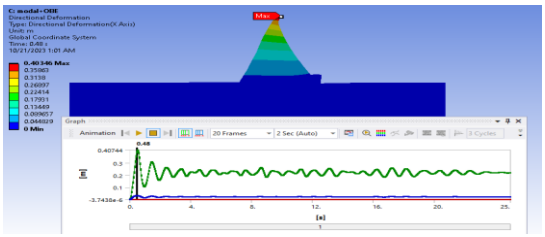

b.directional deformation (MWL+OBE

3.

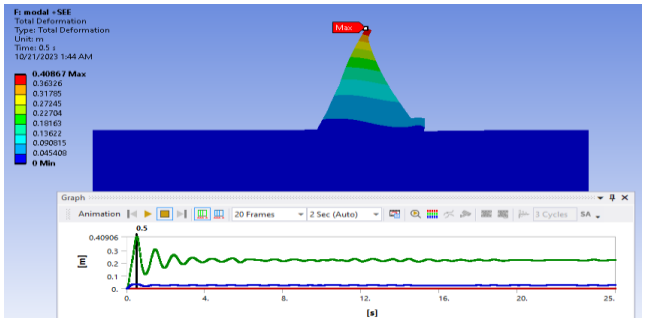

a.total deformation (MWL+SEE)

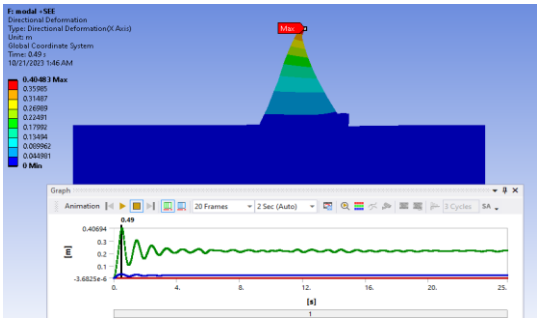

b.directional deformation (MWL+SEE)

Figure 4. 6 figure showing dam deformation in model analysis for the three loading cases

Observation: The above table tries to show the deformation of the dam crest in various loading cases. The dam deforms 10.71 cm along the upstream direction when the operating basis earthquake is faced with it at the end of the construction stage(empty reservoir) which is shown in the picture below. A relatively small amount of deformation is seen in this loading case but in the full reservoir cases at load combination 3 has 40.96 cm deformation along the dam body and 40.69 cm. deformation of the dam crest is observed and it is almost similar to the deformation that occurred at load combination 2 which is 40.95 cm total deformation 40.59 cm deformation in the downstream direction. However, the direction of deformation is identical in both load combinations 2 and 3.this

is a very different observation we see. Gibe III dam is a big dam which is 243 m high and this elongation enables the dam responding similarly for intervals of ground motions.

4.3.4. Dam Crest Acceleration Profile

In modal analysis, the whole structure is assumed to be vibrating at a certain natural frequency. This frequency enables the structure to withstand the worst scenario exposed in the lifetime. The acceleration profile tries to show how the dam body tries to interact with respect to the ground acceleration.

Table 4. 5 figure showing dam crest acceleration of Gibe III dam (modal analysis)

Loading condition	Earthquake ground motion	Reservoir condition	Acceleration (m/s2)	
			total	directional
Load comb.1	OBE in upstream direction	Empty	29.76 Att=0.135 sec	-24.59 At t=0.135 sec
Load comb.2	OBE in downstream direction	Full (normal pool)	15.72 At t=0.16 sec	11.83 At t=0.53 sec
Load comb.3	SEE in downstream direction	Full (normal pool)	15.18 At t=0.02 sec	-11.58 At t=0.52 sec

1.

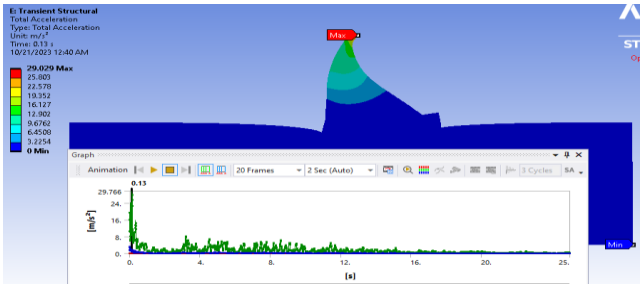

a.total acceleration (empty+OBE)

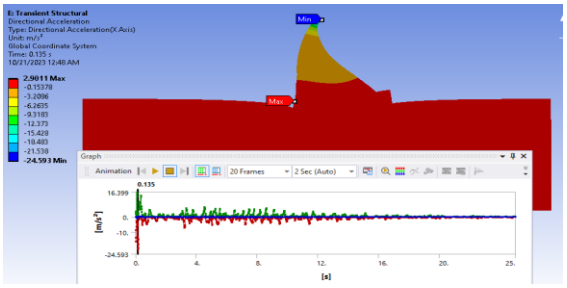

b.directional acceleration (empty+OBE)

2.

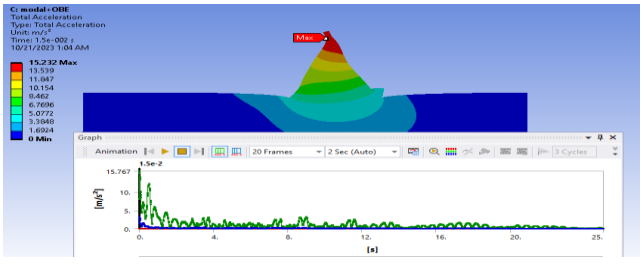

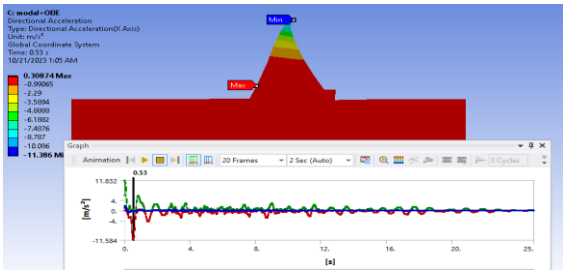

a.total acceleration(MWL+OBE)

b. directional acceleration (MWL+OBE)

3.

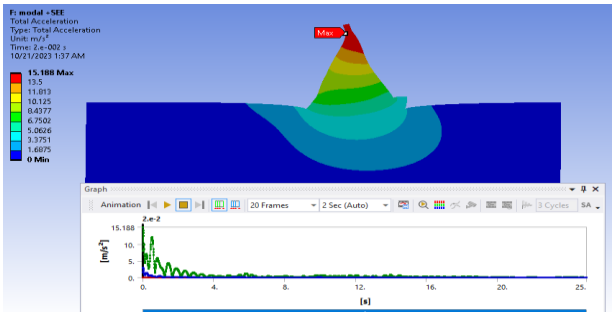

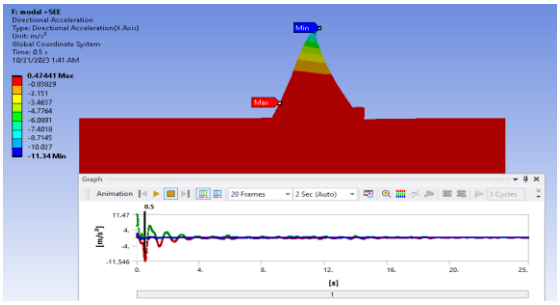

a. total acceleration (MWL+SEE)

b. directional cceleration(MWL+SEE)

Figure 4. 7 figure showing acceleration along the dam body

Observation: The crest acceleration profile table shows that the dam at the empty reservoir has more crest acceleration than the rest load combinations this is due to it having no interacting load other than self-weight and the ground shaking inertia. The dam as a whole shows an acceleration of 29.76 m/s2 while the crest moves at a rate of 24.59m/s2 downstream direction. The rest loading conditions are characterized by a 15.72 m/s2 total dam body and 11.83 m/s2 at downstream side directional acceleration observed in load combination 2, but 15.18 m/s2 total acceleration and 11.58m /s2 downstream directional acceleration is seen as per profile shown on the table and is visualized at the pictures on the above in all cases the dam crest shows an amplified acceleration as it is compared to the ground movement.

4.3.5. Stress Envelope Along The Dam Body

The distribution of stress along the dam body was investigated using the above six mode shapes and it was simulated on the static and dynamic loading cases. The stress typically distributed along the dam body has been shown by the following output below with maximum principal stress and minimum principal stresses which are relatively showing the tensile stress and compressive stress developed along the dam body. the record was taken when the absolute maximum values were seen along the dam body but the software by itself displays the average values of these parameters. Such a record kind is applied by assuming it is used for comparison purposes so that comparison made with the other analysis method is not only dependent on values but it tries to see the regions where stress is critical. To do so the display pictures use stress contours.

Table 4. 6 table showing the maximum and minimum principal stress of the dam

Loading condition	Earthquake ground motion	Reservoir condition	Principal stress (Mpa)	
			Maximum principal	Minimum principal
Load comb.1	OBE in upstream direction	Empty	6.19 at t=0.065 sec	-14.49 at t= 0.445 sec
Load comb.2	OBE in downstream direction	Full (normal pool)	11.9 at t=0.41 sec	-37.9 at t=0.30 sec
Load comb.3	SEE in downstream direction	Full (normal pool)	11.36 at t = 0.38 sec	-38.01 at t=0.34 sec

1.

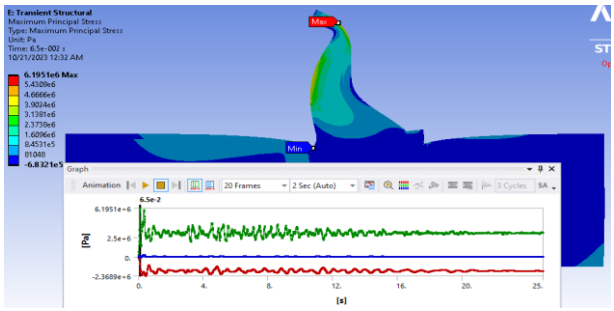

a.maximum principal stress (empty+OBE)

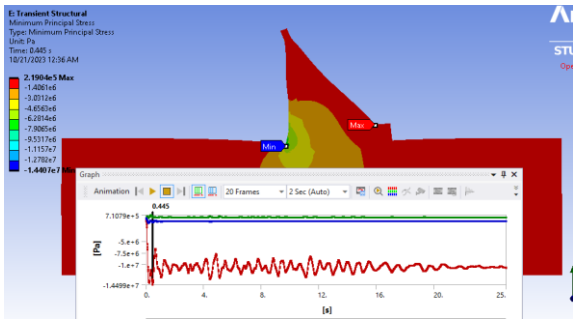

b.minimum principal stress (empty+OBE)

2.

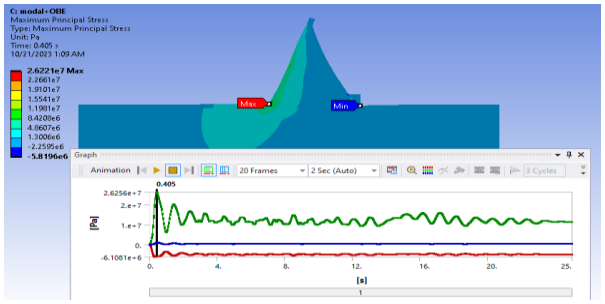

a.maximum principal stress (MWL+OBE)

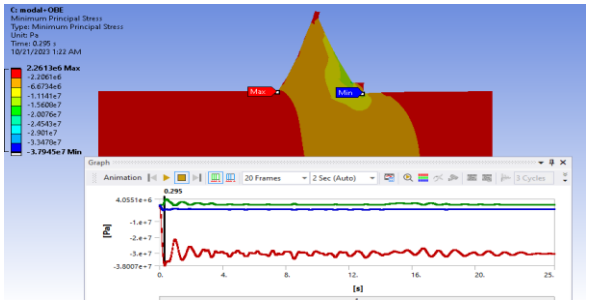

b.minimum principal stress (MWL+OBE)

3.

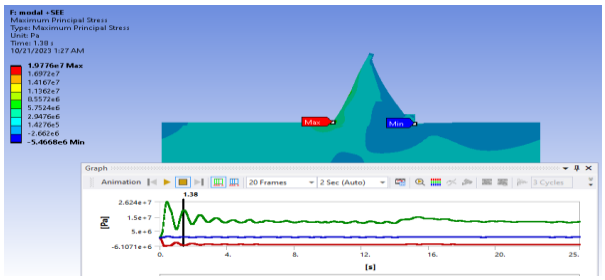

a.maximum principal stress (MWL+SEE)

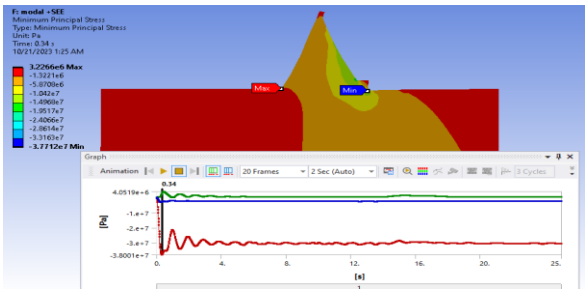

b.minimum principal stress (MWL+SEE)

Figure 4. 8 figure showing maximum and minimum principal stress profile of the dam under modal analysis

Observation : The stresses developed along the dam body at this method of analysis are a little big this is due to the large deformation seen from the foundation as if it is massless and it is assumed to act as a spring where the ground acceleration is directly reflected and transforming without change in rate versus quantity to the dam baseline. As a result, it is expected to have this kind of results. Here the result shown in the table represents analysis results until the material we used has gained its maximum elastic range but there is also another case where the material has resisted this stress by re-arranging its shape versus internal particle interlocks which in turn is practiced with non-linear analysis and the analysis we do here doesn't consider the analysis of joints and materials non-linearity, dam body non-uniformity versus structural complexity. But the dam's heel, toe and areas where slope change was seen were the stress susceptible regions as seen from the picture on the above.

4.4. Transient Analysis (Time History) of Gibe III Dam

The selected gravity dam is simulated including dam reservoir interaction using the Finite Element discretization. The linear transient dynamic analysis adopted in ANSYS2016 and the 2023-R2 student version program was implemented. To investigate the effects of dam water on the time history response of gravity dams, the linear earthquake response of the selected event was determined for the specified case. The dam was subjected to the Morganhill (1984) earthquake on the OBE case and the Hectrmine (1999) earthquake on the SEE case in the upstream-downstream direction as shown below and the results of this analysis are displayed in the next consecutive charts.

Damping: in this analysis the global damping ratio ($\xi = 0.05$) was used.

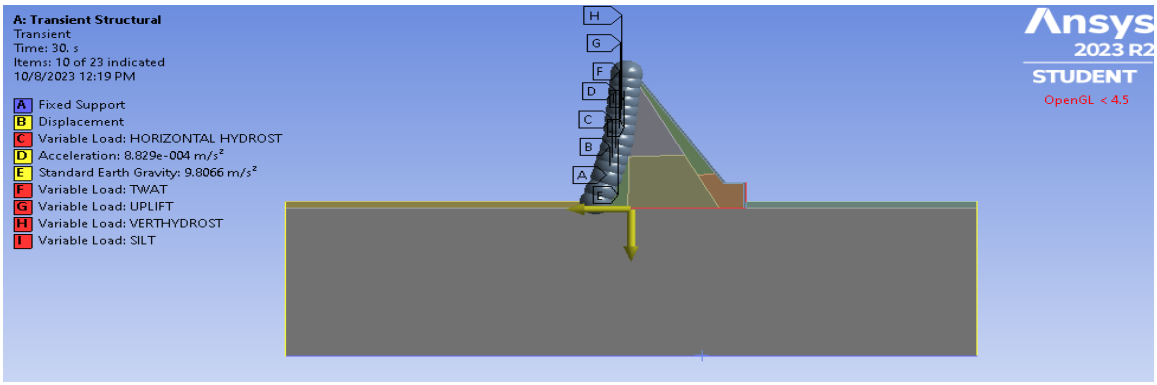

Figure 4. 9 figure showing time history analysis loading

4.4.3. Deformation of The Dam Crest

Deformation under the three loading conditions is shown using the table and color band contours below. Within this analysis, total dam body deformation and dam crest directional deformation were visualized using number values(table) and pictorial descriptions which show deformation profiles at different loading conditions.

Table 4. 7 table showing deformation behavior of Gibe III under time history analysis

Loading condition	Earthquake ground motion	Reservoir condition	Deformation (cm)	
			Total	directional
Load comb.1	OBE in upstream direction	Empty	6.8 at t= 0.89 sec	7.5 at t= 0.29
Load comb.2	OBE in downstream direction	Full (normal pool)	33.54 at t = 0.4sec	-31.54 at t= 0.41 sec
Load comb.3	SEE in downstream direction	Full (normal pool)	33.64at t= 0.395 sec	-31.8 at t= 0.42 sec

1.

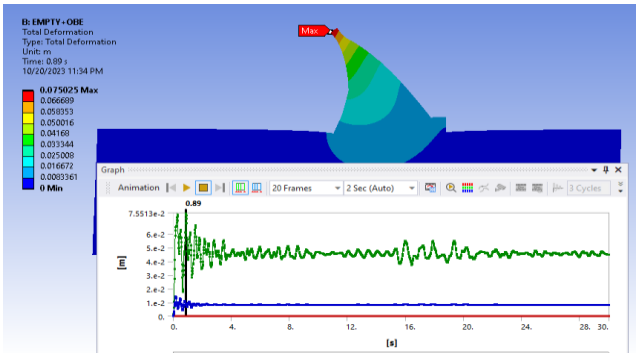

a.total deformation (empty+OBE)

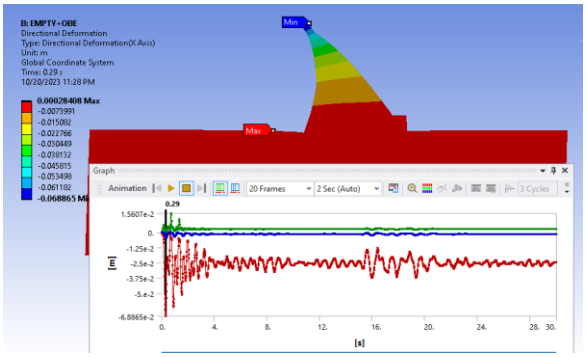

b.directional deformation(emty+OBE)

2.

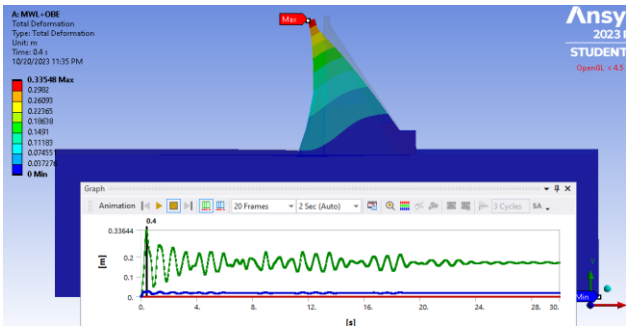

a.total deformation (MWL+OBE

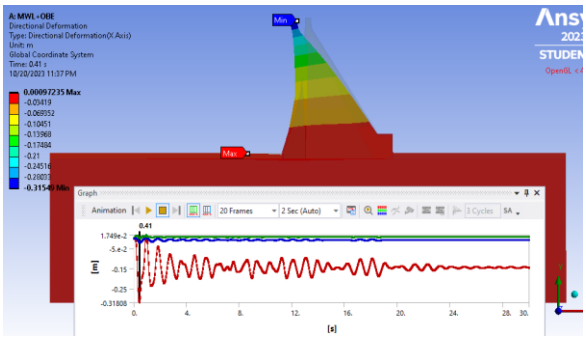

b.directional deformation (MWL+OBE)

3.

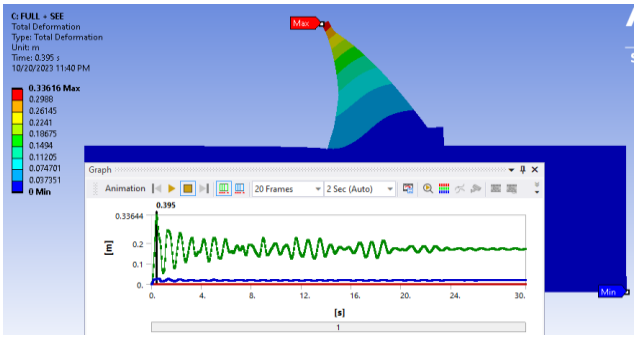

a.total deformation (MWL+SEE)

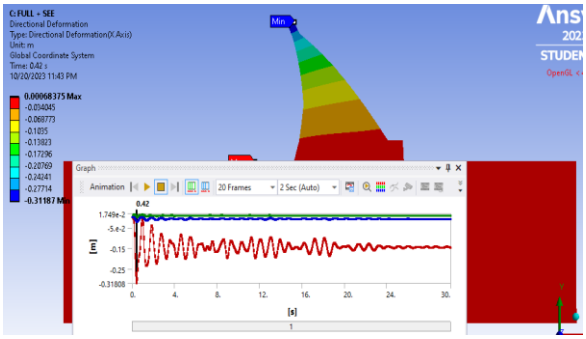

b.directional deformation (MWL+SEE)

Figure 4. 10 figure showing deformation behavior under different loading conditions of Gibe III dam

Observation : as seen from the table above total deformation of the dam is 6.8 cm and 7.5 cm directional in the empty reservoir loading condition. Which is relatively small compared to other loading cases. But in the MWL +OBE case, the dam body deforms 33.54 cm while the dam crest deflects at 31.54 cm to the downstream direction. However, the maximum deformation was seen on the load combination 3(MWL+SEE) which is 31.64 cm total and 31.8 cm directional. The deformation patterns are clearly shown in each picture below. finally, the result is relatively closer to what we did in modal analysis where the comparison will be seen on the next respective pages.

4.4.4. Acceleration at Dam Crest

The dam body versus crest acceleration data is set in the table below and it shows that crest acceleration along the dam body is amplified and is acceptable in different researches. The acceleration on the SEE case is greatest in all cases.

Table 4. 8 table showing acceleration profile of the dam under different loading conditions in time history analysis

Loading condition	Earthquake ground motion	Reservoir condition	Acceleration (m/s^2)	
			Total	directional
Load comb.1	OBE in upstream direction	Empty	16.72 at t=0.16 sec	13.56 at t= 0.036 sec
Load comb.2	OBE in downstream direction	Full (normal pool)	19.93at t=0.37 sec	19.48 at t=0.37 sec
Load comb.3	SEE in downstream direction	Full (normal pool)	19.96at t=0.37 sec	19.63at t=0.356 sec

1.

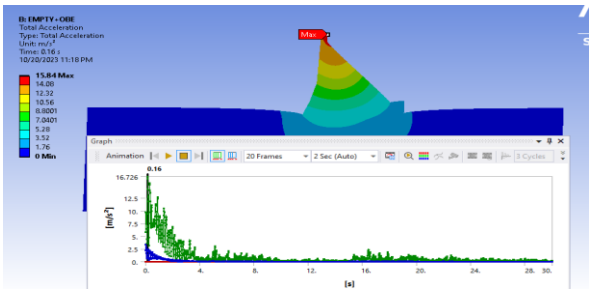

a.total acceleration (empty+OBE)

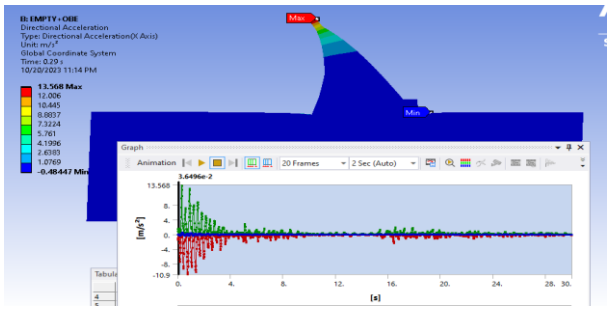

b.directional acceleration (empty+OBE)

2.

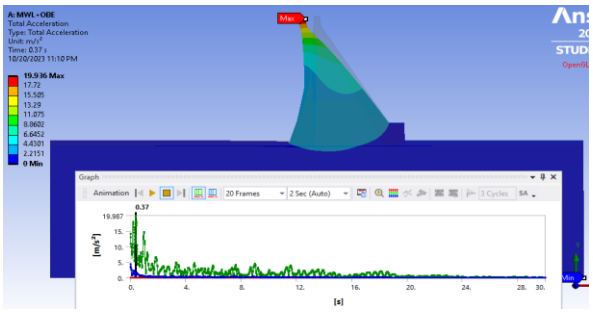

a.total acceleration (MWL+OBE)

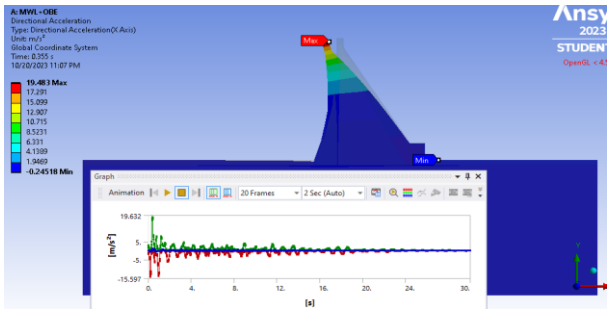

b.directional acceleration (MWL+OBE)

3.

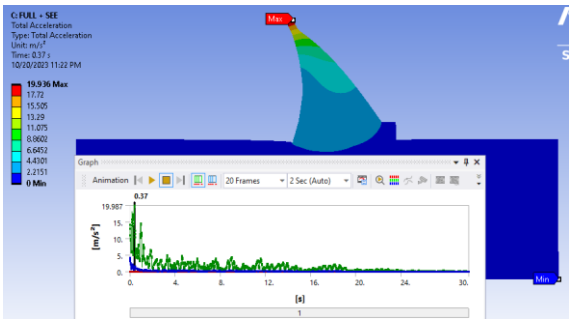

a.total acceleration(MWL+SEE)

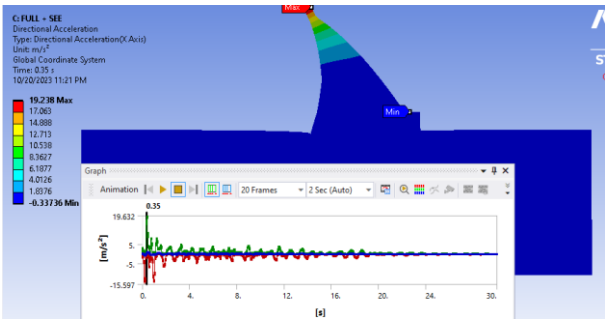

b.directional acceleration(MWL+SEE)

Figure 4. 11 figure showing acceleration behavior of Gibe III dam under time history analysis

Observation : the acceleration profile of the Gilgel Gibe III dam under time history analysis looks as it is seen on the table which displays the number values while the contour profiles are shown on each picture representing every loading scenario. The highest acceleration profile is seen on the third load combination with a value of 19.96 m/s2 on the dam's body while 19.63 m/s2 directional.in general, the acceleration seen on the dam's crest is amplified as it is compared to the ground acceleration we used during the analysis. This is acceptable according to gravity dam design manuals (USACE: USBR) and many types of research done on linear time history analysis of gravity dams on earthquake loading cases.

4.4.5. Stress Distribution Along the Dam

The stress distribution profile is shown using a chart which displays the amount and pictures below showing the stress contours typically describe the distribution along the dam body. In general, stress developed along the dam body is quite similar to what we have seen in the modal analysis.

Table 4. 9 table showing principal stress profile under different loading conditions of Gibe III dam

Loading condition	Earthquake ground motion	Reservoir condition	Stress (Mpa)	
			Maximum principal stress	Minimum principal stress
Load comb.1	OBE/upstream direction	Empty	2.49at t=0.3 sec	-6.57 at t=0.26 sec

Load comb.2	OBE/downstream direction	Full(normal wl)	6.29 at t=0.53sec	-48.46 at t=0.54 sec
Load comb.3	SEE / downstream	Full (MWL)	6.3at t=0.55 sec	-54.5 at t= 0.53sec

1.

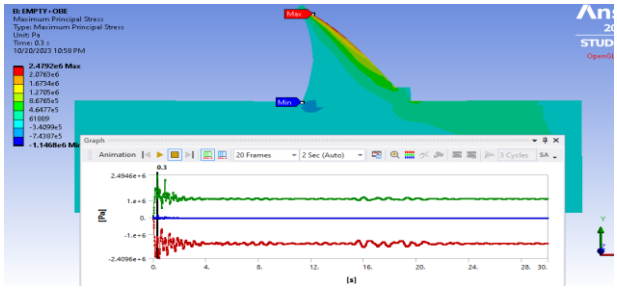

a.maximum principal stress (empty+OBE)

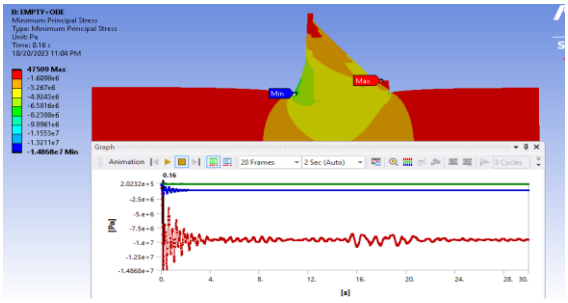

b.minimum principal stress (empty+OBE)

2.

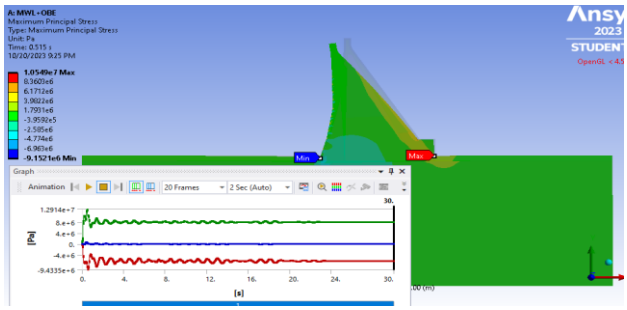

a.maximum principal stress (MWL+OBE)

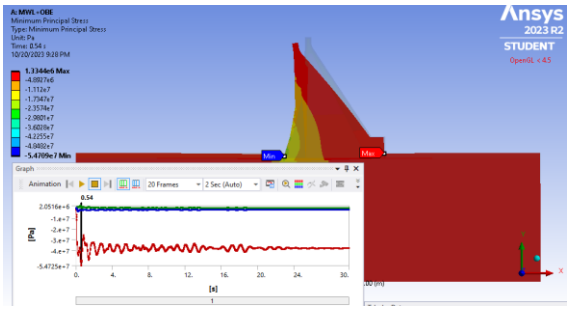

b.minimum principal stress (MWL+OBE)

3.

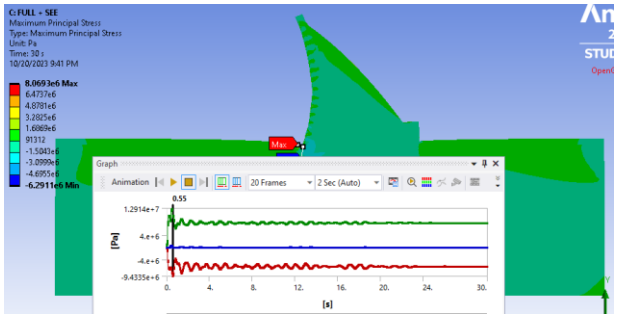

a.maximum principal stress (MWL+SEE)

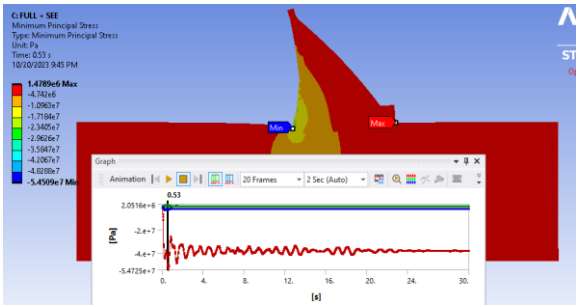

b.minimum principal stress (MWL+SEE)

Figure 4. 12 figure showing maximum and minimum principal stress contour of Gibe III dam under time history analysis

Observation : the chart shows the maximum amount of stress developed along the dam body in mega Pascal. Which was decided to be the absolute maximum for the ease of identifying the stress susceptible regions and comparison purposes. The maximum principal stress is usually considered as the tensile stress developed under the dam tensile regions was not more than 4.4 Mpa but here the values observed are greater than this value except for the stress shown on the empty reservoir case and this doesn't mean that the dam is not stable these numbers show the dam needs non-linear dynamic analysis for further investigation and decision. The same is true for minimum principal stresses (compressive stresses) developed at the dam's compressive loading regions. On the other hand, this study aims to show the distribution of stress along the dam body using the pictures below with time histories versus contours on the dam body. As seen from the pictures the stresses are developed at the dam's heel, toe or regions at the upstream/downstream slop near the dam crest or at the dam crest.

4.4.6. Result Summary and Validation

In the case of dynamic analysis, the two methods modal and time history methods play a vital role especially time varying loads exist in the real environment. Both methods are effective within a specific intensity of loading in this study, the two methods with different loading conditions but the same load history and distribution to parameters are set to be used in comparison.

4.3.4.1.Directional deformation

Both internal and exterior loads induce deformation and damage to dams. These loads determine the deformation of the dam for the sake of safe resistance of loading actions. Most researches show the deformation of concrete dams with different heights, uses directional deformations to show the stability status. In this case two gravity dams be taken for the comparison of the result obtained in this study. The first dam is a concrete arch dam modeled with ANSYS and its height is relatively as high as gibe III among other dams studied by this method. While in the second dam it was modeled in ABACUS with height 1/2 as high as Gibe III dam, but it is an RCC gravity dam. In both dams the deformation is investigated along the crest of each dam. Deformation along Gibe III RCC dam was determined on its crest. Using the above criteria we will like to see the proportionality of the

deformation occurred along the crest of two dams and the deformation along dam crest of gibe III concrete gravity dam.

1. B. Poursartip and V. Lotfi. (2008) try to clarify the directional deformation of dam crest in different regions Using the Shahid Rajaee concrete arch dam over a rigid foundation. The dam is 138 m in height with a crest length of 420 m. and the directional deformation stated here is comparatively show the deformation is increasing as the reservoir height is increasing. This study shows that the height of the dam and the deformation occurred have direct relationship. deformation observed on Gibe III dam is no longer worse since the height of the dam is almost 75% greater than Shahid Rajaee dam. And the maximum deformation here is 24.17cm downstream direction while the Gibe three dam's is 31.8 cm downstream direction on TMH and 40.69cm upstream in modal analysis.

Reservoir height(m)	location	Maximum displacement(cm)
20-40	Right corner(dam crest)	-21.33
40-80	Right corner(dam crest)	-22.96
80-130	Right corner(dam crest)	-24.17

2.N. Salman Movahedi and B. Aminneja (2016) declare that the crest deformation of the Latyan dam of height 107m was analyzed using ABACUS with full reservoir condition. It was analyzed using dynamic analysis under earthquake loading. The study finally showed that the crest displacement of the dam under earthquake loading was 30.72cm.In most cases, the deformation is observed towards the down-stream direction but in the first loading case, it is along the up-stream direction

Table 4. 10 table showing dam crest deformation of Gibe III dam under time history and modal analysis

Loading condition	Earthquake ground motion	Reservoir condition	Deformation (cm)		Remark
			TIME HISTORY	MODAL	
Load comb.1	OBE in upstream direction	Empty	7.5	-10.7	Occurred at dam crest
Load comb.2	OBE in downstream direction	Full (normal pool)	-31.54	40.59	Occurred at Dam crest

Load comb.3	SEE in downstream direction	Full (normal pool)	-31.8	40.69	Occurred at dam crest

As seen from the above two works one with a proportionality relation between deformation and height of the RCC dam, while the second with determined result, the deformation obtained through the analysis using seismic loading varies as the dam height. Deformation seen as a result of earthquake loading on Gilgel Gibe III dam is on the right proportion.

4.4.6.2.Tensile Stress (Maximum Principal Stress)

As per USACE: EP 1110-2-12 (1995) and EM 110-2- 6051(2003) Direct tensile strength measurements on core samples will serve as the foundation for determining the tensile strength of RCC. Cores from test-fill placements created with the suggested design mixes must be taken and placed with the suggested consolidation for the final design of new dams **.**

a. Location of critical tensile stress. : Critical tensile stresses are located at the upstream and downstream faces of the dam. The tensile stress distribution within the dam mass is of interest to help establish zone boundaries for superior, higher-strength RCC mixes that may be required to control cracking near the faces.

b. Allowable Tensile Stresses: The tensile strength or capacity of the plain concrete used in the computation of demand capacity ratio(DCR) is obtained from the uni-axial splitting tension tests or the static tensile strength $f_t = 1.7 f'^{\frac{2}{3}}_c$ where in which fc' is the compressive strength of the concrete. A performance curve displays the permissible level of damage based on the linear-elastic analysis (USACE, 2003 and 2007, USBR, 2006)

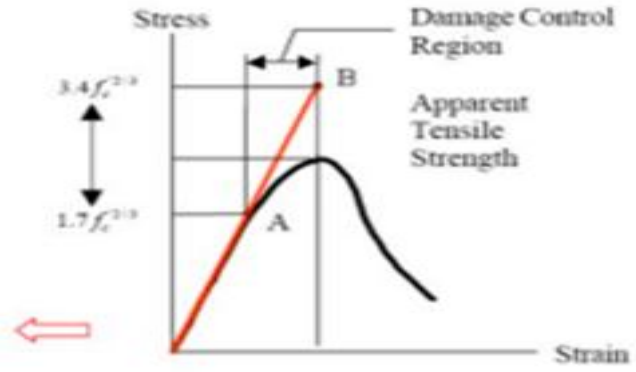

Table 4. 11 figure showing stress-strain performance

For a dam's linear transient dynamic analysis, a DCR of two is the maximum allowed. This translates to a stress demand of twice the concrete's static tensile strength. The stress demand associated with a DCR of 2 corresponds to the concrete's so-called "apparent" dynamic tensile strength, which is utilized to assess the outcomes of linear dynamic analysis, as shown by the stress-strain curve in the previous image. Based on the fact that it is described above the maximum strain developed through the dam's body is set to be twice the demand capacity ratio i.e. $f_t = 1.7f_{c^{\frac{2}{3}}} equivalent\ to\ 0.32f_{c^{\frac{2}{3}}} = 2.2Mpa\ the\ elastic\ range$ So the maximum principal stress is located at RCC 5 (the concrete zone covering dam outer zone)on the dam body which is 18 Mpa and For DCR of 2, which is the elastic plastic range(apparent tensile strength) is $f'_t = 2 * 0.32 * f_{c^{\frac{2}{3}}}) = 4.4\ Mpa.$

Table 4. 12 table showing maximum principal stress (tensile)

Loading condition	Earthquake ground motion	Reservoir condition	Maximum principal stress		Remark
			TIME HISTORY	MODAL	
Load comb.1	OBE in upstream direction	Empty	2.56	6.19	Located at RCC5
Load comb.2	OBE in downstream direction	Full (normal pool)	6.29	11.9	Located at RCC5
Load comb.3	SEE in downstream direction	Full (normal pool)	6.3	11.36	Located at RCC5

The maximum principal stress (tensile stress developed in the dam body in time history analysis) is over this range, except for the stress developed in the empty reservoir case, while in the modal analysis, the results are more than what we expect in the empty reservoir case. That means modal analysis has a little bit of an exaggerated result, and according to this result, the analysis type is set to be non-linear elastic dynamic analysis.

4.4.6.3. Compressive stress (Minimum Principal Stress)

The maximum principal stress is equivalent to the concert's compressive strength. In most cases, the compressive strength of the RCC is 20.7 Mpa. But here all the results except load combination 1 are above the concrete strength of the dam since the compressive stress is observed at the dam's

upstream face and downstream face versus toe, and heel. RCC5 was the concrete zone where these regions are lying, whose compressive strength is 20.7 Mpa.

Table 4. 13 table showing summary of minimum principal stress

Loading condition	Earthquake ground motion	Reservoir condition	Minimum principal stress		Remark
			TIME HISTORY	MODAL	
Load comb.1	OBE in upstream direction	Empty	-6.67	-14.49	Located at RCC5
Load comb.2	OBE in downstream direction	Full (normal pool)	-48.4	-37.9	Located at RCC5
Load comb.3	SEE in downstream direction	Full (normal pool)	-54.7	-.38.01	Located at RCC5

4.5. Comparison Between Modal Analysis and Time History (FEM) Analysis

The charts and discussions made in this unit show a clear similarity and differences of the two analysis methods. The observations seen on this study are summarized and offered below:

- During the computation of each analysis method loads applied in the time history method will used as they are computed rationally but in modal analysis, applied loads must be changed into cyclic or vibratory loads so that there should be computation error which makes the difference.
- There are different cases where the modal method is very efficient, others where there is no clear winner between time history methods and modal methods,
  - Speed: The modal method ought to be quicker if we have many more time or frequency steps than shapes. substantially quicker than the direct(TMH) approaches. This is a result of the drastic decrease in DOF. For instance, the modal technique might only need 20, 100 or 1000 mode shapes for a model with 1 000 000 DOF. The modal model is several orders of magnitude smaller and thus faster because each mode shape represents one DOF. Calculations that can't be done directly are needed to calculate the shapes (modes). the transient analysis is a time-integration procedure so that performing numerical analysis on each time step with the appropriate DOF needs more work trajectory than modal method.

- Time history: CPU time is 2 hours and 40 minutes while modal analysis is 16-20 minutes maximum so that the modal analysis is time effective.

Time history **Modal**

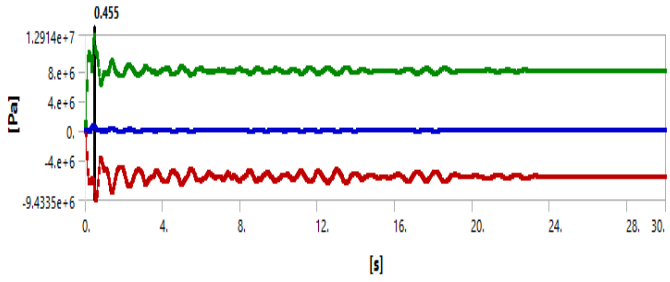

a. Time history of stress distribution (MWL+OBE)

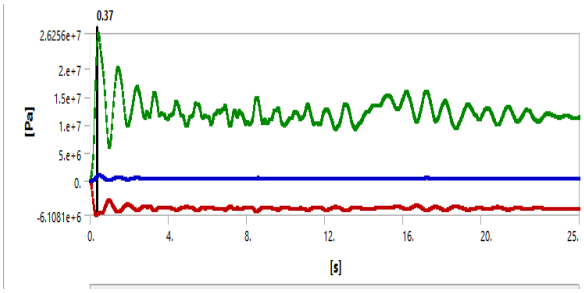

a. Time history of stress distribution (MWL+OBE)

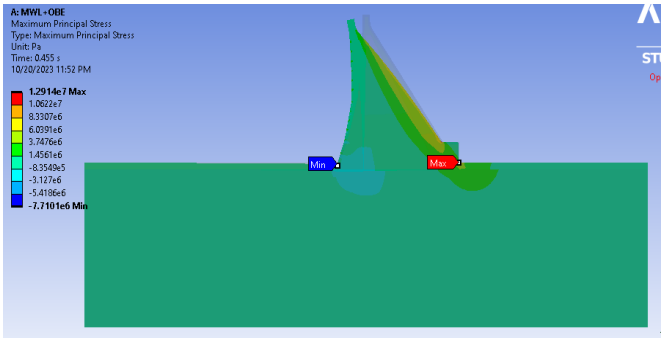

b. Stress distribution pattern(MWL+OBE

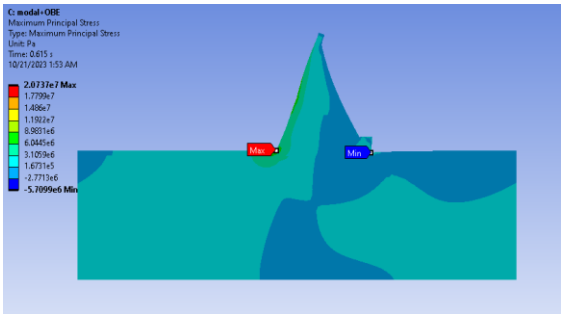

b. Stress distribution pattern(MWL+OBE

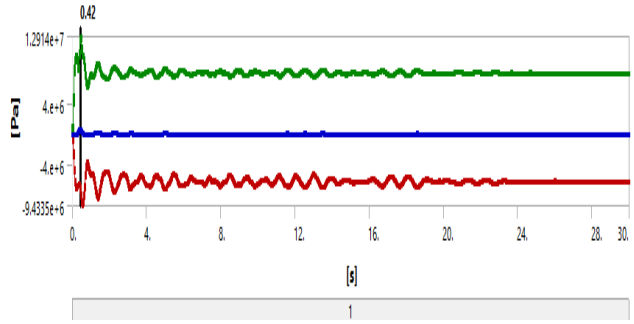

C. Time history of stress distribution (MWL+SEE)

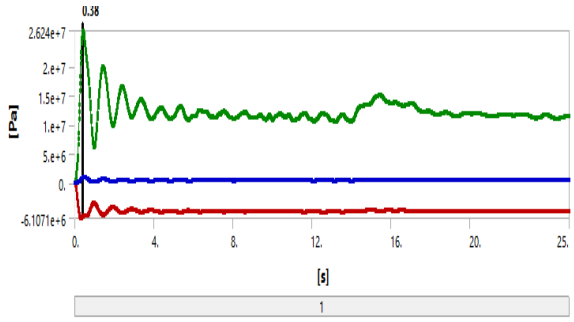

C. Time history of stress distribution (MWL+SEE)

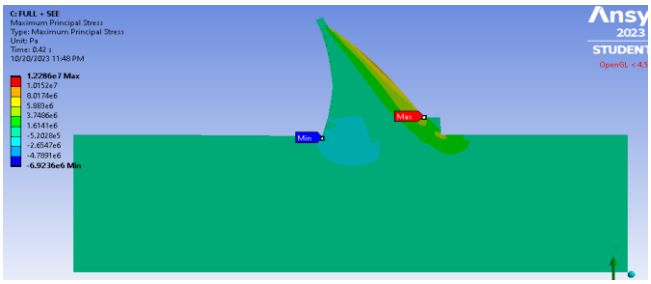

d. Stress distribution pattern(MWL+SEE)

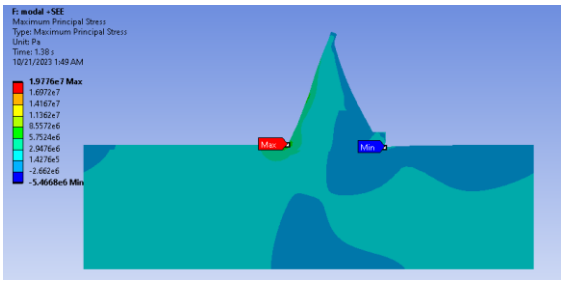

d. Stress distribution pattern(MWL+SEE)

Figure 4. 13 figure showing relative comparison of principal stress distribution between modal and time history analysis

- Stress distribution along the dam body: As seen from the pictures above stress distribution contour versus time history of the two analysis methods are quite different this is due to time history analysis is a direct method, it accounts the non-linearity of dam cross section versus material non linearity. We can also apply any load in the time history method directly with the distribution type but in the case of modal analysis it doesn't account non-linearity behaviors.
- The time history method is a tedious process of analysis but it tells the exact demarcation of parameters and properties of a given material and it is better to use such an analysis for the wise use of resources plus knowing the exact behavior of a material.

5. CONCLUSIONS AND RECOMMENDATIONS

5.1. Conclusions

This study finally presents the comparison between linear time history(FEA) and modal analysis methods according to results of the case study conducted on Gilgel Gibe III dam for the effect of two types of seismic loadings, the operation basis earth quake (OBE) and serviceable evaluation earthquake (SEE). The linear dynamic analysis adopted in ANSYS2016 and the 2023-R2 student version program was implemented. To investigate the effects of dam water on the response of gravity dams, the earthquake response of the selected event was determined for the specified case. The dam was subjected to the Morganhill (1984) earthquake on the OBE case and the Hectrmine (1999) earthquake on the SEE case in the upstream-downstream direction. Linear dynamic finite element analysis was conducted utilizing the two basic methods on the dam with seismic loading as the main case to observe the difference in dam's response against the three (extreme loading)combinations chosen together with inertia developed by the ground motion on the two analysis methods. Finally it was reached on the following conclusions:

1. Gibe III is a big dam and had complex geometrical setup, modeling and computation of mathematical works need attention so that computational and simulation accuracy enables the designers to set the appropriate dimensioning of the dam versus effective utilization of materials as well as the safety of the dam structure. According to this approach, the two methods give similar deformation behavior on the Gilgel Gibe III dam where the maximum value occurs at the dam crest. Stress developed over the dam body has been visualized with a very similar expected regions with different pattern of distribution except a little variation in magnitude which was occurred due to the nature of applying loads, accountability of non-linear behaviors as the time history method accepts time varying loadings directly and accounts non-linearity that the final result obtained in such method describes the effect of direct application but in the case of modal analysis it doesn't account non-linearity versus obeys time varying loads as loads varying in a time-frequency domain.
2. According to this study the time history method of analysis gives relatively an accurate result this is due to the method by itself uses the numerical evaluation of the whole structure computed based on what would the response of the structure in a very pre-defined small time changes through loading time steps as compared to the modal analysis. Modal analysis, on the other

hand, entails determining the natural modes of vibration and associated frequencies of a structure. This method analyzes the response in the frequency domain after the structure is generally excited at a small number of known excitation locations. The frequencies and mode shapes discovered by modal analysis offer a concise description of the structure's dynamic behavior, which can be helpful for both design and understanding of the structure's general behavior in terms of initial deformation. For instance, modal analysis is more appropriate for big and complicated structures than the time history technique since it is often faster and more computationally efficient, but it does not provide as much information on the structure's response over time.

3. The time history method, on the other hand, offers a more thorough view of the reaction but may require more processing power, particularly for large and complicated structures. Unfortunately, the modal analysis makes it easy to get wrong answers by not calculating enough mode shapes and/or not requesting static shapes.
4. The analysis made in this study on Gilgel Gibe III dam using both modal and time history analysis gives an insight for further investigation works while tries to visualize techniques for the determination of stresses, and deformation with comparable values in time history and modal analysis methods. knowing the distribution of stress along the dam body, and the critical region's stress becomes worse without doubt.

5.2. Recommendations

This study is believed to address basic concepts in linear lime-history analysis and modal analysis methods for the different users. It tries to give an emphasis on the linear basic dynamic 2-dimensional plain strain analysis which is apparently utilizing the two methods and the following basic ideas are left as points to be recommended for those who need to read and use this research for further work.

1. **The need for integrating two analysis methods in design of large structures**:-. For large and complex structures like Gilgel Gibe III RCC dam, using the two methods of analysis interchangeably enables to know the structures different cross sections in a very profound design parameters (stress, deformation) for optimized use of materials in time history method while efficient use of time in modal analysis. The modal analysis is effective for

preliminary design purposes since it doesn't account non-linearity behaviors so that it doesn't optimize the material resources but it is time effective .

2. **Options for further analysis**:- This study conducts linear elastic dynamic analysis applying time history and modal analysis using 2- dimensional plain strain finite element modeling and Results obtained show if the structure is big enough like the GIBE III RCC dam its cross sectional variability, joints and interfaces between different sections of the structure with nonhomogeneous material property seeks the linear analysis not showing the real behavior of the dam so that considering the realistic property of materials the type of analysis advised to encounter will be non-linear dynamic time history analysis using the 3D-modeling approach.
3. **Recommending the Establishment of National Guideline for Design and Analysis of Dam Structures**: the study uses different countries national code and international design and analysis requirement manuals with previous works. For that manner compiling this work effectively was very tedious due applying different standards accordingly. Now dam construction industry is at its youngest stage in our country and we have also dams in this time, there must a continuous investigation of these structures with respect to safety and serviceability considering natural phenomena like earth quake. Establishment of the national guideline for the design and analysis of dam structures ensures the designers to compile their work effectively in design of new and analysis of safety issues in existing dam structures.

REFERENCES

1. ACI318-11, 2011. Building Code Requirements for Structural Concrete , 38800 Country Club Drive Farmington Hills, MI 48331 U.S.A.
2. Aman Ali,(2020), Seismic Vulnerability Analysis of Major Ethiopian Dams with Emphasis on Dam Safety Evaluation, PHD desertation Addis Ababa university.
3. Anil K. Chopra. (2012). dynamics of structures theory and applications to earthquake engineering, University of California at Berkeley
4. Awulachew, S. B. Y., A. D.; Loulseged, M.; Loiskandl, W., Ayana, M.; Alamirew, T. (2007). International Water Management Institute: Water Resources and Irrigation
5. Ayele. Atalay, (2016), Probabilistic seismic hazard analysis (PSHA) for Ethiopia and the neighbouring regions, Addis Ababa university.
6. B. Poursartip and V. LotfiModal, (2008). Analysis of Concrete Arch Dams In Time Domain Including Dam-Reservoir Interaction, The 14th World Conference on Earthquake Engineering, Beijing, China
7. EEPCO.(2009). Environment impact assessment report on Gibe III dam project, Addis Ababa, Ethiopia.
8. EEPCO.2007. Stability Analysis Main Report On Gibe III Dam, Addis Ababa Ethiopia
9. EEPCO . 2007. Seismic Hazard Assessment on Gibe III Dam (Level One Design) Report. Addis Ababa Ethiopia
10. EEPCO.2008. Foundation Geotechnical Level One Design Report on Gbe III dam, Addis Ababa Ethiopia
11. Elsayad M.A., Attia W.A.E., and Belal A.M, Finite Element Analysis of Concrete Gravity Dam Under Seismic Loads, Arab Academy for Science, Technology & Maritime Transport, Cairo University
12. Getinet Melesse, Habtamu Melesse, Devadass T. 2021. Determining the reference basic wind speed in Ethiopia and comparing with compulsory Ethiopian standard CES 145, 2015, ELSVIER

13. Ernest K. Schrader (2022). A presentation on RCC Dam Design: Analyzing Stress and Stability, Renewable Energy World, California.

14. Eugenia Correa Saracco Patrick Lucas Bochnak, (2020). Design of RCC gravity dam and FEM modelling in GeoStudio Longtan dam, Division of Water Resources Engineering Department of Building & Environmental Technology, Lund University

15. Niranjan Dilip Patil . (2022). 3d Finite Element Analysis of Dam using Direct Time History Method- A Review, International Journal of Engineering Research & Technology (IJERT)

16. Pandimani and GMRIT Ravindra Vipparthy. (2022). Static and free vibration analysis of gravity dam under the influence of hydrostatic pressure using ANSYS finite element models, research square, UK

17. Richard Malm. (2016). Guideline for FE analyses of concrete dams, Energiforsk, E-mail: kontakt@energiforsk.se | www.energiforsk.se

18. Senait Assefa Demeke, (2017). Numerical modelling of RCC dam with special consideration on lift joints under earthquake conditions, UNESCO-IHE Institute for Water Education, Delft, the Netherlands

19. Shayma Al Baghdady and Linnea Khan, (2018) Designing Roller compacted concrete (RCC) dams, Royal Institute of Technology (KTH), Stockholm, Sweden TH

20. Quentin Shaw. (2017). Concrete Dam Types and The Circumstances And Conditions That Favour One Type Over Another, SANCOLD Conference, Tshwane, South Africa

21. EB225.01. (2003).Design Manual For Small Rcc Gravity Dams, Portland Cement Association 5420 Old Orchard Road Skokie, Illinois,

22. Mark T. Jones and Merrell L. Patrick. 1989. The Use of Lanczos's Method to Solve the Large Generalized Symmetric Definite Eigenvalue Problem, Institute for Computer Applications in Science and Engineering NASA Langley Research Center Hampton, Virginia 23665-5225.

23. USBR Guide for Analysis of Concrete Dam Structures using Finite Element Methods, Denver, Colorado

24. US Army of Corps of Engineers, Gravity Dam design, Manual number 1110-2-2200, Washington DC

25. US Army of Corps of Engineers, Engineering and design of time history analysis of hydraulic structures, Manual number 1110-2-6050, Washington DC

26. US Army of Corps of Engineers, Engineering and design of time history analysis of hydraulic structures, Manual number 1110-2-6051, Washington DC

27. US Army of Corps of Engineers, Engineering and design of time history analysis of earthquake, Manual number 1110-2-6053, Washington DC

28. U.S. Department of the Interior Bureau of Reclamation. 2018. Evaluation of Numerical Models and Input Parameters in the Analysis of Concrete Dams, Denver, Colorado

29. USBR. 1976. Design Manual For Concrete Gravity Dams (Design Of Gravity Dams). Denver Colorado.

30. USACE: EM 1110-2-2100. 2005. Engineering and Design of Stability Analysis Of Concrete Structures

31. Md. Hazrat Ali*, Md. Rabiul Alam, Md. Naimul Haque, Muhammad Jahangir Alam , (2011). Comparison of Design and Analysis of Concrete Gravity Dam, scientific research journal (http://www.SciRP.org/journal/nr),

32. Mohammad Ejaz Shahir and Priyanka Dhurvey.(2017). Seismic Response of Concrete Gravity Dam in Afghanistan, International Research Journal of Engineering and Technology. Volume: 04 Issue: 06 | June -2017

33. Clough, R., and J. Penzien. (1993). Dynamics of Structures, Second Edition. McGraw-Hill, Inc. ISBN 0-07-011394-7.

34. Edward L. Wilson. (2000). Three-Dimensional Static and Dynamic Analysis of Structures A Physical Approach With Emphasis on Earthquake Engineering,

35. Boresi, A. P. (1985). Advanced Mechanics of Materials. John Wiley & Sons. ISBN 0-471-88392-1.

36. Hughes, Thomas. (1987). The Finite Element Method - Linear Static and Dynamic Finite Element Analysis. Prentice Hall, Inc.

37. Wilson, E. L. (1962). "Dynamic Response by Step-By-Step Matrix Analysis," Proceedings, Symposium On The Use of Computers in Civil Engineering. Labortorio Nacional de Engenharia Civil. Lisbon, Portugal.

38. P. Novak, A.I.B. Moffat, C. Nalluri and R. Narayanan, 2007, Hydraulic Structures Fourth Edition, Taylor and Francis. London and USA.].

39. Pavol Lengvarský, Jozef Bocko. (2013).Theoretical Basis of Modal Analysis, American Journal of Mechanical Engineering, 2013, Vol. 1, No. 7, 173-179

40. Ioannis Koutromanos, James McClure and Christopher Roy, 2018, Fundamentals of Finite Element Analysis, Linear Finite Element Analysis, Wiley And Son's Limited, River Street, Hoboken, Nj 07030, USA

41. Martin Wieland and R. Peter Brenner, 2004, Earthquake Aspects Of Roller Compacted Concrete And Concrete-Face Rockfill Dams, 13th World Conference on Earthquake Engineering, Canada,

42. Kuo, J. S.-H. (1982). Fluid-structure interactions: Added mass computations for incompressible fluid, University of California, College of Engineering, Earthquake Engineering

43. Zienkiewicz, O.C. (1971) The finite element method in engineering science. McGraw-Hill, London.

44. Ioannis Koutromanos, James McClure AND Christopher Roy, 2018, Fundamentals of Finite Element Analysis, Linear Finite Element Analysis, WILEY AND SON'S LIMITED, River Street, Hoboken, NJ 07030, USA

45. B. Poursartip and V.Lotfi. 2008. Modal Analysis Of Concrete Arch Dams In Time Domain Including Dam-Reservoir Interaction 14th World Conference in Earthquake Engineering. Bejing China

46. N. Salman Movahedi and B. Aminneja. (2016). Seismic Performance Assessment Of Latyan Concrete Buttress Dam Subjected To Different Records Including Reservoir Effects By Finite Element Method, Journal of Fundamental and Applied Sciences. ISSN 1112-9867

47. ANSYS Inc. ANSYS. 2013. Mechanical APDL Advanced Analysis Guide. Release15.0

48. ANSYS Inc. 2015. ANSYS Modeling and Meshing Guide ANSYS Release 9.0

49. ANSYS Inc. 2016. Fundamental FEA Concepts and Applications A Guidebook for the Use and Applicability of Workbench Simulation Tools from ANSYS, Inc.
50. Pavol Lengvarskýa and Jozef BockoTheoretical, (2013), Basis of Modal Analysis, American Journal of Mechanical Engineering, 2013, Vol. 1, No. 7, 173-179
51. ZHANG Huidong , WANG Yuanfeng , LI Zheng and WANG Rixuan4, (2008), Seismic Time History And Non-Linear Analysis Of Large-Scale Power House Structure, The 14 th World Conference on Earthquake Engineering October 12-17, 2008, Beijing, China.
52. Kalyan Kumar Mandal & Damodar Maity, (2016). Transient Response of Concrete Gravity Dam Considering Dam-Reservoir-Foundation Interaction, Journal of Earthquake Engineering, http://dx.doi.org/10.1080/13632469.2016.1217804
53. S.Yu. Fialko, E.Z. Kriksunov and V.S.Karpilovsky . 2003. A block Lanczos method with spectral transformations for natural vibrations and seismic analysis of large structures in SCAD software, research gate, June 3-6, 2003, Gliwice, Poland

APPENDIX 1.
Sample load calculation

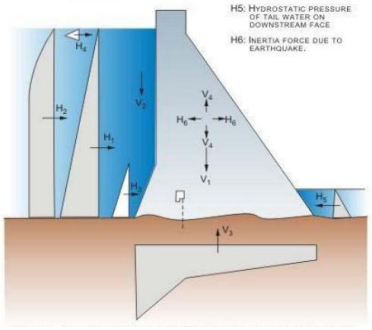

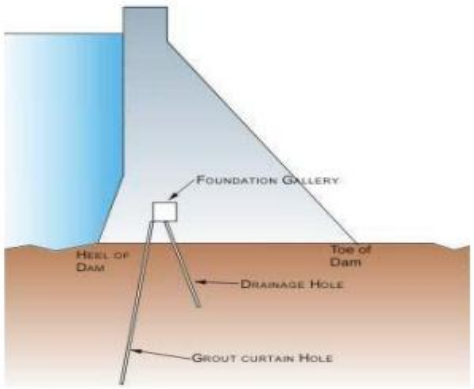

Gibe III RCC Dam				
Hydrostatic pressure distribution				
Horizontal direction				
Unit weight of water:		γ_w=	9.81	KN/m3
Maximum depth of water		H_{max}=	222	m
Horiz. hydrostatic pressure, pH, at any depth, zi, from top water surface				
			$p_h = \gamma_w * Zi$	
Vertical hydrostatic pressure, pv, at any depth, zi, from top water surface				
			$p_v = \gamma_w * Zi$	
Horizontal hydrostatic pressure				
Yi (m)	zi	p_h (KN/m2)		
0	222	2177.82		
10	212	2079.72		

20	202	1981.62		
30	192	1883.52		
40	182	1785.42		
50	172	1687.32		
60	162	1589.22		
70	152	1491.12		
80	142	1393.02		
90	132	1294.92		
100	122	1196.82		
110	112	1098.72		
120	102	1000.62		
130	92	902.52		
140	82	804.42		
150	72	706.32		
160	62	608.22		
170	52	510.12		
180	42	412.02		
190	32	313.92		
200	22	215.82		
210	12	117.72		
220	2	19.62		
222	0	0.00		
Vertical hydrostatic [ressure				
Xi (m)	Yi (m)	zi	p_h (KN/m2)	
0	0	222.00	2177.82	
5	14.43	207.57	2036.26	
10	28.54	193.46	1897.84	

14.32	40.91	181.09	1776.49	
18	55.87	166.13	1629.74	
22	71.25	150.75	1478.86	
26	88	134.00	1314.54	
29.09	100	122.00	1196.82	
33	139.61	82.39	808.25	
35	170.62	51.38	504.04	
37	179.1	42.90	420.85	
39.88	208	14.00	137.34	
39.88	222	0.00	0.00	

Uplift pressure

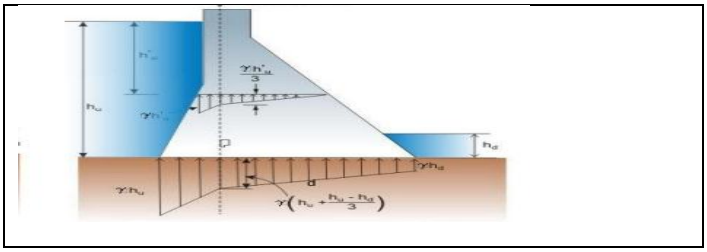

	Uplift pressure distribution				
			H3 = K (H1-H2)*(L-X)/L + H2=	84	m
			H1=	222	m

			H2=	7	m
			L=	193	m
			X=	20	
			K= 0.25 - 0.50 --- =	0.4	
	Xi (m)	Formula	p_v (KN/m2)		
	0	$\gamma w * H_1$	2177.82		
	10		1501.36		
	20	$\gamma w * H_3$	824.90		
	30		781.19		
	40		737.48		
	50		693.77		
	60		650.05		
	70		606.34		
	80		562.63		
	90		518.91		
	100		475.20		
	110		431.49		
	120		387.77		
	130		344.06		
	140		300.35		
	150		256.64		
	160		212.92		
	170		169.21		
	180		125.50		
	190		81.78		
	193	$\gamma w * H_2$	68.67		

Appendix. 2.
Hydrodynamic load calculation

Hydrodynamic interaction effects (Westergaard Added Mass , 1933)

Max.depth of water @ dam section; $H =$ 222 m

Horiz.acceleration coefficient, $\rho_w =$ 1000 kg/m3

Width of added mass water:

$$b_i = \frac{7}{8} * \sqrt{H_i(H_i - Z_i)}$$

$$\alpha_i = \frac{7}{8} * \rho_w * \sqrt{H_i(H_i - Z_i)}$$

Node, ni	Point masses		Zi	H_i =H-Zi	bi	αi	Node	Ai	mi = Ai*ρw (kg)
	X-Coordinate	Y-Coordinate							
1	0.0000	0.0000	0.0000	222.0000	194.2500	194250.000	1	6098.931	6098931.40
2	6.6500	19.0000	19.0000	203.0000	185.7516	185751.598	2	4811.132	4811132.10
3	14.3201	40.9146	40.9146	181.0854	175.4390	175439.047	3	3984.034	3984034.00
4	18.1716	56.3206	56.3206	165.6794	167.8104	167810.371	4	3160.325	3160325.10
5	21.8096	70.8727	70.8727	151.1273	160.2714	160271.389	5	2655.154	2655154.30
6	25.4477	85.4249	85.4249	136.5751	152.3598	152359.768	6	2467.153	2467152.70
7	29.0857	99.9770	99.9770	122.0230	144.0142	144014.224	7	2427.501	2427500.60
8	30.9284	118.4037	118.4037	103.5963	132.6956	132695.643	8	2118.732	2118732.10
9	32.4209	133.3292	133.3292	88.6708	122.7651	122765.081	9	1746.507	1746507.10
10	33.9135	148.2548	148.2548	73.7452	111.9570	111957.043	10	1525.485	1525484.90
11	35.4060	163.1803	163.1803	58.8197	99.9876	99987.554	11	1473.601	1473600.70
12	36.8986	178.1059	178.1059	43.8941	86.3749	86374.911	12	1252.982	1252981.50
13	38.3911	193.0314	193.0314	28.9686	70.1695	70169.486	13	1113.447	1113447.20
14	39.8837	207.9570	207.9570	14.0430	48.8556	48855.615	14	598.643	598642.70
15	39.8837	222.0000	222.0000	0.0000	0.0000	0.000	15	100.000	100000.00
									35433626.40

Appendix 3
Site-specific spectrum calculation

2. Type 2: Elastic Response Spectrum

2.1 Type 2: Horizontal Elastic Response Spectrum (Surface wave magnitude, Ms > 5.5)

2.1.1 For 5% damping case

Damping ratio: ξ= 5

Damping correction factor: $\eta = \sqrt{(10/(\xi+5))}$ = 1.00

Parameters to describe the horizontal elastic response spectrum

Ground Type	S	T_B	T_C	T_D
A	1	0.15	0.4	2

Fund. natural period of vibration of dam / empty case T = 0.7 sec.

Fund. natural period of vibration of dam / full reservoir case: T= 1.1 sec.

$$0 \le T \le T_B: \quad S_e(T) = a_g \cdot S \cdot [$$

$$T_B \le T \le T_C: \quad S_e(T) = a_g \cdot S \cdot$$

$$T_C \le T \le T_D: \quad S_e(T) = a_g \cdot S \cdot$$

$$T_D \le T \le 4s: \quad S_e(T) = a_g \cdot S \cdot$$

Equations to be used:

T (sec)		Sa / a_g				
	0.00	1.0	0.340			
	0.05	1.5	0.510			
	0.10	2.0	0.680			
T_B	0.15	2.5	0.850			
	0.20	2.5	0.850			
	0.25	2.5	0.850			
	0.30	2.5	0.850			
	0.35	2.5	0.850			
T_C	0.40	2.5	0.850			
	0.60	1.67	0.567			
	0.80	1.25	0.425			
	1.00	1.00	0.340			
	1.20	0.83	0.283			
	1.40	0.71	0.243			
	1.60	0.63	0.213			
	1.80	0.56	0.189			
T_D	2.00	0.50	0.170	Damping	5	%
	2.20	0.41	0.140	T =	0.7	sec.
	2.40	0.35	0.118	Sa/ a_g =	1.43	

	2.60	0.30	0.101	a_g=	0.10	g
	2.80	0.26	0.087	Sa=	0.14	g
	3.00	0.22	0.076			
	3.20	0.20	0.066	For T =	1.1	sec.
	3.40	0.17	0.059	Sa/ a_g =	0.91	
	3.60	0.15	0.052	a_g=	0.10	g
	3.80	0.14	0.047	Sa=	0.09	g
	4.00	0.13	0.043			
	4.20	0.11	0.039			
	4.40	0.10	0.035			
	4.60	0.09	0.032			
	4.80	0.09	0.030			
	5.00	0.08	0.027			
	5.20	0.07	0.025			
	5.40	0.07	0.023			
	5.60	0.06	0.022			
	5.80	0.06	0.020			
	6.00	0.06	0.019			
	6.20	0.05	0.018			
	6.40	0.05	0.017			
	6.60	0.05	0.016			
	6.80	0.04	0.015			
	7.00	0.04	0.014			
	7.20	0.04	0.013			
	7.40	0.04	0.012			
	7.60	0.03	0.012			
	7.80	0.03	0.011			
	8.00	0.03	0.011			
	8.20	0.03	0.010			
	8.40	0.03	0.010			
	8.60	0.03	0.009			
	8.80	0.03	0.009			
	9.00	0.02	0.008			
	9.20	0.02	0.008			
	9.40	0.02	0.008			
	9.60	0.02	0.007			
	9.80	0.02	0.007			
	10.00	0.02	0.007			